Synthesis and Characterization of Thermogelling Copolymers for Drug Delivery Applications

by

Nasim Ghasemi

A thesis submitted in partial fulfillment of the requirements for the degree of

Doctor of Philosophy

in

Pharmaceutical Sciences

Faculty of Pharmacy and Pharmaceutical Sciences
University of Alberta

Abstract

Thermo-reversible hydrogels, or thermogels, are a category of gel forming materials that are liquid at lower temperatures but turn into gel at higher temperatures. Thermogels are explored for different applications in drug delivery and tissue engineering fields. In this context, the development of biocompatible and biodegradable hydrogels that can safely be used in human is of great interest .In this thesis, the development of thermo-reversible hydrogels from block copolymers based on a block of poly(ethylene glycol) (PEG) and two blocks of functionalized poly(ε-caprolactone) was explored. In the first chapter, we investigated the effect of the ring-opening polymerization method (bulk versus solution polymerization) on the properties of prepared block copolymers such as molecular weight, molar mass dispersity, as well as thermo-responsive gelation, and viscoelastic properties of block copolymer solutions in water. Our results showed in block copolymers based on poly(ethylene glycol) as hydrophilic middle block and poly(α-benzyl carboxylate-ε-caprolactone) as the hydrophobic lateral blocks (abbreviated as PBCL-PEG-PBCL) the presence of a specific concentration of a high molecular weight subpopulation was crucial for the formation of thermo-reversible and viscoelastic PBCL-PEG-PBCL hydrogels. The appearance of this subpopulation was attributed to the formation of partially cross-linked or branched polymers during ring opening polymerization of α-benzyl carboxylate-ε-caprolactone by PEG. To test this hypothesis, in the next step, we synthesized chemically cross-linked PBCL-PEG-PBCLs by the manual introduction of different nucleophilic cross-linkers to PBCL-PEG-PBCL copolymers. The effect of the type and/or molar ratio of cross-linker to polymer on the formation of viscoelastic thermogels was then investigated. This step sheds light on the required conditions for the synthesis of PBCL-PEG-PBCLs capable of formation of viscoelastic thermogels around 30°

C. Such viscoelastic thermogels were prepared using chemical cross-linking of PBCL-PEG-PBCL by PEG400 at PEG400/BCL molar ratio of 4:10. In the next chapter, we characterized the effect of benzyl carboxylate conversion to carboxyl groups in partially cross-linked PBCL-PEG-PBCL copolymers, on the thermo-gelling behaviour of produced structures (abbreviated as PCBCL-PEG-PCBCL) in water. The results showed the hydrophilic/lipophilic balance in the polymer structure affects the formation of viscoelastic thermo-gels from partially cross-linked PCBCL-PEG-PCBCL copolymers under study, with the thermo-gels to be formed for PCBCL-PEG-PCBCL with around 35-65 percent COOH substitution on the polymeric backbone. Finally, we developed polymeric micelle loaded liposomal formulation (or lipocell) through encapsulation of triblock copolymer of poly(α-carboxyl-co-benzyl carboxylate-ε-caprolactone)-b-poly(ethylene glycol)-b-poly(α-carboxyl-co-benzyl carboxylate-ε- caprolactone) (PCBCL-PEG-PCBCL) conjugated to doxorubicin (abbreviated as PCB(CL-DOX)-PEG-PCB(CL-DOX)) in liposome via the freeze-thaw method. The success in the encapsulation of polymeric micelles inside liposome was assessed with a transmission electron microscope (TEM) employing either a negative staining or a cryogenic TEM technique (cryo-TEM). The results of this study identified the required synthesis condition leading to the preparation of viscoelastic thermogels based PBCL-PEG-PBCL and PCBCL-PEG-PCBCL. It also set the foundation for the preparation of polymeric micelles encapsulated liposomes or lipocells, as a new nanocarrier for future applications in drug delivery.

Preface

This thesis is an original work by Nasim Ghasemi under the supervision of Dr. Afsaneh Lavasanifar (Faculty of pharmacy and pharmaceutical sciences) at the University of Alberta.

Chapter 2 and parts of **Chapter 3 and 4** are included in a patent application. Ghasemi, N.; Vakili, M. R.; Lavasanifar, A. As "**Triblock copolymers and thermo-reversible hydrogels**" U.S. 63/182,4222. 2021.

Chapter 2 of this thesis has been published as Ghasemi, N.; Vakili, M. R.; Lavasanifar, A. "**Defining Role of a High-Molecular-Weight Population in Block Copolymers Based on Poly(α-Benzyl Carboxylate-ε-Caprolactone) and Poly(Ethylene Glycol) on the Formation of Thermo-reversible Hydrogels**" in ACS Appl.Polym.Mater. 2021, 3 (5), 2608–2617. I conceived the experimental design and performed the experiments, data analysis, and wrote the first draft of the manuscript and conducted editions on the manuscript based on reviewers' comments. Vakili, M.R Assisted in conceptualization, validation of data and analysis, and editing of the manuscript. Lavasanifar, A supervised the development and assisted in conceptualization, validation of data and analysis, funding acquisition, and contributed to manuscript editing.

Chapter 3 has been published as Ghasemi, N.; Vakili, M. R.; Lavasanifar, A. "**Cross-linking of triblock copolymers of functionalized poly(caprolactone) and poly(ethylene glycol): The effect on the formation of viscoelastic thermo-gels**" in Reactive and functional polymers.171, 105167 (2022). My role was data curation, analysis, writing of the original draft, and visualization of the results. Vakili, M.R assisted in conceptualization, supervision, validation, writing-review, and editing. Lavasanifar, A supervised the development and assisted in conceptualization, validation of data and analysis, funding acquisition and contributed to manuscript editing.

Chapter 4 of this thesis will be submitted for publication as Ghasemi, N.; Vakili, M. R.; Lavasanifar, A. "**Polymer characteristics leading to the formation of viscoelastic thermo-gels in partially cross-linked copolymers based on benzyl carboxylate/carboxyl substituted PCL and PEG"** I did the experimental design and performed the experiments, data analysis and wrote the first draft of the manuscript. Vakili, M.R assisted in conceptualization, validation of data and analysis, and editing of the manuscript. Lavasanifar, A supervised the development and Assisted in conceptualization, validation of data and analysis, funding acquisition, and contributed to manuscript editing.

Chapter 5 of this thesis will be submitted for publication as part of a future manuscript Ghasemi, N.; Vakili, M. R.; Lavasanifar, A. **"Preparation and characterization of lipocells, liposomes encapsulating polymeric micelles, as a promising new nano-drug delivery system"** I conducted experimental design and synthesis, data analysis, and wrote the original manuscript. Vakili, M.R assisted in conceptualization, supervision, and validation of data. Lavasanifar, A supervised the development and assisted in conceptualization, validation of data and analysis, funding acquisition and contributed to manuscript editing.

Dedication

To

My lovely parents, for always loving and supporting me

My amazing husband, Milad, for his patience, love, friendship, and endless support

My little son, Taha, whose laughter always fills my heart with happiness, hope, and love

Acknowledgments

My Ph.D. accomplishment would not have been possible without the presence of special people during my research at the University of Alberta.

First and foremost, I would like to extend my heartfelt appreciation to my supervisor, Prof. Afsaneh Lavasanifar for her guidance, patience, support, and encouragement. She patiently corrected my mistakes, showed me the way to do research, and helped me to overcome challenges during my Ph.D. journey. I take great pride and great pleasure that I've been able to be her student and member of her lab. Thanks, Dr. Lavasanifar for your support not only in my educational experiences but also in my personal life.

- I sincerely thank Dr. Mohammad Reza Vakili for training me in the lab and for all the kind words and encouragement that I received from him during my studies.
- I sincerely thank my supervisory committee members, Dr. Carlos Velazquez Martinez, Dr. Raimar Loebenberg, Dr.Joao Soares, and Dr.Philip Choi.
- I sincerely thank Dr. Vishwanatha Somayaji for the acquisition of NMR data; Dr.Lingyun Chen for providing me access to her lab at the University of Alberta. Dr. Christin Allen for accepting me as a visiting student and providing me access to her lab.
- I sincerely thank my lab mates, Dr.Igor Pavia, Dr.Hanan Al Lawati, Dr.Zahra Shire, Dr. Sams Sadat, Parnian Mehinrad, Dr. Mohammed Saeid Waleed, Dr. Forugh Sanaee, Dr. Nazila Safaei Nikouei, Dr. Hoda Soleymani Abyaneh, Dr. Shyam Garg, Asma saqr and all of my friends for their help and support and creating a friendly environment in the lab.
- I sincerely thank the Faculty of Pharmacy and Pharmaceutical Sciences and the University of Alberta for accepting me into this Ph.D. Program and for supporting me during the course of my Ph.D. program.

- I would like to thank the Natural Science and Engineering Research Council of Canada (NSERC) for their financial support of my research.
- I will never be able to express my deep gratitude to my parents and my husband. Their encouragement has always been with me during my studies, and their support made it possible for me to attend and complete this Ph.D. program.

Table of Contents

List of Figures

List of Tables

List of Abbreviations

ABCs	Amphiphilic Block Copolymers
ANOVA	Analysis of variance
BCL	α-Benzylcarboxylate ε-caprolactone
CCL	Carboxylate ε-caprolactone
CDCL3	Deuterated chloroform
ε-CL	Caprolactone
CGC	Critical gel Concentration
Da	Dalton
DLS	Dynamic light scattering
DOX	Doxorubicin
DSC	Differential Scanning Calorimetry
FDA	Food and drug administration
G'	Storage Modulus
G"	Loss Modulus
GPC	Gel permeation chromatography
h	Hour
HLB	Hydrophilic/hydrophobic Balance
L	Litre
LCST	Lower Critical Solution Temperature
M	Molar
MDSC	Modulated Differential Scanning Calorimetry

mg	Milligram
min	Minute
mL	Millilitre
Mn	Number average molecular weight
Mw	Weight average molecular weight
MW	Molecular weight
nm	Nanometer
NMR	Nuclear magnetic resonance
Pa.s	Pascal. Second
PBCL	Poly(α-Benzylcarboxylate ε-caprolactone)
PBCL-PEO-b-PBCL	Poly(α-benzyl carboxylate-ε-caprolactone)-polyethylene oxide-block-poly(α-benzyl carboxylate-ε-caprolactone)
PCBCL	Poly(α-Benzyl carboxylate-co-α-carboxyl-ε-caprolactone)
PCCL	Poly(α-carboxylate ε-caprolactone)
PCL	Poly(ε-caprolactone)
Pd/C	Palladium, 10% on activated charcoal
PDI	Poly dispersity index
PDLLA	Poly-DL-lactide
PEG	Polyethylene glycol
PEO	Polyethylene oxide
PEO-b-PCL	Polyethylene oxide-block-poly(ε-caprolactone)
PLA	Poly L-lactide
PLGA	poly(lactic-co-glycolic acid)

PLLA	Poly(L-lactic acid)
PNIPAm	Poly(N-isopropylacrylamide)
PPO	Poly(propylene oxide)
PTX	Paclitaxel
rpm	Round per minute
T	Absolute Temperature
THF	Tetrahydrofuran
μL	microlitre
UCST	Upper Critical Solution Temperature
W/W	Weight per weight

Chapter 1. General Introduction

1.1 Stimuli-responsive copolymers and their application in drug delivery

Stimuli-responsive polymers or smart polymers are macromolecules that can be triggered for a change in their properties by various external or physiological stimuli including[1] temperature [2–5], pH [3,6,7], light [8], electric and magnetic fields [9]. Table 1-1 shows various pros and cons of currently developed stimuli-responsive drug delivery systems. The external stimuli can cause observable or detectable changes in the morphology or molecular bond of polymers which can induce macroscopic changes in shape, color, and function [10]. The concept of a stimulus-responsive drug delivery system was reported for the first time in 1978 by the use of thermo-sensitive liposomes for the enhanced local release of drugs by hyperthermia [11]. Then smart polymers have found numerous applications in medicine specially drug delivery [3–5,12–14], chemotherapy [15], self-healing [16], and anti-bacterial materials [17]. Tables 1-2 exhibit examples of different stimuli-responsive copolymers as drug delivery systems. Between different stimuli-responsive polymers, considerable attention has been paid to temperature-responsive polymers due to their sharp changes in properties upon exposure to small changes in environmental temperature [1,18,19]. Temperature-responsive polymers can divide into 2 categories: polymers with negative temperature sensitivity and positive sensitivity. Polymer with a negative temperature sensitivity which defines as the lower critical solution temperature (LCST) is in a homogeneous mixed phase at a temperature below LCST due to hydrogen bond formation between water and hydrophilic polymeric parts. By increasing the temperature above the LCST, the hydrophobic interaction between the hydrophobic polymeric parts dominates and causes polymeric network collapse then phase separation occurs. On the other hand, the positive sensitivity of polymers defines by upper critical solution temperature (UCST) which leads to collapse in the polymeric network at a temperature below UCST, while swelling occurs at a temperature higher than UCST.

Table 1-1. Advantages and disadvantages of various stimuli-responsive drug delivery systems currently developed [1,7,25–27].

Stimulus	Advantages	Limitations
Temperature	1. Simple synthesis and formulation 2. Ease of control based on critical solution temperature 3. Stability during circulation 4. Applicable *in vitro* and *in vivo* 5. Simplicity of active molecule incorporation 6. Ability to deliver hydrophilic and lipophilic drugs	1. Design a safe and sensitive system that can respond quickly to slight temperature changes 2. Injectability issues under administration conditions 3. Low mechanical strength 4. Instability of thermolabile drugs 5. Burst release of the incorporated drug
pH	1. Suitable for delivery of anticancer drug 2. Suitable for thermolabile drugs	1. Poor stability before reaching a target 2. Low mechanical strength
Light	1. Ease of control for triggering drug release	1. Inconsistent response to the stimuli 2. Dark toxicity of light-responsive polymers
Electric field	1. Gradual and pulsative release of drugs possible	1. Surgical implantation is required 2. Difficulty in optimizing the magnitude of electric field

Table 1-2. Example of stimuli-responsive copolymers applied for drug delivery.

Copolymer	Type of Stimuli-Responsiveness	Drug	Reported application in the preclinical stage	Ref
PLGA-PEG-PLGA	Temperature	Exenatide	Treatment of type II diabetes	20
PCL-PEG-PCL	Temperature	Paclitaxel	Prevention of colorectal cancer metastasis	21
GC/OHC-PEO-PPO-PEO-CHO	pH	Paclitaxel and Doxorubicin	Prolongation of the survival rate of B16F10 tumor-bearing mice	22
PEG-b-CPCL	pH	Ibuprofen/Camptothecin	Delivery of multiple drugs for oral drug delivery	23
PEG-PCL/Gold nanorod hybrid NPs	Light	Doxorubicin	Remote near-infrared triggered drug release	24

1.1.1 Physical forms of stimuli-responsive polymers

Stimuli-responsive polymeric materials (SRPMs) have been utilized in various physical forms :

1. Cross-linked hydrogels (permanently cross-linked)
2. Reversible hydrogels
3. Micelles
4. Modified interfaces

Hydrogels are a 3D network of polymer chains formed through physical or chemical cross-linking of polymers at specific functional group sites. The cross-linking makes the polymeric network water-insoluble, but the hydrophilic polymer may still absorb water and swell. The cross-link density of hydrogels can affect the swelling ratio and inner structure of hydrogels [28,29]. Reversible Stimulus responsive polymeric materials (SRPMs) are the ones that show the formation of a three-dimensional network in response to stimuli such as pH, temperature, light, electric field, etc. Thermo-reversible hydrogels are made from SRPMs that show the solution to gel (sol-gel) transition by an increase in temperature. In this category of SRPMs, usually, gelation and formation of three-dimensional polymer networks are triggered by the formation of hydrophobic interactions leading to physical cross-linking in aqueous media. This category of hydrogels is mostly used for the formation of injectable hydrogels for depot drug delivery [30].

In addition to smart hydrogels, smart polymeric micelles have gained popularity in recent years for different applications. Micelles form by self-aggregation of amphiphilic block copolymers in aqueous media. Smart polymeric micelles can be formed through the introduction of ionizable, or cleavable functional groups to either hydrophobic or hydrophilic blocks of block copolymers. In this case, upon exposure to stimuli dissociation, or association of block copolymers can be

triggered, and/or core or shell forming groups can get released from the micellar structure leading to a change of morphology in the micellar system.

Micelle formation can happen at a low concentration of block copolymers (above critical micellar concentration) by entropic-driven force. At a higher concentration of block copolymers, called critical gel concentration (CGC), the interaction between micelles increases, and reversible hydrogels can form [28,31,32].

Also, surfaces such as polymers, silica, and metal can be functionalized with stimuli-responsive polymers to produce a smart interface between liquid and solid phases for applications such as biomedical, bioelectronics, and catalysis [28].

1.1.2 Methods for the preparation of Stimuli-responsive hydrogels

1.1.2.1. physically cross-linked hydrogels

Stimuli-responsive hydrogels can be prepared by physical or chemical cross-linking methods. Physically cross-linked hydrogels can be prepared without cross-linking agents, organic solvents, and photo-irradiation, and the final hydrogel is reversible. Nevertheless, there is some difficulty in controlling of some variable factors such as gelation time, the pore size of the network, and degradation time in physically cross-linked hydrogels. Physical cross-linking between polymeric chains can occur using a variety of physicochemical interactions such as hydrophobic interactions, hydrogen bonding, charge condensation, steriocomplexation, or supramolecular chemistry as illustrated in figure 1-1 [33]. Amphiphilic copolymers can often form physically cross-link in an aqueous environment by changing temperature. For amphiphilic block copolymers base on PEG and PCL, hydrophobic interaction between polymeric chains is the most common mechanism of gelation. Mechanism of physical gelation driven by hydrophobic interaction is shown in figure 1-1 A. By increasing the temperature hydrophobic domain in amphiphilic copolymers prefers

aggregation to minimize interaction with the surrounding water and maximize the solvent entropy. The sol-gel temperature depends on the length of the hydrophobic block, polymer concentration, and chemical structure of the polymer. Increasing the concentration and hydrophobicity of the hydrophobic segment leads to a larger driving force for the aggregation of block copolymers and/or micelles and lowers the gelation temperature. Some common hydrophobic segments such as poly (propylene oxide) (PPO), poly (lactide-co-glycolic acid)(PLGA), poly(N-isopropyl acrylamide)(PNIPAM), poly(urethane)(PU) and poly(caprolactone)(PCL) can undergo reverse thermal gelation near the physiological body temperature by hydrophobic interaction mechanism.

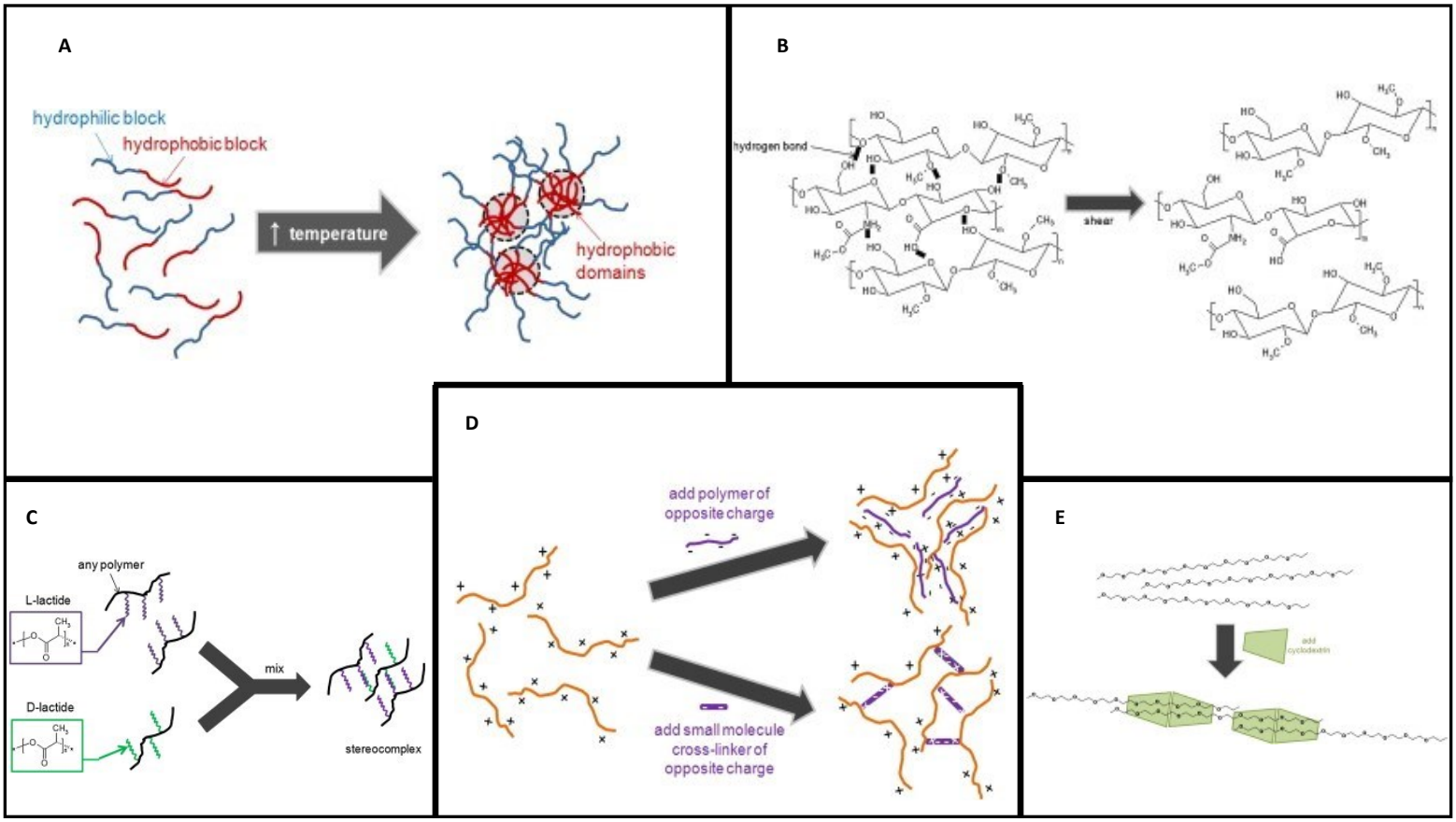

Figure 1-1. Mechanism of physical gelation driven by: **A.** Hydrophobic interaction. **B.** Hydrogen bonding. **C.** Steriocomplexation. **D.** Electrostatic interaction and **E.** Supramolecular chemistry. (Adapted from: Hoare TR, Kohane DS. Hydrogels in drug delivery: Progress and challenges. Polymer. 2008;49(8):1993–2007).

Physical gelation can also occur through hydrogen bonding interaction between the compatible polymeric chain. Hydrogen bonding can be used to formulate injectable hydrogels while shearing the mixture (for example forcing the solution by needle) can disrupt the weak hydrogen bond and facilitate injection. Figure 1-1B shows physical gelation via hydrogen bonding between methylcellulose and hyaluronic acid while the hydrogen bonds break under shear. The hydrogen-bonded networks are not stable in vivo and can dilute and disperse due to the influx of water.

Stereocomplexation is another form of physical gelation which refers to the association between polymer chains or small molecules of the same chemical composition, but with different stereochemistry, as shown in figures 1-1C. However, stereocomplexation is limited to the small range of polymers that have stereochemistry. Also, small changes in the chemical composition of the polymer can significantly weaken or eliminate the stereochemical interaction.

Physical gelation by electrostatic interaction can occur by adding the polymer with an opposite charge or adding a small molecule with an opposite charge as a cross-linker as shown in figure 1-1D. Charge interactions have been widely used in drug delivery specially using pH change as a trigger.

Supramolecular chemistry is a newer category of physically cross-linked hydrogels which uses supramolecular chemistry (ordered arrangement of molecules assemblies and the intermolecular bond), as illustrated in figure1-1E, poly(ethylene oxide) can be cross-linked using cyclodextrin to form a reversible hydrogel which is injectable [33–36]. Table 1-3 gives an overview of the various in-situ gelling system which were physically cross-linked by discussed methods.

Table 1-3. Overview of polymer systems, cross-linking methods, and medical applications of hydrogels.

Copolymer	Cross-linking method	Application	Reference
PLGA-PEG-PLGA	Hydrophobic interaction	Using physical gelling as an injectable sustained-release carrier for a PEGylated drug	[37]
PEO-PPO-PEO	Hydrophobic interaction	Pluronic used in drug delivery, gene and cancer therapy	[38]
PCL-PEG-PCL	Hydrophobic interaction	In situ gel-forming controlled drug delivery system	[39]
Carboxyl methyl cellulose (CMC)	Hydrogen bonding	Tissue Engineering, bioprinting, drug delivery, and cancer therapy	[40,41]
Poly (vinyl alcohol)	Hydrogen bonding	Tissue Engineering for repairing and regenerating tissues and organs	[42]
PEG-PLLA/PDLA diblock and triblock	Stereocomplexation	Controlled delivery carrier	[43,44]
dex-HEMA-MAA + dex-HEMA-DMAEMA	Ionic interaction	Delivery of pharmaceutically active proteins	[45]

1.1.2.2. chemically cross-linked hydrogels

In this category, hydrogels are formed through covalent cross-linking of polymer chains together. The chemically cross-linked hydrogel can provide better mechanical stability compared to physical gels, which prevent dilution of hydrogel and diffusion of the polymers away from the site of injection. However, the cross-linking agents are often toxic and there is a possibility of unwanted reaction in chemical cross-linking which produces by-products or branched polymer [35,36]. The chemically cross-linked hydrogel can be synthesized by adding a small molecule as a cross-linker to reactive pre-polymers or through polymer-polymer cross-linking which is pre-functionalized with reactive functional groups [36].

1.1.3 Hydrogels based on polycaprolactone and polyethylene glycol

Hydrogels made from amphiphilic block copolymers containing both hydrophilic and hydrophobic units represent many advantages and applications compared to other hydrogels. The hydrophobic part in hydrogels improves their mechanical properties and structural stability compared to simple hydrogels. Importantly, the presence of both hydrophobic and hydrophilic segments in amphiphilic hydrogels allows them to carry hydrophilic and/or hydrophobic drugs [46–48]. Among different synthetic polymers, PEG was used as a hydrophilic part in most hydrogels due to its excellent properties such as versatility of its chemistry, good solubility in aqueous and organic solvents, and excellent biocompatibility. On the other hand, the long-term biodegradability of PEG is a disadvantage that can be compensated by using biodegradable polymers like polyesters along with PEG [49,50]. In 1999, Choi et al synthesized di-block and triblock copolymers based on PEG and polyester [51]. Among polyesters, PCL found versatile applications in biomedical applications due to biocompatibility, hydrophobicity, biodegradability, and crystallinity. Generally, PEG/PCL copolymers are synthesized by ring opening polymerization of cyclic ester monomer (ε-caprolactone) in the presence of PEG as the initiator mostly with the help of proper catalyst such as Stannous octoate [52]. Rofg opening polymerization (ROP) is an important aspect in polymer chemistry that involves chain-growth polymerization, where the tail end of initiator polymer acts as a reactive site and cyclic monomer can bind by opening the ring for effective elongation of polymer. The reactive site of the initiator can be cationic, anionic, or a radical but ε-caprolactone mostly react following the attack of the anionic initiator as shown in figure 1-2. The ring opening polymerization can be performed either as a bulk or solution polymerization [53]. In bulk polymerization, no solvent is used and the PEG as the initiator is mixed in a melted condition with the catalyst and monomer. The polymerization usually occurs at high temperatures and there is a

possibility inadequate uniformity in heat transfer leading to the non-uniformity of polymer molecular weight distribution. Use of organic solvents in the polymerization reaction can lower the temperature needed for polymer synthesis, enhance heat transfer and the monodispersity of the polymer population synthesized.

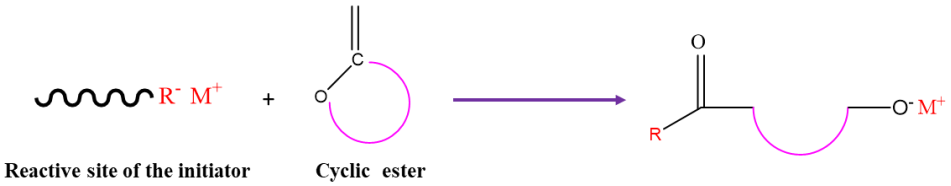

Figure 1-2. Illustrating the reaction for the ROP of the cyclic ester by anionic initiation

Linear copolymers of PCL/PEG can be formed as AB, ABA, or BAB copolymer (A is PCL and B is PEG segment) based on the ratio of PCL to PEG. Table 1-4 shows a summary of different forms of PCL/PEG copolymer making hydrogels, that appeared in the literature in the past decade along with their synthetic method, and application.

Table 1-4. Overview of polymer systems, cross-linking methods, and medical applications of hydrogels.

Copolymer	Synthetic method	Description and applications	Ref.
PEG-PCL-PEG	ROP catalyzed by Sn $(Oct)_2$ and hexamethylene diisocyanate as coupling agent	PEG-PCL-PEG hydrogel is used for preventing local breast cancer recurrence and improving incision wound healing in a mouse model	54
PEG-PCL-PEG	ROP catalyzed by Sn $(Oct)_2$ and hexamethylene diisocyanate as coupling agent	Hydrogel composite of PEG-PCL-PEG, collagen, and nano-hydroxyapatite used for guided bone regeneration.	55
PEG-PCL-PEG	ROP catalyzed by Sn $(Oct)_2$ and hexamethylene diisocyanate as coupling agent	PEG-PCL-PEG hydrogel is used as an injectable drug delivery system for the release of insulin.	56
PCL-PEG-PCL	ROP of PCL incorporated with cyclic ether and catalyzed by Sn $(Oct)_2$	PCL-PEG-PCL hydrogel used for sustained release of PTX-incorporated nanoparticles synergized by a burst release of Dox.HCL	57
PEG-PCL-PEG	ROP catalyzed by Sn $(Oct)_2$ and hexamethylene diisocyanate as coupling agent	PEG-PCL-PEG used for ocular drug delivery of diclofenac sodium	58,59
PCL-PEG-PCL	ROP catalyzed by Sn $(Oct)_2$ Bulk-photo cross-linking	Photo cross-linked PCL-PEG-PCL hydrogel used in cartilage tissue engineering.	60
PEG-PCL-PEG	ROP catalyzed by Sn $(Oct)_2$ and hexamethylene diisocyanate as coupling agent	PEG-PCL-PEG modified via cyclic ether pendant group to improve storage modulus, injectability, biodegradability, and sol-gel transition controllability	61
PCL-PEG-PCL	ROP catalyzed by Sn$(oct)_2$ Bulk	Combination of PCL-PEG-PCL hydrogel and Chitosan-multi walled carbon nanotubes used for doxorubicin delivery.	62
PCL-PEG-PCL	ROP catalyzed by Sn $(Oct)_2$ Bulk	The microsphere of PCL-PEG-PCL/Alginate hydrogel improved skin wound healing.	63
PCL-PEG-PCL	ROP catalyzed by Sn $(Oct)_2$ Bulk	Injectable PCL-PEG-PCL hydrogel is used for sustain-release hyaluronic acid delivery to improve the lubricity of artificial joints.	64
PCL-PEG-PCL	ROP catalyzed by Sn $(Oct)_2$ Bulk	PCL-PEG-PCL hydrogel composite with the poly (D, L-lactide) electrospun nanofiber membrane used for guided spinal fusion.	65
PCL-PEG-PCL	Combination of ROP and RAFT-Solution	Amphiphilic copolymer based on PCL and PEG synthesized via a combination of ROP and RAFT for delivery of anethole.	66
PCL-PEG-PCL	ROP catalyzed by Sn $(Oct)_2$ Bulk	Magnetic-PCL-PEG-PCL nanoparticles are used as anticancer drug carriers.	67
PCL-PEG-PCL	ROP catalyzed by Sn $(Oct)_2$ Bulk	Temperature and pH-responsive pentablock copolymer used for controlled release of insulin incorporated chitosan	68

PCL-PEG-PCL	ROP catalyzed by Sn $(Oct)_2$ cellulose nanowhisker (CNW), as a cross-linker	Effect of PEG length on phase segregation, crystallization, and thermal stimuli responsiveness in PCL-PEGx-PCL copolymer investigated for tissue engineering applications.	[69]
PCL-PEG-PCL	ROP catalyzed by Sn $(Oct)_2$ Bulk	Nanocarrier of PCL-PEG-PCL synthesized for co-loading of docetaxel (DTX) and quercetin (Qu) to decrease side effects of the drug.	[70]

1.1.4 Effect of PCL and PEG molecular weight on solubility and thermo-responsive behavior of PCL-PEG-PCL block copolymer

1.1.4.1 The effect of PCL block molecular weight on thermo-gelling behaviour of PEG/PCL copolymers

In constant PEG block molecular weight, increasing the PCL molecular weight (chain length), elevate the micellar stability and improves the hydrophobicity of the copolymer backbone. Considering the hydrophobic interaction is the driving force for the creation of PEG/PCL physical hydrogel, in constant PEG block length, the surge in the PCL block length decreases critical gelation concentration (CGC) and lowers critical gelation temperature (LCGT) while upper critical gelation temperature(UCGT) increase. Increasing the molecular weight of hydrophobic PCL block leads to a reduction of critical micellar concentration(CMC) and an increase in micellar stability then gelation occurs at lower temperatures and lower concentrations also micelles will be broken at higher temperatures and UCGT increase [59].

1.1.4.2 The effect of PEG block molecular weight on thermo-gelling behaviour of PEG/PCL copolymers

In 2008, Liu *et al* investigated the effect of the PEG molecular weight on the gelation of PCL-PEG-PCL triblock copolymer through the inverse flow method. They reported in constant molecular weight of PCL(1000 Da), by increasing the PEG molecular weight from 1000 to 1540 Da, the sol region window became bigger and shifts to a lower concentration. This was attributed to the improved solubility of the copolymer by increasing PEG block length. However, CGC and LCGT declined which might be caused by increase in the total molecular weight of the copolymer. On the other hand, in 2009, Gong et al reported an increase in LCGT and UCGT when the molecular weight of the PCL block was kept constant, and the PEG molecular weight was increased the gelation window shifted to a higher temperature and concentration. This was attributed to a decrease in the hydrophobicity of copolymer due to a decline in PCL/PEG ratio [59,71].

1.2 Characterization of triblock copolymers

1.2.1 Gel permeation chromatography (GPC)

Gel permeation chromatography(GPC) or size exclusion chromatography (official IUPAC name) is one of the most commonly used techniques for polymer characterization. The main application of GPC technique is to provide information on the molar mass averages and molar mass distribution of polymer. It can also provide valuable information about chemical composition distribution (CCD), Intrinsic viscosity distribution, branching, functionality, chain length, and conformation of polymers. Figure 1-3 shows the GPC system used in our study (Agilent 1260 Infinity), which consisted of a manual injector, pump, Refractive Index detector (RI), dual-angle light scattering detector, viscometer detector, a series of two columns (Styragel HR2 and styragel HR 4E from waters) and a column oven. In GPC, the separation process of polymer samples occurs based on the size or precisely, the molecular hydrodynamic volume of polymer molecules. The GPC column stationary phase (typically a cross-linked gel) is composed of very small porous material with different sizes.

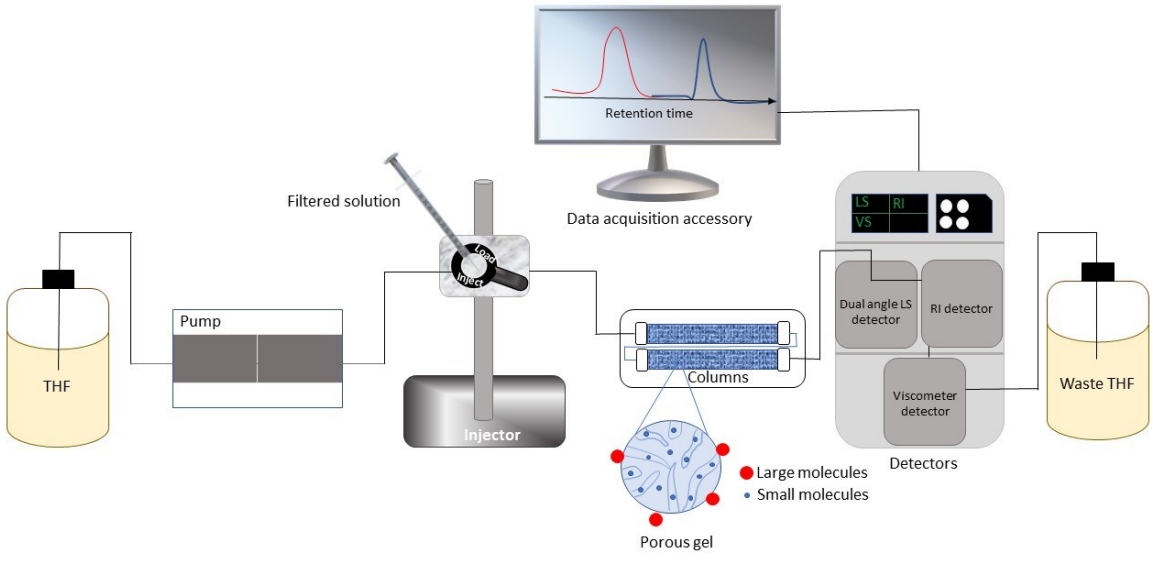

Figure 1-3. Diagram of gel permeation chromatography (GPC) equipment used in this study.

Smaller molecules (marked in blue) can diffuse deeply into more pores and as a result of spending more time in pores, elute from the GPC column after larger molecules. Based on this principle, polymers will be separated based on their molecular size and show different elution times from the column [72,73]. For every GPC system regardless of analysis methods (Conventional calibration, universal calibration, or triple detection), standards with narrow size distribution are used to determine instrument constants and detector offsets. In our studies, the GPC instrument was calibrated with a set of polystyrene standards covering a molecular weight range of 160-200,000 g/mol. The GPC Agilent 1260 Infinity is equipped with RI, viscometer, and light scattering detector to offer not only precise data, but also information that is only available in case of multiple detector combinations. The RI detector can measure sample concentration or refractive index increment (dn/dc) based on Eq.1-1, while n_0 is the refractive index of the solvent.

The dual-angle light scattering detector is used to measure the absolute molecular weight of polymers independent of any standard calibration. Light scatter detector works based on the fact that the light from the incident beam hit some molecules in the sample and cause light scattering. The key point is that the intensity of the scattered light is directly related to the molecular weight of molecules (M_w) in the sample based on the Rayleigh equation (Eq.1-2). At angle 0 and low concentration (A_2 is negligible), the Rayleigh equation is simplified to Eq.1-3 [74,75].

$$RI_{area} = \frac{RI_{cal}}{n_0} . \frac{dn}{dc} = \text{Conc}_{\text{sample}} . V_{\text{inj}} \qquad \text{Eq.1-1}$$

$$\frac{K_{opt} . C}{R_\Theta} = \frac{1}{M_w . P_\Theta} + 2A_2 . c \qquad \text{Eq.1-2}$$

$$R_\Theta = K_{opt} .c. M_w \qquad \text{Eq. 1-3}$$

K_{opt}: optical constant for polarized light.
c: concentration of the sample.
R_Θ: R_θ is the excess Rayleigh scattering ratio of the solution above that of the pure solvent, measured at angle θ.
P_Θ: particle scattering function or angular dissymmetry.
A_2: second virial coefficient- related to the sample/solvent interaction.

The viscometer detector provides the valuable property of polymers which is viscosity (η). The combination of a viscometer detector with a light scatter detector can provide high-value information on samples such as hydrodynamic size, branching, and conformation of polymers. The theory behind the viscometer detector is the solution containing dissolved macromolecules would be more viscose compared to the solvent and it causes pressure differential in 4 capillaries of viscometer (Figure 1-4). The DP is equal to the difference between the pressure drop of R_3 and R_4 and IP is integral pressure. whenever the sample flows through R_1, R_2, and R_3 the delay column passes solvent to R_4, then the viscosity calculates based on the below equation:

$$\eta = \frac{4DP}{IP-2DP} \qquad \text{Eq. 1-4}$$

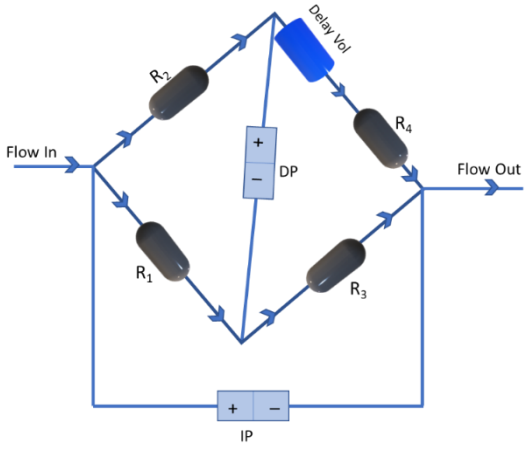

Figure 1-4. The capillary bridge used in viscometer

1.2.2 Nuclear Magnetic Resonance (NMR) spectroscopy

Nuclear Magnetic Resonance (NMR) spectroscopy is one of the most powerful, sensitive, and versatile techniques based on the magnetic properties of specific nuclei. The NMR was commercialized in the 1950s and quickly became a crucial tool for chemical research. When molecules are placed in a strong magnetic field, the nuclei of some atoms behave like a magnet and by applying the radio frequency waves, the nuclei will resonate at their specific frequency. These resonant frequencies are then measured and converted into an NMR spectrum. The NMR spectrum is a plot of the intensity of absorption (or emission) on the vertical axis versus frequency on the horizontal axis. In the NMR, the position of lines shown in "part per million" (ppm) using the chemical shift scale, then the position of the NMR peaks becomes independent of the field strength. The chemical shift scale is set up by agreeing to the reference compound and using the below equation while υ is the frequency of the NMR line and υ_{ref} is the frequency of reference compound [76].

$$\delta(ppm) = 10^6 \times \frac{\upsilon - \upsilon_{ref}}{\upsilon_{ref}}$$

The effective magnetic field can also be affected by the orientation of neighboring nuclei. This effect is known as a spin-spin coupling which can cause the splitting of the signal into two or more lines.

NMR can be applied to liquid and/or solid material for the characterization of polymer hydrogels, determination of the mechanism of gelation, and self-assembly of polymer network [77,78]. In this work, we used Bruker Avance III HD 600 MHz spectrometer to look over some polymer characteristics like the degree of polymerization (DP), a number average molecular weight (M_n), and the percentage of debenzylation for block copolymers under study. Figure 1-5 depicts the ^1H

NMR spectrum of PBCL-PEG-PBCL block copolymer in $CDCL_3$ and peak assignments. The DP and M_n of block copolymers were calculated by comparing the area under the peak of methylene protons of the PEG block (CH_2CH_2O-, δ=3.65 ppm) to the methylene protons of the PBCL backbone (-OCH_2-, δ= 4.1 ppm).

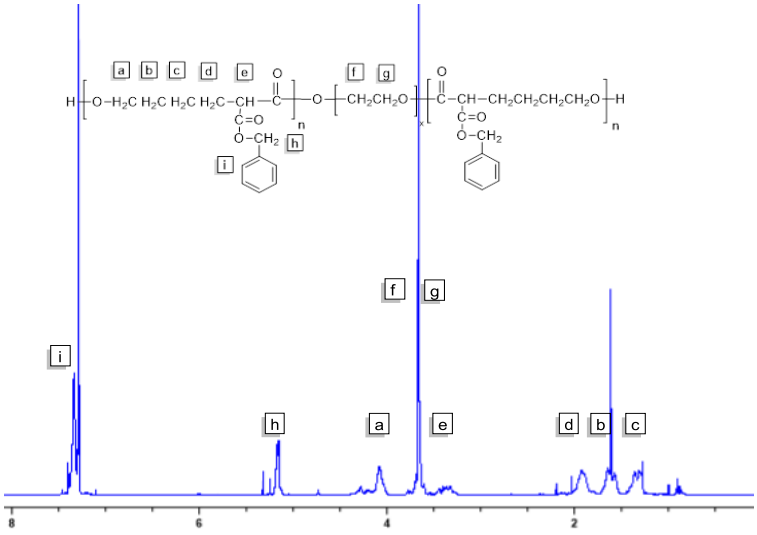

Figure 1-5. ^1H NMR spectrum of PBCL-PEG-PBCL block copolymers in $CDCl_3$ and peak assignments.

1.3 Characterization and aqueous solution behavior of triblock copolymers

Evolution of gel formation, determination of sol-gel transition, and viscoelastic properties of an aqueous solution of copolymers as a function of temperature captured in small amplitude oscillatory shear rheology and vial inversion tests. This section briefly described the methods and parameters used to investigate the thermo-responsive behavior of polymer solutions.

1.3.1 Vial inversion or inverse flow method

The vial inversion or inverse flow method is a traditional way employed to examine the successful formation of the hydrogel. In this method vial containing polymer solution was equilibrated at 4°C overnight, then the vial was immersed in a water bath. The temperature of the water bath increased gradually from 10 to 50°C. The vials containing the above samples were equilibrated for 15 min at each temperature. If the liquid inside the vial did not flow for the first 30 seconds, the sample was regarded as a gel.

1.3.2 Using Rheology to characterize viscoelastic properties of polymer solutions

The term "Rheology" was defined in 1929 by Professor Bingham of Lafayette college as the *study of the deformation and flow of matter* [79]. In other words, rheology explains the relationship between the stress (amount of force applied to a given area of the sample) and strain (deformation). The ratio of stress to strain gives key information about the properties of materials. In 1868, Maxwell defined the mechanical model that described elastic deformation with a spring (Hook's law) and viscoelastic deformation by dashpot (Newton's law) for the viscoelastic liquids. In 1928, Voigt proposed a parallel arrangement of spring and dashpot for the viscoelastic solid. A viscose material can be modeled by dashpot as shown in Figure 1-6 A. when stress or force is applied to an ideal viscous material, it starts to deform until the stress is removed. The required energy for deformation dissipated within the fluid mostly as heat. In this case, the ratio of stress to the rate of strain defines as viscosity (η). On the other hand, the ideal elastic material like spring (Figure 1-6 C) deforms proportionally to the given stress as long as the elastic limit is not exceeded and will return to the initial shape whenever stress is removed. In this case ratio of stress to strain to define as elastic modulus (G). Majority of the materials are both viscous and elastic and classified as a viscoelastic material. Therefore, it is possible to combine spring and dashpot in series, which is

called the Maxwell model representative of viscoelastic liquids. A viscoelastic solid material can be shown by the Kelvin-Voigt model that combined spring and dashpot in parallel (Figure 1-6 B) [80,81]. The most common method for measuring the viscosity and viscoelasticity properties of fluids, semi-solids, and solid materials is using a rheometer. In this study, we used Discovery Hybrid Rheometer (DHR) in parallel plate geometry for measuring the viscoelastic properties of polymer solutions in water.

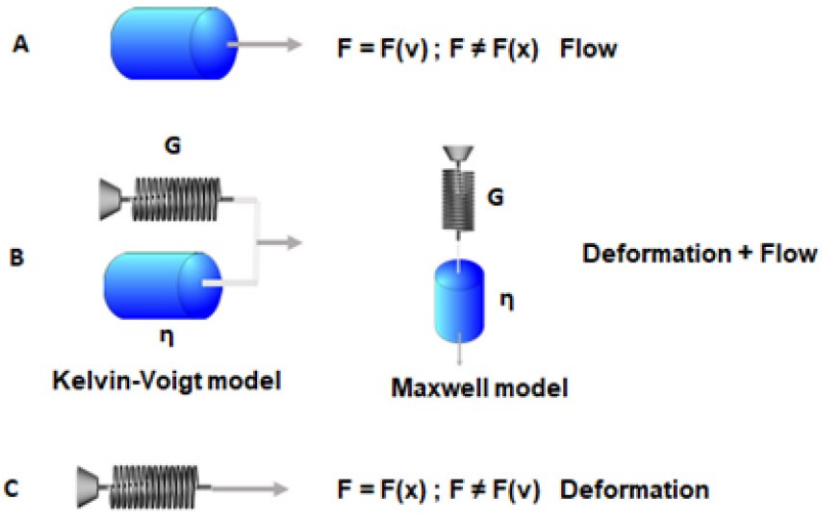

Figure 1-6. Represent of **A:** An ideal liquid (dashpot), **B:** Maxwell model to describe a simple viscoelastic liquid and Kelvin-Voigt model for a simple viscoelastic solid, **C:** An ideal solid (spring)

DHR uses controlled stress measurement, an oscillatory torque (the force that rotates material) applied to the upper plate and the resultant deformation is measured. The ratio of the applied complex stress to the measured complex strain gives the complex modulus (G^*) and the phase lag between the deformation and torque is shown by phase angle (δ). If the material is an ideal elastic, stress and strain are in phase and $\delta=0^{\circ}$, while for purely viscous materials, stress and strain are out

of phase and show δ value of 90°. For the viscoelastic material $0^{\circ} < \delta < 90^{\circ}$ and $\delta = 45^{\circ}$ represent the boundary between the viscous and elastic behavior of polymers.

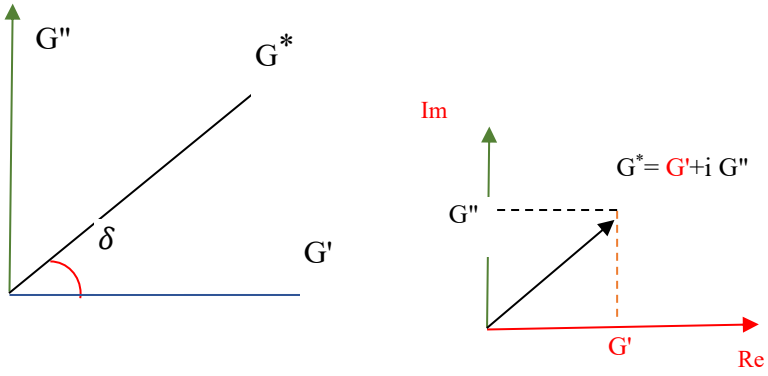

$$G' = G^{*}\cos\delta \qquad \text{Eq. 1-5}$$

$$G'' = G^{*}\sin\delta \qquad \text{Eq. 1-6}$$

$$G^{*} = \sqrt{(G'^{2} + G''^{2})} \qquad \text{Eq. 1-7}$$

$$\tan\delta = G''/G' \qquad \text{Eq. 1-8}$$

Figure 1- 7. Relationship between G', G"and G*

Despite several theories and a large number of published experimental methods to determine gel point, still, there is debate regarding the best way to measure sol-gel transition temperature for different polymer systems.

In 1986, Winter and Chambon focused on the polymerization of polydimethylsiloxane (PDMS) and tried to define a model for the gel point (Winter-Chambon criteria). They observed a power-law behavior between modulus (G' and G") and measurable frequency domain (Eq. 1-9 and Eq. 1-10). Based on Eq. 1-11, in the particular case when n=1/2, G'= G" and the gel point can easily measure at a single frequency. This simplification of the formula is so useful for some irreversible gels where the frequency remains constant during experimental runs [82,83].

$$G'(\omega) \approx \omega^{n} \qquad 0 < \omega < \infty \qquad \text{Eq. 1-9}$$

$$G''(\omega) \approx \omega^{n} \qquad 0 < \omega < \infty \qquad \text{Eq. 1-10}$$

$$G'(\omega) = \frac{G''(\omega)}{\tan n\pi/2} = \frac{G''(\omega)}{\tan\delta} \qquad \text{Eq. 1-11}$$

1.4 Dynamic light scattering (DLS) measurements of self-assembly of copolymers

Dynamic light scattering (DLS), also known as photon correlation spectroscopy (PCS) is a non-invasive technique for measuring the size of particles and molecules in suspension. DLS is a useful technique with numerous applications in science and industry [84–88]. In 1845, George stokes found that friction between moving particles is proportional to its radius and solvent viscosity. Later (1905), Einstein established the brownian motion theory (random movement of particles due to the bombardment by the solvent which quantifies by translational diffusion coefficient (D)) and the Stokes-Einstein equation which relate the diffusion coefficient (D) of the particle to its hydrodynamic radius (Rh) and viscosity of medium (η) according to Eq. 1-12 where KB is Boltzman coefficient (1.380 × 10-23 kg.m2.s-2. K-1) and T is the absolute temperature [88].

$$D = \frac{K_B T}{6\pi\eta R_h} \qquad \text{Eq. 1-12}$$

Based on the Stokes-Einstein equation DLS can measure the hydrodynamic radius of particles or molecules which is the radius of a hard sphere that diffuses at the same speed as the particle being measured.

The self-assembly of copolymers under study was determined using MALVERN Nano-ZS90 ZETA-SIZER (Malvern Instruments Ltd, Malvern, UK) equipped with laser at a wavelength of 633 nm using intensity function.

1.5. Differential Scanning Calorimetry (DSC)

Differential Scanning Calorimetry (DSC), is a powerful technique that has contributed significantly to understanding the thermodynamic properties of the solid, liquid, powder, and film samples for different applications such as food, drug, and polymer industry [89].

The traditional DSC analyzes the thermal behaviour of samples by measuring the difference in heat flow between a sample and inert reference as both are subjected to a linear change in temperature [90]. The Modulated DSC was commercialized in 1992 and could overcome most of the limitations of traditional DSC such as measurement of heat flow and heat capacity in an experiment. Modulated DSC increased resolution, and sensitivity, and ability to determine transitions of samples more accurately.

The DSC or MDSC can calculate total heat flow based on the bellow equation

$$dH/dt = Cp\ dT/dt + f(T,t) \qquad \text{Eq. 1-13}$$

Where Cp is the heat capacity of the sample, and dT/dt is the rate of temperature changes. T is the absolute temperature and f (T.t) is a function of time and temperature expressing the calorimetric response of the chemical or physical reaction [91].

Determination of sol-gel transition for thermo-responsive hydrogels is one of the applications of MDSC which appears in the thermograms as an endothermic peak.

1.5. Research proposal

1.5.1. Central hypothesis

This thesis examined the central hypothesis that polymerization method, molecular weight distribution, chemical or physical cross-linking, and hydrophilic-lipophilic balance can affect the thermo-gelation of triblock copolymers based on PEG and functionalized PCL.

1.5.2. Rationale

Thermo-sensitive hydrogels based on PCL and PEG attracted considerable attention for biomedical applications specially in the drug delivery field due to their biodegradability, biocompatibility, and relative hydrophobicity [92]. Compared to other PEG/polyester thermo-gels such as PLGA-PEG-PLGA (ReGel®), PEG/PCL block copolymer has slow degradation. This is dues to the high crystallinity and hydrophobicity of the PCL segment. However, this extremely slow degradation and high crystallinity may not be desirable in specific applications [93]. Furthermore, the lack of functional groups in PCL structure reduced the capacity of PEG/PCL hydrogels to incorporate drugs with having hydrophilic functional groups. Therefore, through using conventional PEG/PCL hydrogel, it might be difficult to achieve target drug concentrations incorporated into the gel or achieve slow drug release for such chemical entities.

Our research group has previously reported on the synthesis of amphiphilic triblock copolymers based on PEG and functionalized PCL (α-benzyl carboxylate-ε-caprolactone) (PBCL), as the hydrophobic lateral blocks (abbreviated as PBCL-PEG-PBCL) using bulk ring opening polymerization [94,95]. The synthetic process developed for the triblock copolymer in our lab was found not to produce polymers capable of forming thermogels at aqueous media in a consistent manner feasible for large-scale production. Therefore, the objective of the present research was

to develop a reproducible and scalable process for the preparation of temperature-responsive gel forming triblock copolymers based on PEG and functionalized PCL.

In the first step, we tried to modify the method of polymerization for the synthesis of PBCL-PEG-PBCL copolymer and focus on the identifying a polymerization method that can lead to the production of PBCL-PEG-PBCL thermogels. Thus, we defined for the first-time the effect of molecular weight distribution of amphiphilic PBCL-PEG-PBCL block copolymer on their temperature-induced sol-gel transition in water. This step was very crucial since the results provided an understanding of the polymer characteristics that can affect thermo-responsive gelation and viscoelastic properties of PBCL-PEG-PBCL solutions in water. The results of this study identified a role for a higher than expected molecular weight population in the synthesized copolymers, for the formation of thermogels in water from PBCL-PEG-PBCL. The formation of this high molecular weight population was attributed to partial cross-linking of the polymer by PEG or impurities of the monomer in the ROP reaction.

In the second step, to test the above hypothesis, we attempted to manually introduce different chemical cross-linkers to PBCL-PEG-PBCLs prepared using ring opening polymerization of purified monomer by PEG. The data in this chapter confirmed formation of thermogels from PBCL-PEG-PBCL polymers that were partially cross-linked with PEG 400.

In the third step, we identified the effect of hydrophilic lipophilic balance in partially debenzylated and cross-linked PBCL-PEG-PBCLs, on the formation of thermogels. Finally, we explored the ability of PEG/BCL copolymer for encapsulation in liposomes as a new promising nano-platform in drug delivery.

1.5.3. Specific objectives

1. To assess the effect of polymerization method (bulk versus solution), and polymerization time on the characteristics of PBCL-PEG-PBCL copolymers and their temperature-responsive sol-gel transition.

2. To study the effect of different cross-linkers (PEG 400, polycaprolactone triol, and trimethylolpropane ethoxylate) on the formation of partially cross-linked PBCl-PEG-PBCL co-polymers prepared by bulk and solution polymerization and assess the thermo-reversible gelation of the products.

3. To investigate the effect of benzyl carboxylate reduction on carboxyl group in partially cross-linked PBCL-PEG-PBCL copolymers synthesized by bulk or solution polymerization on their thermo-reversible gelation.

4. To synthesize and characterize PCB(CL-DOX)-PEG-PCB(CL-DOX) incorporated liposome (or liposcells) as a novel DDS and assess the morphology of the prepared systems through cryogenic electron microscopy.

Chapter 2. The defining role of a high molecular weight population in block copolymers based on poly (α-benzyl carboxylate-ε-caprolactone) and poly (ethylene glycol) on the formation of thermo-reversible hydrogels

The content of this chapter was published in :

Journal of **ACS Applied polymer materials**

2.1 Introduction

Thermo-gelling polymers, i.e., those forming aqueous colloidal dispersions or sol at low temperatures, but turning to gel at higher temperatures, have been the focus of much interest in biomedical fields [96,97], particularly for drug delivery [5,73–77], tissue engineering [32,98–100] and other medical applications [101–103]. In this context, polyester-based thermo-gels are very attractive biomaterials, because of their biodegradability under physiological conditions and biocompatibility of their degradation products [104]. Polyesters such as block copolymers of poly(D, L-lactide-co-glycolide)-*b*-poly(ethylene glycol)-*b*-poly(D,L-lactide-co-glycolide) (PLGA-PEG-PLGA), known as ReGel® [105], and poly(ε-caprolactone)-b-poly(ethylene glycol)-b-poly(ε-caprolactone) (PCL-PEG-PCL) are reported to exhibit reversible sol-gel transition around physiological temperature in aqueous media [13].

Despite the development of several thermo-gelling polyester-based biomaterials, prior reports on polymeric characteristics that can affect their thermo-responsive gelation and their viscoelastic properties are scarce in the literature [106–109]. Nevertheless, a role for the chemical structure [110,111], molecular weight, molecular weight distribution [112,113] (MWD), and hydrophilic/hydrophobic block length [114–116] of PEG-poly(ester) block copolymers on their thermo-gelling behavior is implicated. One of the few studies on this subject has been conducted by Ding *et al* who examined the influence of molar-mass dispersity ($Đ_M$) of ReGel®, on its sol-gel transition temperature (T_{gel}) in aqueous media. They found a positive correlation between $Đ_M$ and the transition temperature of ReGel®, irrespective of the average molecular weight of the PLGA-PEG-PLGA polymers [113,117]. However, the source of an increase in the $Đ_M$ of the polymer or processing conditions that can

affect the $Đ_M$ and, in turn, control the thermo-responsive sol-gel transition of ReGel® has not been clarified [118,119].

Our research group has previously reported on the synthesis of biodegradable triblock copolymers based on PEG, as the hydrophilic middle block, and poly(α-benzyl carboxylate-ε-caprolactone) (PBCL), as the hydrophobic lateral blocks (abbreviated as PBCL-PEG-PBCL) using bulk ring-opening polymerization [94,95,120]. The objective of the current research was to investigate the synthesis conditions and/or polymer characteristics that can lead to the production of thermo-gelling PBCL-PEG-PBCLs with enhanced viscoelastic properties. In this context, using a fixed monomer to initiator molar ratio (α-benzyl carboxylate-e-caprolactone (BCL) to PEG ratio) we first assessed the effect of polymerization time in bulk versus solution ring-opening polymerization, on the characteristics of the synthesized PBCL-PEG-PBCL block copolymers. The properties that were evaluated included the average molecular weights, molar-mass dispersity $Đ_{M,}$ and intrinsic viscosity of prepared polymers. In the second step, the thermo-responsive self-assembly, gelation, and rheology of block copolymer solutions in aqueous media were investigated. Our results revealed that the formation of thermo-reversible PBCL-PEG-PBCL hydrogels is dependent on the existence of a polymer population with a higher-than-expected molecular weight at around 40 % molar concentration of the block copolymer sample, irrespective of the polymerization method. Solution polymerization enabled better control over the weight percentage of this high molecular weight population of PBCL-PEG-PBCL, under current synthesis conditions. Partial cross-linking and/or branching of PBCL-PEG-PBCL under current synthesis conditions was implicated as a potential reason for the formation of this high molecular weight population.

2.2 Experimental section

2.2.1 Materials

α-Benzyl carboxylate-ε-caprolactone (BCL) was synthesized by Alberta Research Chemicals Inc (ARCI), Edmonton, Canada, based on a previous report by our group [121]. Biphenyl (≥99%) and dihydroxy poly(ethylene glycol) (PEG) (Mw = 1450) were purchased from Sigma-Aldrich (St. Louis, MO). Solvents such as tetrahydrofuran, dichloromethane, and hexane were chemical reagent grade and purchased from Sigma-Aldrich (St. Louis, MO).

2.2.2 Synthesis of triblock copolymers

Ring-opening polymerization of cyclic esters such as lactide, glycolide, or ε-caprolactone in the presence of PEG as the initiator is a commonly used method for the synthesis of poly(esters)-PEG-poly(ester) block copolymers. In this reaction, several types of metal catalysts such as aluminum alkoxides, zinc butoxides, and most commonly tin(II) 2-ethyl hexanoate (Sn(Oct)2) is used [52,122–125]. Here, polymerization of PBCL-PEG-PBCL copolymers was performed by ring-opening polymerization of BCL by dihydroxy poly(ethylene glycol) (PEG) as initiator using bulk and solution polymerization. Synthesis of PBCL-PEG-PBCL has been described in our previous publication [95]. In the current study, polymerization was accomplished in the absence of any catalyst to limit the rapid PBCL chain growth and keep the degree of polymerization of PBCL low. In brief, 0.6 g of monomer (BCL) and 0.19 g PEG were dehydrated at 70°C under vacuum for 3 h, then added to an ampule and sealed under vacuum. In solution polymerization, biphenyl (30%wt of monomer) was mixed with other ingredients, then the ampule was sealed under vacuum. The

polymerization reaction was carried out at 160℃ for 15-25 h according to the preassigned conditions summarized in Table 2.1. The polymerization was quenched by cooling down the reaction container to ambient temperature. Prepared triblock copolymers were then purified by dissolving in tetrahydrofuran (THF), followed by precipitation using anhydrous ethyl ether and the supernatant decantation. The product was dried under a vacuum for 24 h.

2.2.3. Characterization of synthesized triblock copolymers

Purified polymers were dissolved in $CDCl_3$ at a concentration of 5 mg/mL. ^1H NMR spectra of copolymers acquired by Bruker 600 MHz NMR were used to calculate the degree of polymerization (DP) of caprolactone blocks and then the number of average molecular weight (Mn) of copolymers. The DP of caprolactone blocks was calculated by comparing the area under the peaks of methylene protons of the PEG block (CH_2CH_2O-, δ=3.65 ppm) to the methylene protons of the PBCL backbone (-OCH_2-, δ= 4.1 ppm). The M_n of the PEG block was considered 1450 g/mol for these calculations (Figure S2-1).

Retention time, average molecular weights (MW), molar-mass dispersity ($Đ_M$), intrinsic viscosity (η), and conformation of prepared block copolymers were estimated by gel permeation chromatography (GPC) (Agilent 1260 infinity with refractive index, light scatter, and viscometer detectors) equipped with 2 columns (Styragel HR2 and Styragel HR 4E from Waters). The instrument was calibrated with a set of polystyrene standards with molecular weights ranging from 160 to 200,000 g/mol. Polymer samples (5-10 mg/mL) were dissolved in THF (HPLC grade) and filtered with a nylon syringe filter (pore size: 0.45 μm). Then 200 μL of samples were injected into GPC which was operated at a THF flow rate of 0.7 mL/min at 35 °C. The elution time for all

polymers was 30 min. During this time, the GPC chromatogram came back to the baseline but for clarity of presentation, elution time was selected from 14-24 min in all GPC graphs.

2.2.4. Phase diagram or inverse flow method

The sol-gel transition of block copolymers under study in water was examined by the inverse flow method at a polymer concentration of 15 % (w/w). Each vial contained 1 mL of copolymer solution and all samples were equilibrated at 4 °C overnight before measurement. Vials were immersed in a water bath at 30°C and equilibrated for 15 min. If the vial content did not flow for at least 30 s in an inverted position, the sample was considered a gel.

2.2.5. Dynamic Rheological Measurements

The viscoelastic behavior of the hydrogels at a concentration of 15 % as a function of a rise in temperature between 10-50 °C was investigated by Discovery Hybrid Rheometer (TA instruments) in parallel plate geometry and auto gap set mechanism with a heating rate of 1 °C/min, and angular frequency (ω) 10 rad/s. The viscosity, storage, and loss modulus of the copolymer solutions were measured as a function of temperature.

2.2.6. Characterization of thermo-responsive self-assembly of PBCL-PEG-PBCL

The block copolymer samples (10 mg) were dissolved in 1 mL of acetone, then 10 mL of distilled water was added to this solution dropwise. The mixture was stirred for 24 hours at room temperature to evaporate the acetone and reach a final polymer concentration of 1 mg/mL. The size of aggregates (intensity Z-average) as a function of a rise in temperature between 10-50 °C was measured using MALVERN Nano-ZS90 ZETA-SIZER with a laser beam at a wavelength of 633 nm. The scattered light was detected at an angle of 173°. The heating rate was 1 °C/min.

2.2.7. Statistical analysis

The results are reported as average ± standard deviation (SD) of three independent measurements on a single batch of polymer unless mentioned otherwise. The statistical analysis was processed using GraphPad Prism software, version 8.3.1 (GraphPad Software Inc., La Jolla, CA, USA). The significance of differences between results was assessed by one-way ANOVA analysis followed by Sidak's multiple comparison test where $\alpha=0.05$ was set as the level of significance.

2.3. Results

2.3.1. Synthesis and characterization of triblock copolymers

Block copolymers of PBCL-PEG-PBCL were synthesized by ring-opening polymerization of BCL initiated by dihydroxy PEG without any catalyst using two methods of bulk and solution polymerization at different polymerization times (15-17.5 hours for bulk and 17-25 h for solution polymerization) as summarized in Table 2-1. The reaction times were chosen based on our pilot studies that have shown relatively similar DP for the PBCL segment (based on ^{1}H NMR data), for the polymers produced by the two methods of polymerization at the corresponding reaction times. The scheme for the synthesis of PBCL-PEG-PBCL triblock copolymers is shown in figure 2-1.

To optimize the solution polymerization of BCL with dihydroxy PEG using biphenyl as a solvent, different quantities of biphenyl were used in the polymerization reaction while other parameters such as the ratio of BCL to PEG and reaction temperature were kept constant. Optimum yield and degree of polymerization were achieved at a biphenyl concentration of 30 wt% of the monomer (data not shown). Therefore, 30 wt% biphenyl was selected to prepare triblock copolymers through solution polymerization in further studies.

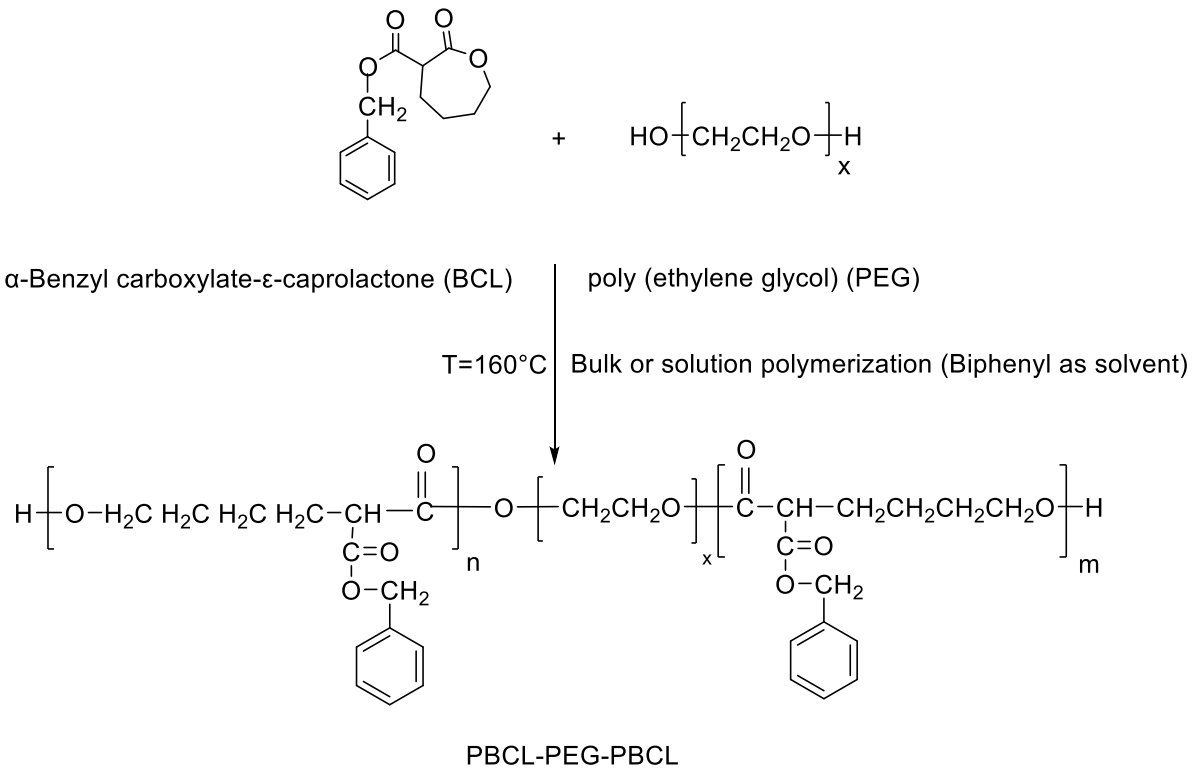

Figure 2-1. Scheme for the synthesis of PBCL-PEG-PBCL triblock copolymers by bulk and solution polymerization. n,m= 1-18, x= 33

2.3.1.1. The effect of polymerization time on the average molecular weights and molecular weight distribution of block copolymers prepared by bulk versus solution polymerization.

Characteristics of prepared polymers are summarized in Table 2-1. In general, the yield of reaction for solution polymerization was significantly higher than the bulk method in this study. The polymerization time also showed a positive correlation with the DP of prepared block copolymers, irrespective of the method of polymerization (Table 2-1).

Table 2-1.Characteristics of synthesized PBCL-PEG-PBCL triblock copolymers (theoretical MW of copolymers was 6030 g/mol) (n=3).

Sample[1]	Polymerization Time (h)	DP [2]	M_n [3] (Da)	M_n [4] (Da)	$\frac{Mn(GPC)}{Mn(NMR)}$	Yield (%)	Appearance in water at 30°C
B_{15}	15	10.4±0.30 [a]	4080±85	5300±85	1.3	79±6	sol
$B_{16.5}$	16.5	11.3±0.40 [a]	4270±100	9900±1500	2.3	78±2	sol
B_{17}	17	13.6±0.45 [b]	4880±275	55000±9000	11.3	74±10	gel
$B_{17.5}$	17.5	N/A	N/A	N/A	N/A	N/A	insoluble
S_{17}	17	11.2±0.30 [a]	4200±75	6500±570	1.5	90±5	sol
S_{21}	21	12.5±0.20 [c]	4500±56	13000±530	2.9	93±3	sol
S_{23}	23	12.8±0.20 [bc]	4600±45	31000±10600	6.7	89±6	gel
S_{25}	25	N/A	N/A	N/A	N/A	N/A	insoluble

[1] B stands for Bulk polymerization and S stands for solution polymerization. The number in the subscript shows the reaction time in hours.
[2] Degree of polymerization (DP) of PBCL block measured by ^{1}H NMR.
[3] Number average molecular weight of block copolymers measured by ^{1}H NMR.
[4] Number average molecular weight of block copolymers measured by GPC.
The same superscript letters indicate no statistical significance while different letters mean statistical difference at $P<0.05$.

Using bulk polymerization, increasing the polymerization time from 15 to 17 hours led to a drastic increase in the DP of the PBCL block from 10.4 to 13.6 (approximately 3 units), on average. However, in solution polymerization, the change was more gradual, i.e., a 6 h increase in reaction time (from 17 to 23 h) was needed for a 2-unit increase in the average DP of the PBCL block (Figure 2-2A). A similar trend was observed for M_n based on ^{1}H NMR and GPC (Figure 2-2B & C), indicating a more gradual increase in polymer chain growth enabling better control over polymerization degree in the solution versus bulk polymerization. The M_n(GPC)/M_n(NMR) ratios were always above 1, irrespective of the polymerization method, and elevated with an increase in reaction time. Moreover, the time-dependent increase in M_n(GPC)/M_n(NMR) ratios was more gradual for polymers prepared by solution polymerization (Figure 2-2D). For polymers prepared

by bulk polymerization at 15, 16.5, and 17 h reaction times, the M_n measured by GPC were 1.3, 2.3, and 11.3-fold higher than those from NMR, respectively (Table 2-1, Figure 2-2D). For polymers prepared by solution polymerization at 17, 21, and 23 h polymerization time, the M_ns measured by GPC were 1.5, 2.9, and 6.7-fold higher than the M_ns measured by NMR.

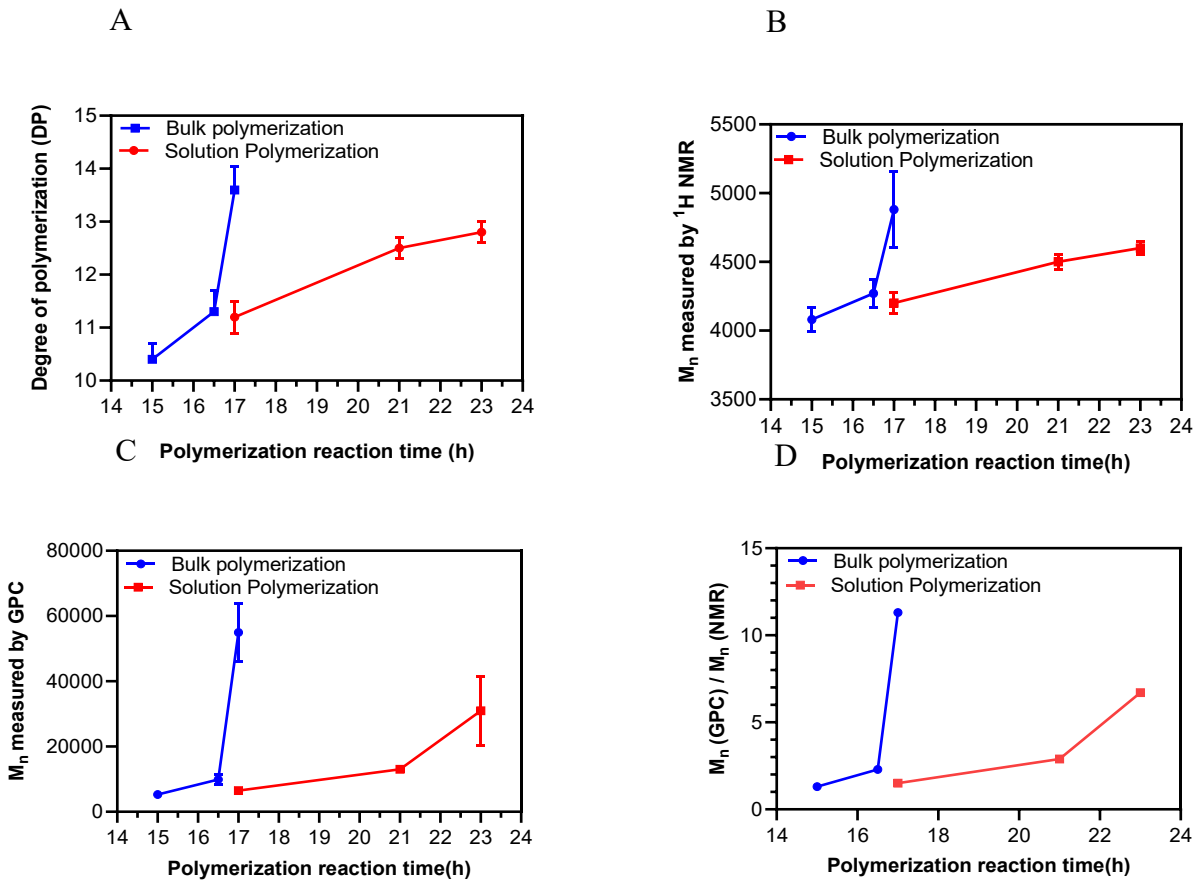

Figure 2-2. The effect of polymerization times on the **A)** Degree of polymerization; **B)** M_n as measured by ^{1}H NMR; **C)** M_n measured by GPC; and **D)** M_n(GPC)/M_n(NMR) for bulk and solution polymerization reactions.

The GPC elution profiles of block copolymers that could form soluble samples in THF are shown in Figures 2-3A and B. The extracted data from GPC is summarized in Table 2-2. Irrespective of the method of polymerization, increasing the reaction time, led to a decrease in the peak maximum retention time of block copolymers. This implies an elevation in the hydrodynamic volume as a

result of an increase in the molecular weight of the block copolymers. As shown in Figure 2-3C and Table 2-2, in particular, B_{17}, S_{21}, and S_{23} samples showed a distinct population of polymers with unexpectedly larger molecular weights. The calculated weight average molecular weight (M_w) for these samples were 188000, 73600, and 147900 g/mole, respectively. This was 31, 12.2, and 24.5-fold higher than the theoretical average molecular weight for these polymers, respectively.

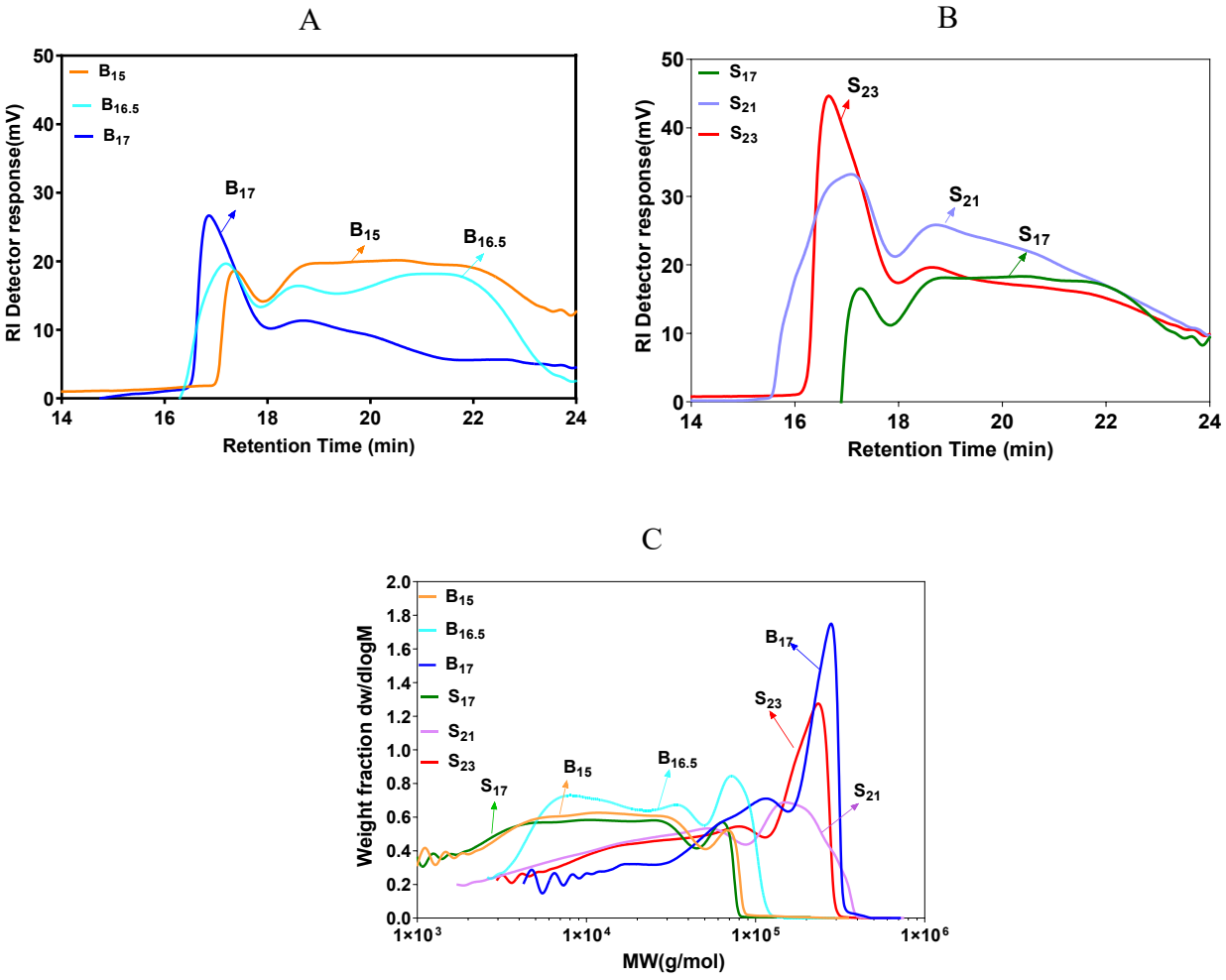

Figure 2- 3. GPC elution profile of **A)** block copolymers prepared by bulk polymerization at different reaction times, i.e., B_{15}, $B_{16.5}$, B_{17}; **B)** block copolymers prepared by solution polymerization at different reaction times, i.e., S_{17}, S_{21}, S_{23}; **C)** Molecular weight distribution of block copolymers prepared by bulk (B_{15}, $B_{16.5}$, B_{17}) and solution polymerization (S_{17}, S_{21}, S_{23}).

Table 2-2. Characteristic of triblock copolymers under study from GPC (n=3).

Sample	Peak Max Retention Time in GPC (min)	$M_w \pm SD$ [a] (g/mol)	$Đ_M \pm SD$ [b]	Intrinsic viscosity ± SD (dl/g)	K (dL/g) [c]	α [c]
B_{15}	20.4	16700±1100	3.1±0.40	0.15±0.01	0.0130	0.31
$B_{16.5}$	16.8	30500±1370	3.1±0.50	0.46±0.04	0.0110	0.38
B_{17}	16.5	188000±9000	3.4±0.24	0.48±0.10	0.0005	0.87
S_{17}	20.3	24600±4600	3.7±0.79	0.07±0.01	0.0190	0.39
S_{21}	16.8	73600±3500	5.7±0.16	0.41±0.08	0.0002	0.76
S_{23}	16.7	147900±54500	4.8±0.18	0.47±0.06	0.0002	0.87

[a] Weight average molecular weight.
[b] Molar mass dispersity (M_w/M_n) measured by GPC.
[c] Mark-Houwink parameters.

2.3.1.2. The effect of polymerization time and method on the intrinsic viscosity of prepared block copolymer populations.

Figure 2-4A and B show the intrinsic viscosity plots of polymer populations for samples under study as a function of retention time and molecular weight analyzed by GPC, respectively. The data shows the existence of a polymer population with higher-than-expected intrinsic viscosity in polymers as defined by the marked region in Figure 2-4A. Moreover, when analyzing the changes in the intrinsic viscosity versus molecular wight for polymer populations (Figure 2-4B), it is evident that the B_{17}, $S_{23,}$ and S_{21} polymers behave differently as these samples showed a particularly steeper increase in their intrinsic viscosity vs molecular weight compared to $B_{16.5}$, $B_{15,}$ and S_{17} (Figure 2-4B).

The average intrinsic viscosity and Mark Houwink constants (α and K) for each sample are also illustrated in Table 2-2. The data shows a positive but non-linear correlation between

polymerization time and α, irrespective of the polymerization method. The α value is similarly higher for the B_{17}, S_{23} and S_{21} polymers compared to $B_{16.5}$, B_{15} and S_{17}.

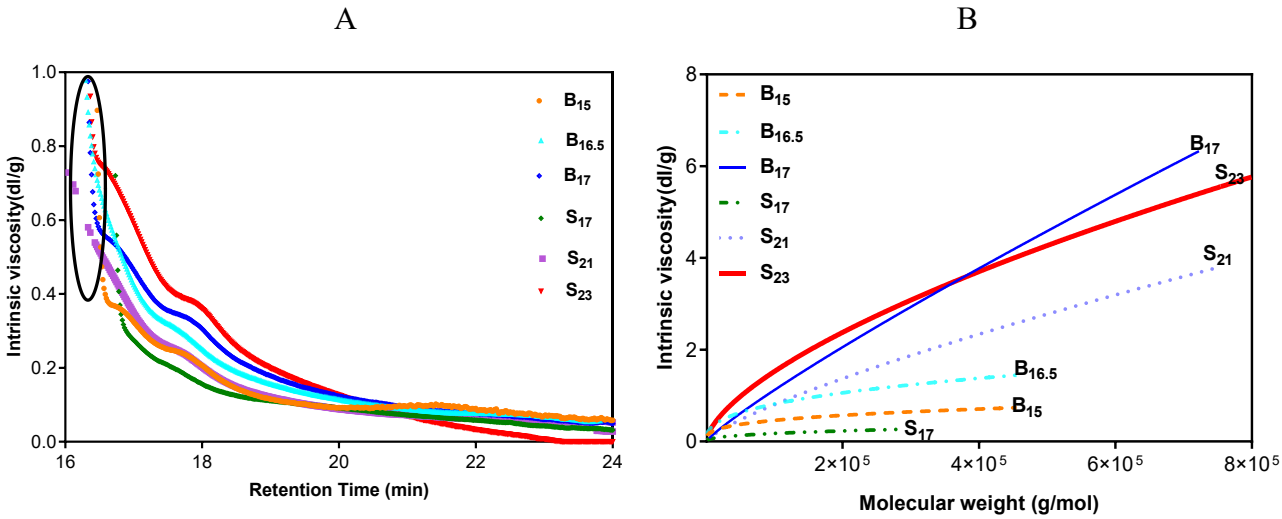

Figure 2- 4. A) An overlay of viscometer elution profiles. **B)** Double log plot of [η] vs M_w from GPC data.

2.3.2. Characterization of the aqueous solutions of prepared block copolymers

2.3.2.1. Thermo-gelation of copolymer solutions in aqueous media as measured by inverse flow method.

Thermo-gelling behaviour of copolymers under study was investigated through the inverse flow method. The $B_{17.5}$ and S_{25} copolymers were insoluble in water, thus, were not studied here. All other polymers become soluble in water at a concentration of 15 wt% at 4°C. Among the aqueous solutions of polymers under study (Table 2-1), only B_{17} and S_{23} showed gel formation at a concentration of 15 wt% at 30°C. Other samples remained soluble in water and did not form a visual gel at this concentration and temperature.

2.3.2.2. Temperature-dependent viscoelastic gelation of block copolymer aqueous solutions

The changes of storage modulus (G'), loss modulus (G"), and complex viscosity (η*) as a function of temperature for aqueous solutions of block copolymers at 15 wt% are shown in Figure 2-5. The B_{15} sample showed typical behaviour of viscoelastic liquids, where both G' and G" modulus decreased as a function of a temperature rise, while G" dominated G'. Also, the η* of these samples decreased as a function of temperature [126]. For the $B_{16.5}$ sample, the G', G" and η* showed a peak between 25-40 ° C, but G" was higher than G' indicating more viscose than elastic behaviour. The B_{17} sample, on the other hand, showed a distinct thermo-gelling behaviour with sol-to-gel transitions around 27-28 ℃, as evidenced by a cross over of the G' and G" graphs. The rise in temperature above 27-28 ℃, also led to an increase in the viscosity of B_{17} aqueous solutions. Further increase in temperature in this sample, led to a decrease in viscosity and a second cross over of the G' and G" graphs at 41 ℃.

A similar trend was observed for polymers prepared by the solution polymerization at 17, 21, and 23 h polymerization time. The S_{17} sample showed similar behaviour to that of B_{15}, representative of liquids, where both G' and G" modulus decreased with increasing temperature below 20 ° C. For this sample, a small increase in loss and storage modulus, as well as viscosity, was recorded between 17-25 °C, but G" dominated G' at all temperatures under study. The S_{21} sample showed similar behaviour to that of $B_{16.5}$, where the values of G', G" and η* showed a peak between 25-30 °C. Similar to $B_{16.5}$, the loss modulus still dominated the storage modulus in this temperature range, indicating the dominance of viscous behavior. The temperature range for the viscous transition was narrower for S_{21} compared to $B_{16.5,}$ however. Like B_{17}, the S_{23} polymer showed a true viscoelastic sol-gel transition at 27 °C, which was reflected by a cross over of G" and G'. A second cross over of the G' and G" graphs was recorded for this sample at 46 °C.

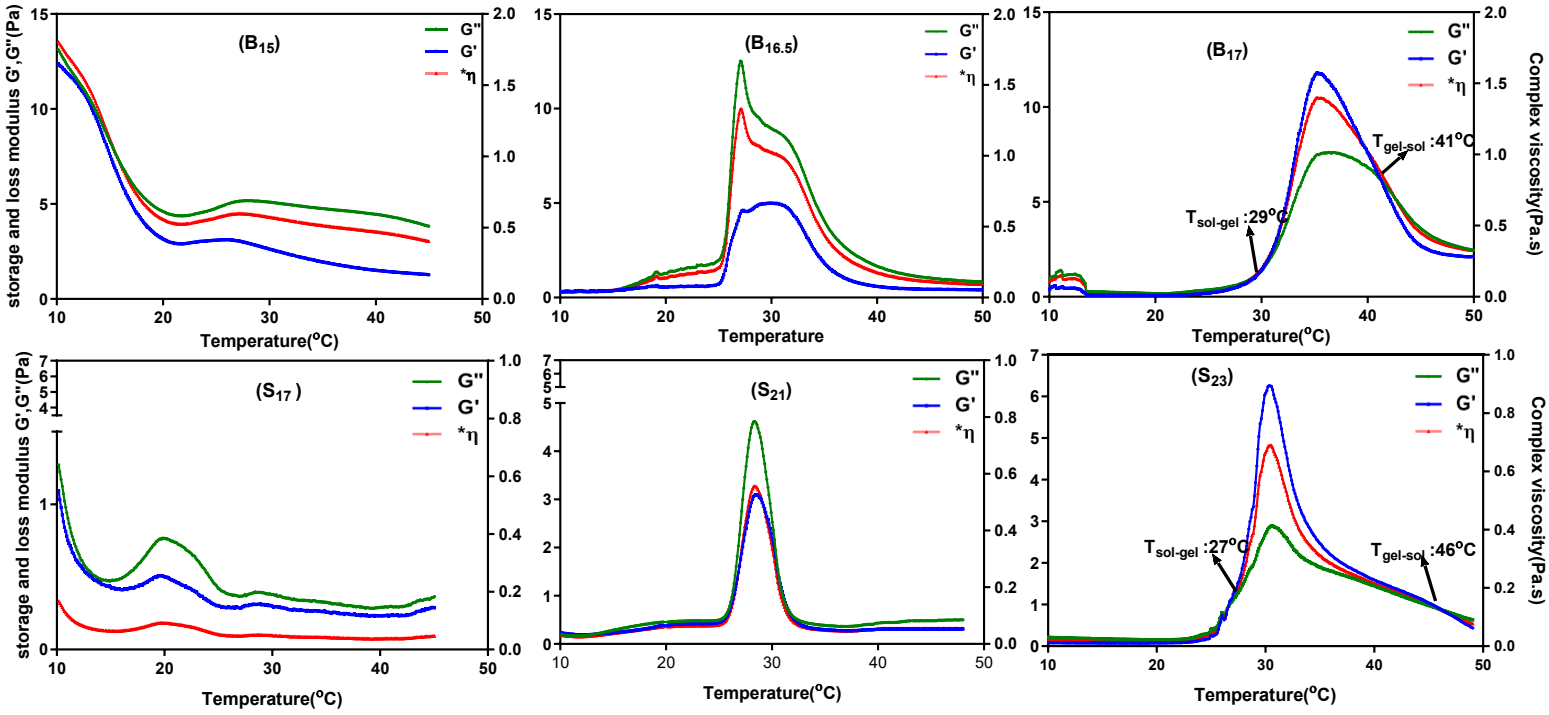

Figure 2-5. Storage modulus(G'), Loss modulus(G") and complex viscosity (η*) of hydrogels under study at 15 % w/w concentration as a function of temperature (heating rate of 1 °C/min).

2.3.2.3. Temperature-dependent self-assembly of block copolymers in aqueous solution.

Figure 2-6A shows the average size of self-assembled structures from copolymers under study at ambient temperature (25 °C) and in water. For polymers made using bulk polymerization, the average diameter of B_{15} and $B_{16.5}$ aggregates in water were similar, but aggregations assembled from B_{17} showed significantly larger sizes at room temperature. For polymers made by solution polymerization, the S_{23} polymers produced relatively larger aggregates at room temperature which were comparable to the self-assembled structures from B_{17} samples. The size of aggregates from S_{17} polymers was, on the other hand, similar to that of B_{15}.

The change in the Z average diameter of self-assembled structures from block copolymers under study (1 mg/mL) as a function of temperature (10-50℃) was assessed by DLS using Zeta Sizer Nano. As shown in Figure 2-6B, there was no significant change in the size of self-assembled structures formed by B_{15} and $B_{16.5}$ as a function of a temperature rise. The B_{17} sample on the other hand showed a significant increase in the size of its aggregates at around 20 °C (Figure 2-6B). In polymers prepared by solution polymerization, no change in the size of aggregates as a function of a temperature rise was observed for the S_{17} sample. The S_{21} sample showed a decrease in size between 10-15 °C and plateaued after. On the other hand, S_{23} showed a thermo-responsive increase in the size of its self-assembled structures between 20-25 ℃, which was similar to that observed for the B_{17} polymers.

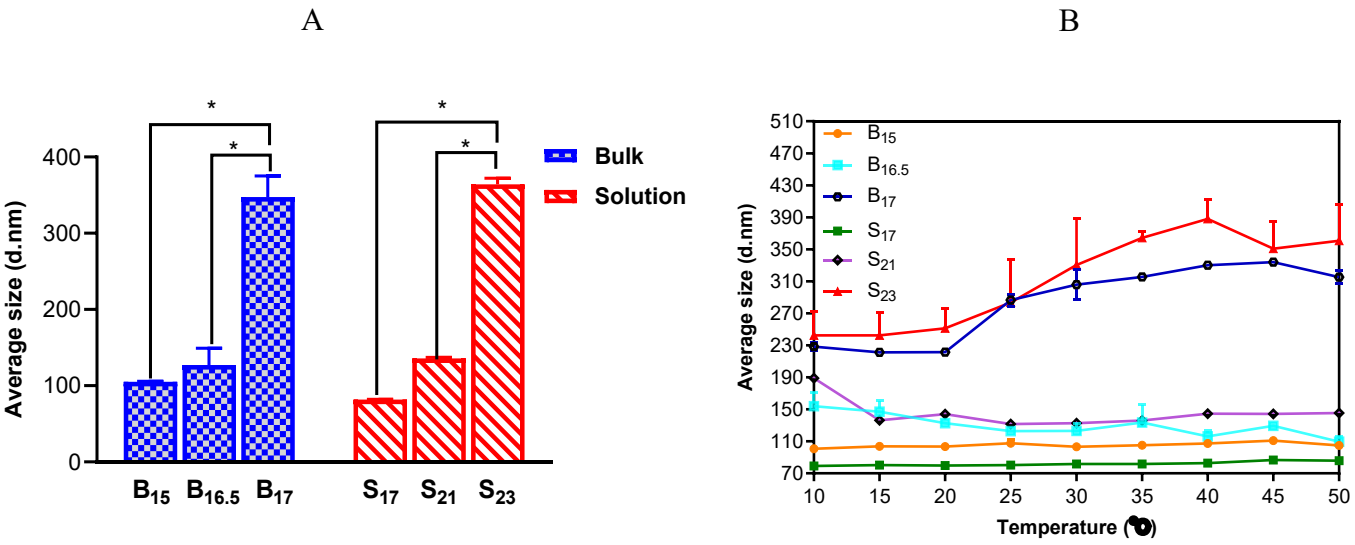

Figure 2-6. A) The effect of polymerization time and method on the size of self-assembled structures from block copolymers under study at 25℃. Results are presented as Mean ± SD (n=3). Asterisks denote significant difference at P<0.05. **B)** Change in the size of self assembled structures from block copolymers as a function of temperature at 1 mg/mL polymer concentration as measured by DLS.

4. Discussion

The development of stable, reproducible, bio-compatible, and viscoelastic thermo-reversible hydrogels is of interest in the field of depot drug delivery and tissue engineering. In the present study, we characterized block copolymers of PBCL-PEG-PBCL synthesized by solution versus bulk polymerization (Figure 2-1) in detail, to define the structural characteristics of these block copolymers that can lead to the formation of viscoelastic thermo-reversible hydrogels.

The results showed in both methods of polymerization, expanding the polymerization time, to increase the DP, $M_{n,}$ and viscosity of the products, as expected. The use of solution polymerization, on the other hand, improved the controllability and yield of the reaction when compared to bulk polymerization (Table 2-1). This was evident from the slope of increase in average DP and M_n of polymers versus time, which was less steep for solution polymerization compared to bulk polymerization (Figure 2-2). The observation was not surprising, since the solvent acts as a diluent facilitating the transfer of heat in the polymerization reaction by reducing the viscosity of the reaction mixture compared to bulk polymerization [127]. The same explanation can also be used to describe the reason for the increase in the yield of polymerization when a biphenyl was used in the reaction.

Interestingly, the GPC data confirmed the formation of a distinct polymer population with higher-than-expected molecular weight (Figure 2-3) as well as intrinsic viscosity (Figure 2-4) in all polymers under study. The proportion of this distinct population seemed to increase as a result of an increase in reaction time. Particularly, for B_{17} and S_{23} samples the proportion of this population became very noticeable and significant, at around 40 % molar concentration (Figures 2-3 and 4).

The formation of long homopolymers of PBCL during the polymerization reaction, cannot explain the distinctly high molecular weight population of block copolymer in the 10-55 KDa MW range,

as the added quantity of the monomer to achieve a theoretical MW of ~ 6 KDa is not enough to produce such large linear polymers (~30-55 KDa). The formation of a distinct and unexpectedly larger molecular weight population may be attributed to the formation of a nonlinear molecular architecture, e.g., branched and/or partially cross-linked polymer populations, in our products. The proportion of this non-linear polymer population increased as a function of an increase in the polymerization time. A higher-than-expected intrinsic viscosity for this polymer population is observed in all samples under study, as well (Figure 2-4A). The higher-than-expected intrinsic viscosity in B_{17}, $S_{21,}$ and S_{23} polymers, in particular, which coincides with a significant proportion of the large molecular weight population in these samples, may indicate the formation of partially cross-linked polymers with a distinctly larger proportion in these samples (Figure 2-4B), rather than branching [128]. In fact, above 17 h (in the bulk polymerization) and 23 h (in the solution polymerization), we observed the formation of solid and insoluble structures. This observation also confirms our explanation for the formation of partially cross-linked structures in PBCL-PEG-PBCL polymers, with particular growth in proportion in the B_{17} and S_{23} samples. Above these time points, it can be speculated that the growth of the cross-linked copolymer population passed the threshold for polymer solubility in water or organic solvents and led to the formation of insoluble polymers.

Remarkably, our further studies showed polymer samples, with at least 40 % (M/M) proportion of this high molecular wight populations (B_{17} and S_{23} samples) are in fact the ones capable of forming thermo-gelling hydrogels with enhanced viscoelastic properties (Figure 2-5). In constant angular frequency, the crossover of the loss (G") and storage (G′) moduli occurs near gel point [129]. Rheological behaviour of polymers under study showed, that only B_{17} and S_{23} can produce thermo-reversible hydrogels with a crossover of G′ over G". Based on GPC results, the same two samples

are the ones showing the highest average M_n (GPC)/M_n (NMR) ratios deviating from their theoretical molecular weights (Table 2-1) as well as the highest αs (Table 2-2). The collection of the above evidence, all points to the defining role of a higher-than-expected molecular weight population in PBCL-PEG-PBCL polymers in the formation of viscoelastic thermo-reversible hydrogels.

Our results also indicated the more gradual pace in the formation of this high molecular weight polymer population, by the solution polymerization. This is particularly indicated by a sharp change in the viscosity profiles of $B_{16.5}$ versus B_{17} samples (only 30 minutes difference in polymerization time) compared to a more gradual profile change for S_{21} and S_{23} samples (2h difference in polymerization reaction) (Figure 2-4B). In general, the solution polymerization seems to be a preferred choice for the preparation of polymers under study as it provides an opportunity for better control of reaction outcome avoiding sharp changes in polymer characteristics. This sharp change in polymer characters coincides with the sudden growth of the high-molecular weight polymer population, within a short reaction time.

In line with the above explanations, we found polymers with thermo-responsive properties (B_{17} and S_{23}) to self-assemble to aggregates of higher diameter compared to other polymers under study. The size of aggregates formed from block copolymers is determined by their molecular weight and/or aggregation number [130]. Here, the B_{17} and S_{23} with significantly higher molecular weight compared to other polymers, self-assembled into particles with a diameter of around 350 nm at ambient temperature. This might reflect larger hydrophobic structures due to branching or cross-linking of the PBCL segment, but further studies are required to elucidate the actual mechanism behind this observation.

In compliance with the result of rheological studies, only two polymers, B_{17} and S_{23}, showed a thermo-responsive increase in the size of their self-assembled structures. Interestingly, the temperature for this transition, coincided with their sol to gel transition temperatures. This may imply a temperature-triggered self-association of polymers with branched and/or partially cross-linked PBCL as the mechanism inducing thermo-reversible gelation of PBCL-PEG-PBCL triblock copolymers in water.

To the best of our knowledge, this is the first report on the role of a higher-than-expected molecular weight polymer population on the formation of thermo-reversible viscoelastic hydrogels based on PEG and PBCL synthesized by bulk vs solution polymerization methods. The evidence from the detailed characterization of polymers and hydrogels under study, strongly points to the formation of partially cross-linked or branched populations in PBCL-PEG-PBCL polymers, to be responsible for the formation of this high molecular weight population. However, further studies are required to characterize the chemical structure of this population better. We propose a nucleophilic acyl substitution reaction between the hydroxyl group of PEGs (particularly those at a shorter molecular weight in the PEG population) and benzyl carboxylate pendant groups on the polymer backbone (Figure 2-7) to explain the mechanism for the partial cross-linking or branching of the polymer. Although the potential for the existence of cross-linking impurities in the monomer or role of hydroxyl terminated PBCL containing polymers as potential branching reactants and/or cross-linkers cannot be ruled out and needs further investigations.

Previous studies have shown gel formation through chemical cross-linking of poly(ester)s where the end groups in the poly(ester) block have been modified with functional groups such as acryloyl groups [131]. In the current study, the cross-linking is assumed to be extended through unique electrophilic sites in PBCL-PEG-PBCL which are the ester pendant groups in the PBCL blocks.

Poly(ethylene glycol) with hydroxyl groups at both ends can only react and act as a cross linker for PCLs containing substituents with good leaving groups (such as benzyl carboxylate in the case of PBCL-PEG-PBCL as shown in Figure 2-7). We found a similar strategy in the literature where a ketoxime linkage as a crosslinker was used to make a gel with keto groups in the polycaprolactone chain [132]. We have also reported on cross-linking of PEO-PCL with propargyl carboxylate pendent groups using diazide PEG as a cross-linker in a previous manuscript but did not conduct GPC studies on the prepared polymers in THF nor studied the formation of hydrogels from these materials [133]. In another study development of PCLs with pendent α-allyl carboxylate groups has been reported to form thermo-responsive hydrogels upon photo cross-linking [134].

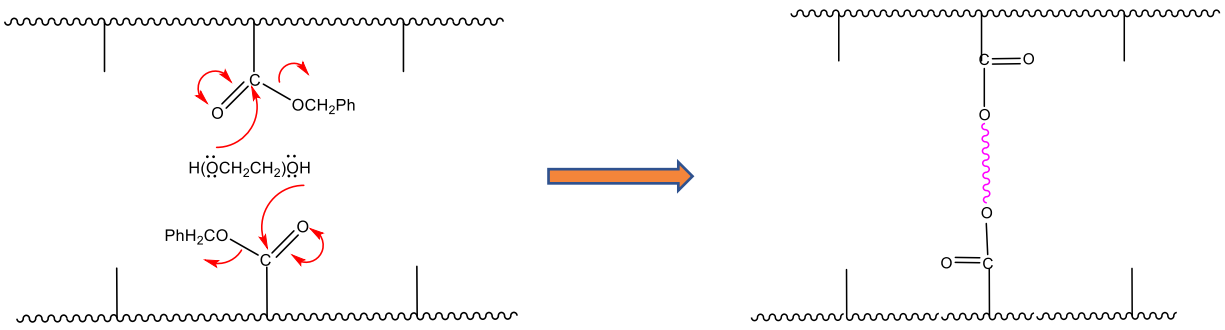

Figure 2-7. Proposed mechanism for the formation of cross-links between PBCL-PEG-PBCL polymer chains.

5. Conclusion

Our results showed the PBCL-PEG-PBCL can be synthesized through both bulk and solution ring opening polymerization, although the solution method of polymerization was proved to provide a better opportunity to control the chain growth during the process. We have provided evidence for the formation of a higher-than-expected molecular weight population with distinctly high intrinsic viscosity in PBCL-PEG-PBCL structure in both polymerization methods, in their GPC profiles. Interestingly the thermo-reversible formation of viscoelastic gels in aqueous media was only observed in polymer samples with around 40 mol % of this population, i.e., B_{17} and S_{23}. In polymer samples with a lower level of high-molecular weight population, viscoelastic gel formation as a function of a temperature rise was not observed. The data have indicated the defining role of this higher-than-expected molecular weight population (which was perhaps formed through partial cross-linking or branching of the PBCL part during polymerization reaction) in the formation of viscoelastic thermo-reversible hydrogels from PBCL-PEG-PBCL block copolymers.

Chapter 3. Cross-linking of triblock copolymers of functionalized poly(caprolactone) and poly (ethylene glycol): The effect on the formation of viscoelastic thermo-gels

The content of this chapter was published in :

Journal of **Reactive and Functional polymers**

3.1. Introduction

Thermo-gelling polymers make flowable solutions in aqueous media below their transition temperature but turn to a semisolid gel upon an increase in temperature [96,135]. Biodegradable thermo-gelling polymers have been the focus of much attention for a variety of biomedical applications [136] including use in a depot or stimulus-responsive drug delivery [3,4,37,106,137–141], tissue engineering [100,131,142–147], prevention of post-operative tissue adhesion [103] and biomaterials for endoscopic submucosal dissection [146]. Gelation in thermo-reversible polymers is commonly induced by non-covalent and usually hydrophobic interactions of polymer chains and/or aggregation of their self-assembled structures [107,108,117]. Chemical gels can also be produced through the covalent cross-linking of the polymers, but chemical gelation is usually irreversible. Chemical gels are, however, usually more elastic, and robust than those formed through the physical interaction of polymer chains. Physical gelation, on the other hand, is commonly reversible, leading to the formation of more flexible and deformable gels. Structures that combine controlled levels of covalent cross-linking and some degree of noncovalent interactions may utilize the advantages of both groups of gels, i.e., show reversible gelation while producing more robust viscoelastic gels [148,149].

Polyester-based thermo-gels have great prospects for application in the biomedical field due to their biodegradability and biocompatibility. In this chemical category, block copolymers of poly(D,L-lactide-co-glycolide)-b-poly(ethylene glycol)-b-poly(D,L-lactide-co-glycolide) (PLGA-PEG-PLGA), known as ReGel® [105], and poly(ε-caprolactone)-b-poly(ethylene glycol)-b-poly(ε-caprolactone) (PCL-PEG-PCL) are reported to exhibit reversible sol-gel transition around the physiological temperature in aqueous media [13]. Block copolymer characteristics such as their

hydrophilic/hydrophobic balance [14,114,115,150,151], molecular weight, and molar-mass dispersity [112,113,124] as well as the chemical structure of copolymers [110,111] are reported to affect the thermo-responsive gelation and viscoelastic properties of produced hydrogels. However, reports on the development of partially cross-linked polymers and the role of cross-link density on the production of thermo-gelling polymers are scarce in the literature [151].

One of the few studies on this subject has been conducted recently by Amirova et al. who synthesized partially cross-linked poly-2-isopropyl-2-oxazoline combining the properties of physical and chemical gels. They found that the synthesized product is bimodal and consists of linear and cross-linked components. Despite the lower proportion of partially cross-linked components, this population dominated the thermo-responsive behaviour and the rheology of the copolymer in aqueous solutions [148]. In a separate study, the same group investigated the effect of crosslinking density on thermo-gelling behaviour and conformational properties of partially cross-linked branched polyethyleneimine (PEI) containing a 2-isopropyl-2-oxazoline unit and discovered a negative correlation between cross-linking mole fraction and lower critical solution temperature (LCST) of the product [152].

Our research group has previously reported on the synthesis of triblock copolymers based on poly(ethylene glycol) as hydrophilic middle blocks and poly(α-benzyl carboxylate-ε-caprolactone) as the hydrophobic lateral blocks (abbreviated as PBCL-PEG-PBCL) [94,120,153,154].

We have recently reported on the defining role of a high molecular weight population in block copolymers PBCL-PEG-PBCL on the formation of thermo-reversible hydrogels (or thermo-gels) with improved viscoelastic properties. The formation of this high molecular weight population was hypothesized to be due to the partial cross-linking or branching of the PBCL-PEG-PBCL structure

by PEG or potential impurities acting as cross-linker, in the reactants during BCL polymerization [154]. Chemical cross-linking of the triblock copolymer can improve the viscoelastic properties of the hydrogels but may restrict the responsiveness of the material to external stimuli such as changes in temperature. A controlled degree of cross-linking for the polymers with appropriate cross-linkers may be used to introduce viscoelasticity to the hydrogel without negatively affecting the physical gelation of the product in response to external stimuli. In the current study, we investigated the validity of this hypothesis through the application of different cross-linkers containing nucleophilic functional groups, including polycaprolactone triol (PCL-triol), trimethylolpropane (TMP) ethoxylate or PEG (200 or 400 Da), following the ring-opening polymerization of purified BCL with PEG. Produced products were then characterized for their molecular weight and molecular weight dispersity by GPC. The effect of the cross-linker and its concentration in the synthesis procedure on the thermo-responsive behaviour and rheology of the bimodal polymer population was investigated. This investigation shed light on the required conditions for the synthesis of partially cross-linked PBCL-PEO-PBCL structures forming reproducible viscoelastic thermo-hydrogels.

3.2. Experimental

3.2.1. Materials

Extra pure α-benzyl carboxylate-ε-caprolactone (BCL) was synthesized by Alberta Research Chemicals Inc (ARCI), Edmonton, Canada. Purification of BCL was accomplished through serial column purifications via dichloromethane and ethyl acetate/hexane system. Then trituration was carried out with hexane and heptane several times to get white, solid, and extra pure powder of BCL. Dihydroxy PEG (MW = 200, 400, and 1450 Da), polycaprolactone triol (M_n=300 Da),

trimethylolpropane ethoxylate (M_n=170 Da), and solvents such as tetrahydrofuran (THF), dichloromethane (DCM), and hexane (chemical reagent grade) were purchased from Sigma-Aldrich (St. Louis, MO).

3.2.2. Synthesis of triblock copolymers

Synthesis of triblock copolymer (ABA) was accomplished through ring-opening polymerization of pure BCL by PEG as described in our previous publication [154]. In brief, the first BCL (0.6 g) and PEG (0.19 g) were dehydrated in a vacuum oven at 70°C for 3h. The polymerization reaction was conducted at 160 °C in an ampule sealed under a vacuum for 10-40 h according to conditions described in Table 3.1. Prepared triblock copolymers were purified by dissolving the products in tetrahydrofuran (THF), followed by precipitation using anhydrous ethyl ether. The sediment was dried under a vacuum for 24 h.

3.2.3. Cross-linking of triblock copolymers by different polyols

Low molecular weight PEGs, i.e., dihydroxy PEG200 and 400 Da, PCL-triol, or TMP ethoxylate were used as cross-linker for the prepared triblock copolymers. In this procedure, bulk polymerization of the pure monomer by PEG (Mw = 1450 Da) was accomplished at 160℃ for 23h as described before. This was followed by the purification of polymers by THF-ethyl ether. Different molar ratios of BCL units in the block copolymer to cross-linker (as summarized in Tables 3-2 and 3-3) were dissolved in 500 µL of dichloromethane and added into a break-seal ampule containing 500 mg of triblock polymer solution in 500 µL dichloromethane. The ampule was kept in a vacuum oven at 50℃ for 2 h and at ambient temperature overnight to evaporate DCM. After, the ampule was sealed again under vacuum and left for 4h at 160℃ in the oven for the nucleophilic reaction of the cross-linker with the PBCL backbone to proceed. Prepared

copolymers were purified by dissolving the product in THF and precipitation using anhydrous ethyl ether. The final product was dried under a vacuum for 24h (Figure 3-1).

3.2.4. Characterization of triblock copolymers and hydrogels

Nuclear Magnetic Resonance (NMR) spectroscopy. Polymers were dissolved in CDCl3 at a concentration of 5 mg/mL, then 1H NMR spectra were recorded using a Bruker Avance III HD 600 MHz. The degree of polymerization (DP) and number of average molecular weight (Mn) of block copolymers were calculated by comparing the area under the peak of methylene protons of the PEG block (CH_2CH_2O-, δ=3.65 ppm) to the methylene protons of the PBCL backbone (-OCH2-, δ= 4.1 ppm). The Mn of the PEG block was considered as 1450 g/mol for these calculations.

Gel permeation chromatography (GPC). Agilent 1260 Infinity II Multi-Detector GPC/SEC system with 3 detectors (Refractive index (RI), light scatter (LS), and viscometer (VS)) was used to obtain data on the peak maximum retention time (PMRT), average molecular weights (M_W) and molar-mass dispersity ($Đ_M$) of the prepared block copolymers. The GPC instrument was equipped with 2 columns (styragel HR2 and styragel HR 4E from waters company) and calibrated with a set of polystyrene standards covering a molecular weight range of 160-200,000 g/mol. Samples (5-10 mg/mL) were prepared in THF (HPLC grade) and filtered with a nylon syringe filter (pore size:0.45 μm). Then 200 μL of samples were injected into GPC which was operated at a THF flow rate of 0.7 mL/min at 35 °C. The elution time for all polymers was 30 min. During this time, the GPC chromatogram came back to the baseline but for clarity of presentation, elution time was selected from 14-24 min in all GPC graphs.

Phase diagram by inverse flow method. The gelation behavior was evaluated by the inverse flow method at a concentration of 150 mg/mL of polymer in water. The vial containing 1 mL of copolymer solution was equilibrated at 4 °C overnight before the test. Then the vial was immersed in a water bath at 30°C and equilibrated for 15 min. If the content of the vial did not flow for 30 s, the sample was considered a gel.

Rheological testing. The rheology test was performed on a Discovery Hybrid Rheometer (TA instruments) in parallel plate geometry with a diameter of 40 mm and an auto gap set mechanism. The copolymer solutions in water (concentration 15 wt%) were prepared and equilibrated at 4 °C overnight. A temperature ramp test was performed to investigate the viscoelastic property changes of hydrogels as a function of an increase in temperature. For temperature ramp, the test was conducted at a strain of 2% (within their linear viscoelastic regions (LVR)), angular frequency (ω) of 10 rad/s, and heating rate of 1 °C/min from 10 to 50°C.

3.2.5. Characterization of the self-assembly of copolymers by DLS

The self-assembly of copolymers was characterized using MALVERN Nano-ZS90 ZETA-SIZER (Malvern Instruments Ltd, Malvern, UK). For sample preparation, 10 mg of the copolymer sample was dissolved in 1 mL of acetone then 10 mL of distilled water was added to this solution dropwise. The mixture was stirred for 24 hours at room temperature to evaporate acetone. The diameter of self-assembled structures was determined with Zetasizer Nano equipped laser at a wavelength of 633 nm using the intensity function. The scattered light was detected at an angle of 173°.

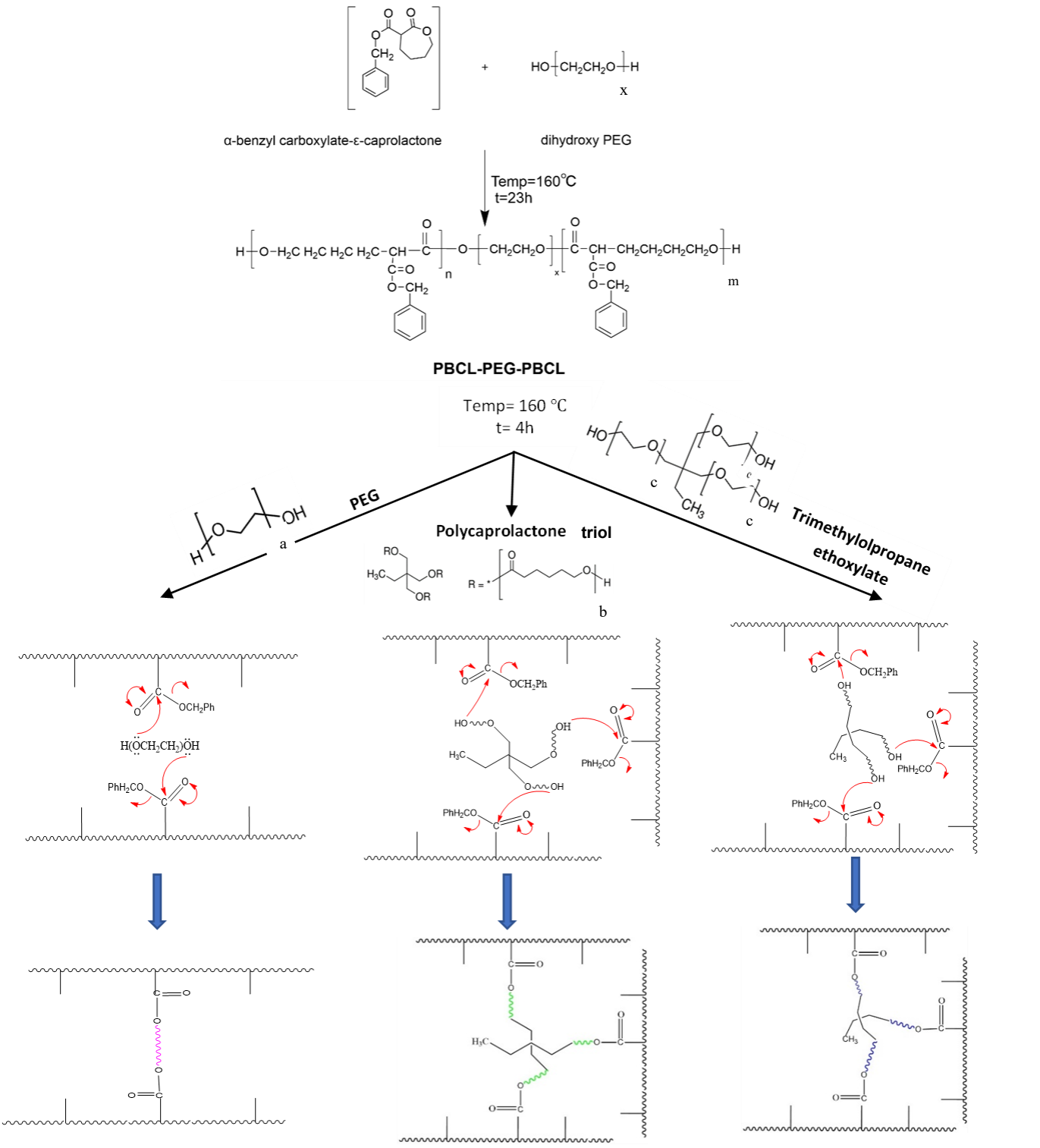

Figure 3-1. Synthesis scheme and proposed models for the preparation of partially cross-linked PBCL-PEG-PBCL copolymers. Depending on the availability and access of the cross-linker to the functional groups on the polymer back bone, the polyol cross linker may react with one, two or, at most, three functional groups leading to branching or cross-linking of the structures by the polyol cross-linker. n, m=1-18, x=33

3.3 Results and discussion

3.3.1. The effect of polymerization time on the molecular weight and molar-mass dispersity of block copolymers synthesized using purified BCL.

As a potential source for the accidental cross-linking in the polymerization of BCL by PEG was the impurities in the monomer, here, we used purified BCL. Polymerization of purified BCL is initiated by PEG (1450 Da) at different polymerization times (10-40 hours) (Table 3-1). The reaction times were chosen based on the results of our previous study [154]. As shown in Figures 3-2A & B, the increase in the reaction times showed a positive and linear correlation with the M_n (as measured by ^{1}H NMR and GPC respectively) of the prepared copolymers. However, even at the maximum reaction time (40 h), DP and M_n(NMR) of the product (8.3 and 3508, respectively) (Table 3-1) were significantly lower than that the expected theoretical values (18 and 6000 g/mol for DP and Mn, respectively). In the current study, the calculated weight average molecular weight (M_w) for B_{40}, was 8866 g/mol. This was only 1.5-fold higher than the theoretical average molecular weight for this sample. This indicates the linear growth of the PBCL chain over time and the absence of any significant proportion of branched/crosslinked structure in the product. In line with this explanation, the highest M_n (GPC)/M_n (NMR) ratio measured for PBCL-PEG-PBCL polymers prepared using purified BCL was 1.50 (Table 3-1) however, based on our previous report [154], the formation of thermo-reversible gels in aqueous media for the synthesized PBCL-PEG-PBCLs was only observed in polymer samples with M_n (GPC)/M_n (NMR) $\geq$ 6.

Table 3-1. Characteristic of copolymers synthesized using ring-opening polymerization of purified BCL by PEG 1450 Da at different reaction times. The theoretical MW of copolymers was 6000 g/mol.

Sample[a]	DP [b]	M_n (Da)[c]	M_n (Da)[d]	M_n(GPC)/M_n(NMR)	M_w (g/mol)	$Đ_M$	Appearance in water at 30°C
B_{10}	2.6	2095	2440	1.16	3433	1.41	Sol
B_{17}	4	2442	2720	1.11	3994	1.47	Sol
B_{23}	6.5	3062	3751	1.23	6104	1.62	Sol
B_{30}	7.2	3236	4747	1.47	7813	1.65	Sol
B_{40}	8.3	3508	5285	1.50	8866	1.68	Sol

a B stands for Bulk polymerization and the number in the subscript shows the reaction time in hours.
b Degree of polymerization (DP) of PBCL block measured by ^{1}H NMR.
c Number average molecular weight of block copolymers measured by ^{1}H NMR.
d Number average molecular weight of block copolymers measured by GPC.

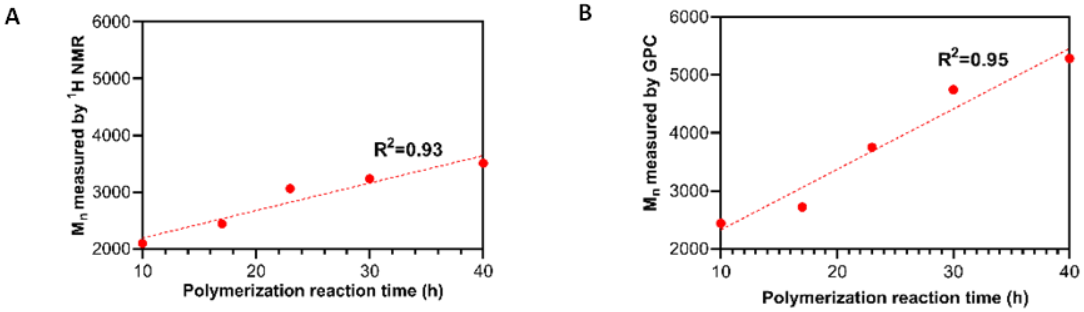

Figure 3- 2. The effect of polymerization reaction times on the **A)** M_n measured by ^{1}H NMR **B)** M_n measured by GPC (dashed line in figures show linear trendline).

By increasing the polymerization time, the GPC elution profiles of synthesized copolymers (Figure 3-3A) showed a decrease in the peak's maximum retention time reflecting an increase in the molecular weights of copolymers. The molecular weight distribution (MWD) of polymers resulting from GPC chromatograms (Figure 3-3B) revealed a similar general shape for all polymers under study, but the weight fraction of the lower molar mass chains slightly decreased as the reaction time progressed. By increasing the polymerization time, the MWD graph of samples skewed to the higher molecular weight area, leading to an increase in the polydispersity index ($Đ_M$) (Table 3-1). All the PBCL-PEG-PBCL polymers prepared using the pure monomer (B_{10}-B_{40}) were

water-soluble at a concentration of 15 wt% and 30°C and did not form a visual gel under this condition, as judged by the inverse flow method (Table 3-1). The collection of the above evidence indicated bulk polymerization of extra pure BCL initiated PEG even in high polymerization time lacked the higher-than-expected molecular weight population observed for the impure BCL in our previous study [154], thus, did not produce thermo-reversible hydrogels in water.

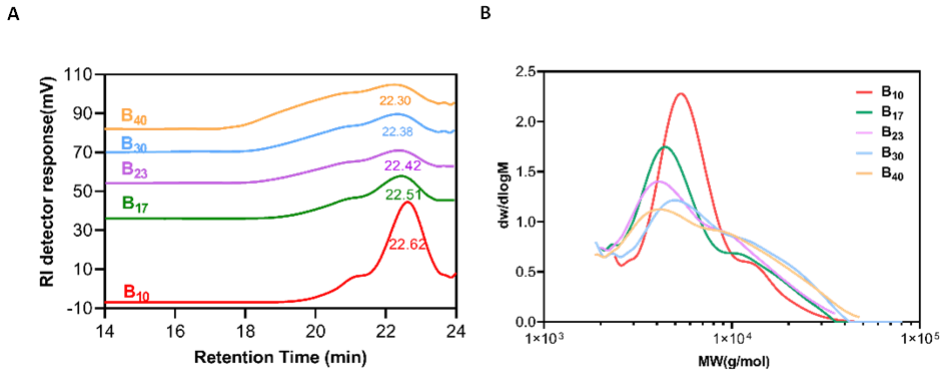

Figure 3-3. A GPC elution profile of copolymers prepared at different reaction times. **B)** Molecular weight distribution of copolymers under study.

3.3.2. The effect of cross-linker on the characteristics and physical gelation of copolymers.

To investigate the effect of cross-linkers on the characteristics of produced polymers thermo-gel formation, a B_{23} sample, with a middle MW among synthesized copolymers was selected. covalent cross-linking of the PBCL-PEG-PBCL was chosen to assess the potential of this approach in producing a reproducible process for the formation of a viscoelastic thermo-gel. For this purpose, three different cross-linkers bearing multi-functional hydroxyl groups in their structure, i.e., PEG 400, polycaprolactone triol, and trimethylolpropane ethoxylate were used at a cross-linker: monomer molar ratio of 4:10.

Table 3-2 shows characteristics of chemically cross-linked B_{23} by different cross-linkers. ^{1}H NMR spectra of the products showed similar DP and M_n for the products of B_{23} reaction with either of the three cross-linkers. Data from GPC showed M_n, M_w, and $Đ_M$ of the products to be similar, irrespective of the type of cross-linker used, as well. The M_n(GPC)/M_n(NMR) ratio was 1.23 for the starting B_{23} polymer. Hence, B_{23} was considered a linear copolymer. The ratio of M_n(GPC)/M_n(NMR) for B_{23} after reaction with either of the three cross-linkers was shown around 8.5 which was around 7 folds larger than that of linear B_{23}. This implied success in partial cross-linking of PBCL-PEG-PBCL irrespective of the cross-linker type. The proposed mechanism for the reaction between the polyol cross-linkers and the PBCL backbone is shown in Figure 3-1. A nucleophilic acyl substitution reaction between the benzyl carboxylate pendant group of the polymer backbone and the hydroxyl groups of cross-linkers was assumed to take place in the reaction.

Although the M_n(GPC)/M_n(NMR) ratio for the products of PCL-triol and TMP ethoxylate cross-linkers implied the success of cross-linking reactions, only the product with PEG 400 as the cross-linker showed the thermo-gelling behaviour in water at 30°C. This was observed despite similarly high M_n (GPC)/M_n (NMR) ratios for polycaprolactone triol, and trimethylolpropane ethoxylate cross-linked polymers to that of PEG400 cross-linked ones (M_n (GPC)/M_n (NMR) of 8.57 and 8.75 versus 8.50), implying a similar degree of cross-linking. The molecular architecture of the final products prepared through the addition of PCL-triol and TMP cross-linkers with three hydroxyl groups (three-point attachment to the backbone), may cause restriction in the freedom of conformations of the polymer backbone. This can hamper the thermal gelation of the product. The difference in the hydrophilicity of the PCL-triol and TMP versus PEG may have contributed to this observation, as well.

Table 3-2. Characteristic of sample cross-linked polymers prepared in the study following reaction of B_{23} with different cross-linkers at a cross linker: BCL ratio of 4:10.

Cross-linker	DP of PBCL	M_n (NMR)	M_n (GPC)	M_n (GPC)/M_n (NMR)	M_w (g/mol)	$Đ_M$	Appearance in water at 30°C
Polyethylene glycol (400 Da)	13	4670	39700	8.50	42500	1.07	gel
Polycaprolactone triol	12	4430	38750	8.75	46300	1.19	sol
Trimethylolpropane ethoxylate	13	4674	40065	8.57	44493	1.11	sol

3.3.3. The effect of PEG molecular weight and molar ratio on the characteristic and physical gelation of synthesized copolymers.

To further investigate the effect of cross-linker, PEGs with different molecular weights (200 and 400 Da) at different molar ratios to the BCL unit in the PBCL block were reacted with PBCL-PEG-PBCL as detailed in Table 3-3. Assessing the characteristics of the prepared copolymers from the ^{1}H NMR spectra showed a similar degree of polymerization and Mn for all products (P_1 to P_7 in Table 3-3). The GPC elution profiles of P_1-P_7 in THF are shown in Figure 3-4A and related data are summarized in Table 3-3. For the P_1 polymer where no cross-linker was used, the peak maximum retention time (PMRT) was recorded at 22.20 min.

The data showed an increasing molar ratio of PEG 200:BCL unit, leading to an increasing trend in the peak with maximum retention time (PMRT) of produced copolymers from 22.62 to 22.76 min. In contrast, when PEG 400 was used as the cross-linker increasing the molar ratio of PEG to that of the BCL unit, led to a decline in PMRT of product from 20.80 for P_5 to 17.18 for P_6 and 15.86 for P_7. As shown in Figure 3-4B and Table 3-3, polymers prepared using PEG 400 as a cross-linker, at a 2:10 and 4:10 PEG: BCL molar ratio, had a distinct population with drastically

increased molecular weights. In these samples, the M_n(GPC)/M_n(NMR) ratio abruptly raised to 6.60 and 8.98, respectively. For P_5 polymer with a PEG 400:BCL molar ratio of 1:10, the M_n(GPC)/M_n(NMR) ratio (2.73) was still higher than the corresponding sample prepared using PEG200 (1.04). Also, the calculated weight average molecular weight (M_w) for P_5, P_6, and P_7 were 36023, 98050, and 185000 g/mol which is 6, 16, and 31-fold higher than the theoretical molecular weight of these samples. Meanwhile, the Inverse flow test at 30℃ for an aqueous solution of samples under study at 15% wt concentration revealed only P_7 can produce a thermo-reversible gel.

Table 3-3. characteristic of synthesized triblock copolymers reacted with different ratios of cross-linker (PEG 200 or 400) to monomer (theoretical MW of copolymer was 6030 g/mol).

Sample	Cross-linker	Molar ratio Cross-linker/ BCL unit in B_{23}	DP	M_n (NMR)	PMRT (min)	M_n (GPC)	M_n(GPC)/M_n (NMR)	M_w (g/mol)	Appearance in water at 30℃
P_1	NA	NA	6	2938	22.20	3925	1.33	6377	Sol
P_2	PEG 200	1/10	6	2938	22.62	3067	1.04	6845	Sol
P_3	PEG 200	2/10	6.4	3037	22.71	3068	1.01	7630	Sol
P_4	PEG 200	4/10	6.1	2963	22.76	3060	1.03	6596	Sol
P_5	PEG 400	1/10	6.7	3112	20.80	8493	2.73	36023	Sol
P_6	PEG 400	2/10	6	2938	17.18	19400	6.60	98050	Sol
P_7	PEG 400	4/10	6.5	3062	15.86	27500	8.98	185000	Gel

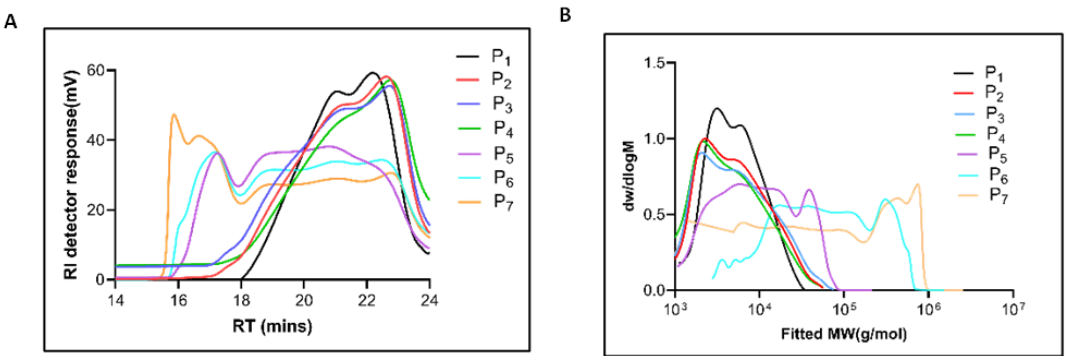

Figure 3-4. A: GPC elution profile and **B:** Molecular weight distribution of copolymers after addition of PEG 200 or PEG 400 as cross-linker at different PEG:BCL molar ratios. The description of each polymer sample is detailed in Table 3-3.

3.3.3.1. The effect of PEG molecular weight and molar ratio on the viscoelastic properties of copolymer aqueous solutions.

Oscillatory rheology was used to probe the temperature dependant viscoelastic properties of the aqueous solution of P_1-P_7 at a concentration of 15 wt% in the temperature range of 10-50℃ (Figure 3-5). In thermo-gelling materials, storage modulus (G'), loss modulus (G"), and complex viscosity (η*) increase proportionally as a function of temperature. When G' is over G", gelation behaviour for the aqueous solution of the copolymer is envisioned. For viscoelastic materials, at the sol-gel transition temperature (sol-gel), we expect G'≈G". Above this temperature G' stays higher than G". At gel-sol transition, again G'≈G" and above this transition G" stays above G' [155].

For the triblock copolymer synthesized without the addition of any crosslinker (P_1), G', G" and η* showed a peak around 20°C. The peak maximum for the G' and G" was 0.50 and 0.76 Pa, respectively and there was no cross over of G' and G" for this sample. Polymers synthesized using PEG 200 as cross-linker (P_2, P_3, and P_4) had moduli below 1Pa. Also, the rise in temperature above 40 °C led to an increase in G', G" and η* while G" was higher than G' at all temperatures under study. On the other hand, polymers that were reacted with PEG 400 had higher moduli. For these

samples, a drastic change in G', G" and η* occurred at a specific temperature range. For the P_6 sample, the value of G', G" and η* showed a peak after 32 °C but loss modulus still dominated storage modulus indicating viscose behavior for this sample. The P_7 sample showed sol-gel transition at 23°C, which was reflected by a cross-over of G' and G". A gel-sol transition was recorded at 42 °C for this polymer, reflected by a second cross-over of G' and G".

Interestingly, the P_7 sample which has shown a thermo-reversible gel formation had shown a high M_n (GPC)/M_n (NMR) ratio (8.50-8.98) as well (Table 3-3). The P_6 sample in which PEG 400 was used at a PEG 400/BCL ratio of 2:10 has shown a lower M_n (GPC)/M_n (NMR) of 6.60 (Table 3-3) and a trend towards viscosity enhancement around 30 C (Figure 3-5) but did not show the thermo-reversible formation of viscoelastic gels. This may reflect the importance of the degree of cross-linking in addition to the structure of cross-linker on the viscoelastic gelation of the constructs under study.

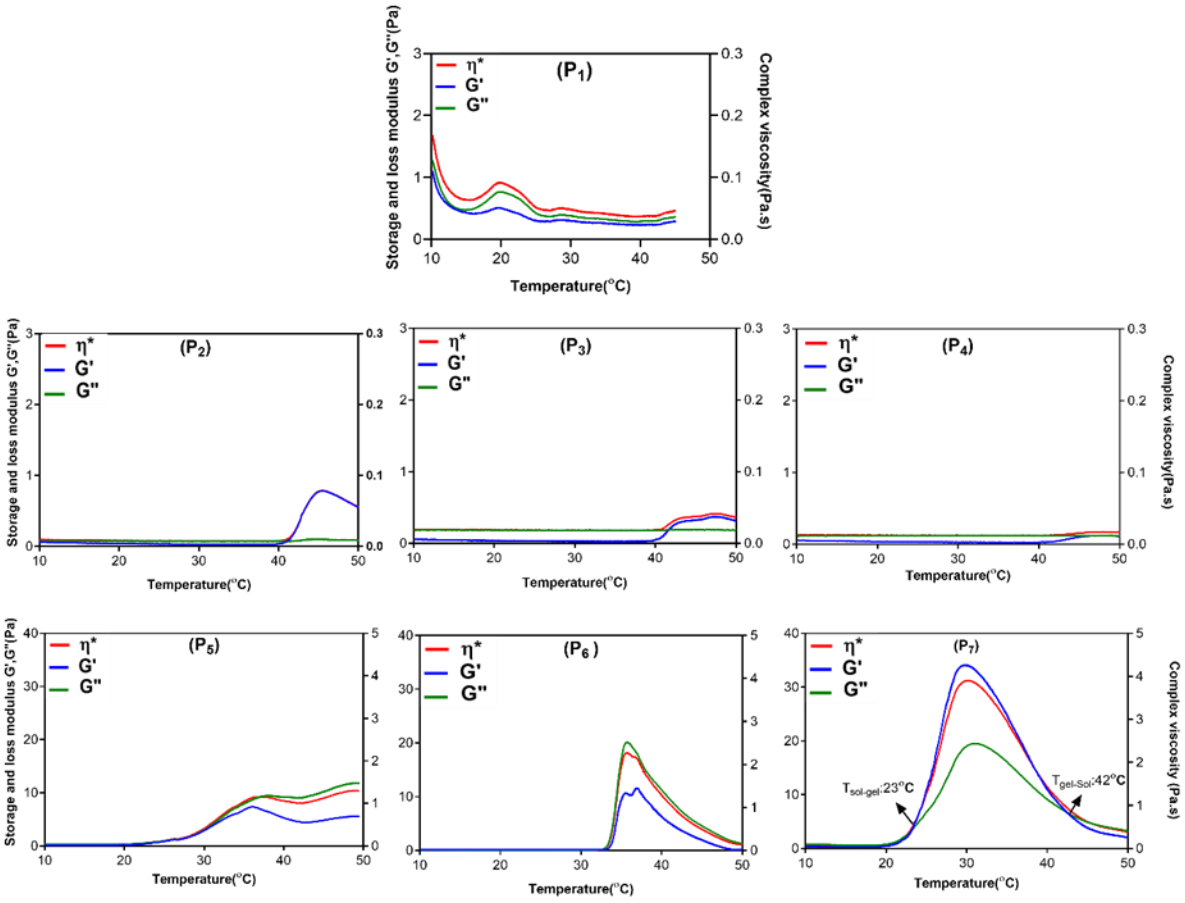

Figure 3-5. Storage modulus(G'), Loss modulus(G"), and complex viscosity (η*) of copolymers aqueous solutions as a function of temperature, concentration 15 wt%, and heating rate 1 °C/min (10-50°C).

3.3.3.2 The effect of PEG molecular weight and molar ratio on temperature-dependent self-assembly of block copolymers in aqueous solutions.

The average size of self-assembled structures for P_1-P_7 samples at ambient temperature in the water is shown in Figure 3-6A. The average size of P_1 aggregate in water was significantly lower than other samples under study. The P_2, P_3, and P_4 aggregates in water showed a similar size. For polymers reacted with different molar ratios of PEG 400 Da, a positive correlation between the aggregate size and the molar ratio of PEG 400: BCL was observed. Remarkably, the P_7 sample

produced significantly larger aggregates at room temperature compared to other samples under study. Figure 3-6B shows the change in the average size of the self-assembled structure for P_1-P_7 as a function of temperature. There was no significant change in the size for P_1-P_4 by raising the temperature from 10°C to 50 °C while P_5 and P_6 samples showed an increase in micellar size after 28 °C. The P_7 sample showed a peak around 20 °C and plateaued after. The size distribution of the self-assembled structure of copolymers (P_1- P_7) is shown in Figure 3-6C. A unimodal distribution with similar intensity was observed for P_1-P_4 while P_5 and P_6 samples showed a bimodal distribution with negligible intensity (≤ 2%) of the second peak in the size distribution graph. On the other hand, for the P_7 sample, bimodal size distribution was significant. While the first peak with a Z-average of 32 nm has 68% intensity, the second peak with an average size of 180 nm has 32% intensity at 30 °C. This may reflect a bulkier structure for the PBCL block due to the partial cross-linking and/or branching of the PBCL segment by PEG 400 Da, which may not be shielded adequately by the micellar shell.

The data confirmed our hypothesis on the effect of partial cross-linking as a potential mechanism for the formation of thermo-reversible and viscoelastic hydrogels from PBCL-PEG-PBCLs. The results of this study can enrich our understanding of the effect of polymer architecture in PEG/PBCL copolymers on their thermo-gelling behaviour.

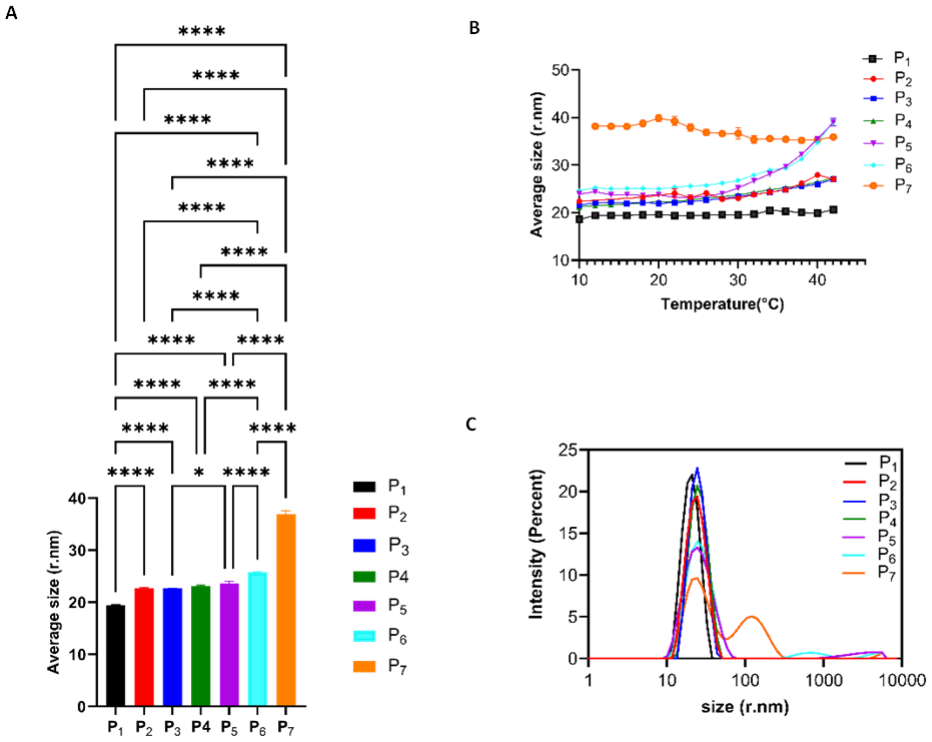

Figure 3-6.A: The effect of PEG molecular weight and ratio (added to PBCL-PEG-PBCL as cross-linker) on the size of self-assembled structures from copolymers under study at 25℃. Results are presented as Mean ± SD (n=3). Asterisks denote significant difference at P<0.05. **B:** Change in the size of self-assembled structures from block copolymers under study as a function of temperature at 1 mg/mL polymer concentration as measured by DLS. **C:** Size distribution of self-assembled structures from block copolymers P1-P7 at 25℃.

3.4. Conclusion

In the present study, for the first time chemically cross-linked PBCL-PEG-PBCL thermogel was synthesized by a two-step procedure: first, ring-opening polymerization of BCL by PEG 1450 as an initiator with low DP and MW; then cross-linking of the produced triblock copolymer by PEG 400 Da. The use of PEG 400 Da at a PEG 400/BCL ratio of 4:10 as a crosslinker for PBCL-PEG-PBCL copolymers, was able to yield a viscoelastic thermo-reversible hydrogel. The data imply a

the role of the degree of cross-linking (reflected by M_n (GPC)/M_n (NMR) ratio) as well as the chemical structure of the cross-linker on the formation of thermo-reversible and viscoelastic physical gels by the structures of under study.

Chapter 4. Polymer characteristics leading to the formation of viscoelastic thermogels in partially cross-linked copolymers based on benzyl carboxylate/carboxyl substituted PCL and PEG

4.1. Introduction

Thermo-hydrogels, defined as aqueous polymer solutions that become gel as a function of a rise in temperature, are of interest in different biomedical fields. For use in biomedical field, thermo-gelling polymers with sol to gel transition temperatures around the physiological range (typically between 25 to 37 ℃) are the subject of particular attention [97,106,145,156–158]. This is owed to their potential application as smart hydrogels for the delivery of pharmaceuticals and/or stimulus-responsive scaffolds for tissue engineering applications [3,131,136,139,143,145,159]. Thermo-gelling polymers with a poly(ester) based structure can add the benefit of biodegradability to the above properties, providing new opportunities in the development of pharmaceutical excipients and/or biomaterials that support *in vivo* tissue/cell implantation or proliferation [160–162]. In this category, copolymers of poly(ethylene glycol) (PEG) and poly(caprolactone) (PCL) as FDA-approved, biodegradable, and biocompatible biomaterials with thermo-gelling properties have been the most focus of a few studies [12,46,56,59,71,92,163–166]. For instance, Bae *et al* found an aqueous solution of PCL-PEG-PCL to undergo a sol-gel transition as a function of an increase in temperature. They found the transition temperature to be dependent on the hydrophilic/hydrophobic balance of the polymer, and the thermal history of the copolymer aqueous solution. They also proposed that the sol-to-gel transition to occur by micellar aggregation, whereas the gel-to-sol transition to occur by increasing PCL molecular motion leading to micellar breakage [71,167].

Despite great potential, the lack of functional groups as well as the high crystallinity and hydrophobicity of the PCL segment, has limited the use of conventional PEG/PCL hydrogels [46,163]. In 2006, our research group has reported on the introduction of functional groups on caprolactone monomer, developing α-benzyl carboxylate-ε-caprolactone (BCL) and further polymerization of this functionalized monomer through bulk ring opening polymerization (ROP)

by methoxy poly(ethylene oxide), leading to the production of methoxy PEO-b-poly(α-benzyl carboxylate-ε-caprolactone) (PEO-b-PBCL) diblock copolymers [121]. We have later reported on the preparation of triblock copolymers through ring opening polymerization of BCL by dihydroxy poly(ethylene glycol) (PEG) leading to the production of PBCL-*b*-PEG-*b*-PBCL [120,153,154]. The benzyl carboxylate groups on PEO-*b*-PBCL and PBCL-*b*-PEG-*b*-PBCL block copolymers prepared by bulk polymerization were also reduced to carboxyl groups at different degrees, leading to the conversion of PBCL blocks in PBCL-PEG-PBCL to poly(α-carboxyl-ε-caprolactone)-co-poly(a-benzyl carboxylate- ε-caprolactone) (PCBCL). In further studies, we investigated the effect of the solution versus bulk polymerization methods on the characteristics of PBCL-PEG-PBCL block copolymers and gelling behaviour of produced polymers in an aqueous environment. In that study, we provided evidence for the presence of a high molecular weight subpopulation in the synthesized PBCL-PEG-PBCL structure. We also showed the defining role of this subpopulation at around 40 % molar concentration in the thermo-reversible transition of aqueous solutions of PBCL-PEG-PBCL to viscoelastic gels. The appearance of this higher-than-expected molecular weight subpopulation was attributed to partial cross-linking or branching of the PBCL block by nucleophilic reactants present in the polymerization procedure [154]. In the present manuscript, we used the PBCL-PEG-PBCL copolymers having this subpopulation of high molecular weight polymers and reduced the PBCL segment using different hydrogenation reaction times (Figure 4-1). The original partially cross-linked PBCL-PEG-PBCL (or PBCL-PEG-$PBCL_{pc}$) copolymers used in the reduction reaction were prepared through either bulk or solution polymerization methods. The partially cross-linked (PC) copolymers based on PEG and carboxyl/benzyl carboxylate substituted PCL blocks (abbreviated as PCBCL-PEG-$PCBCL_{PC}$) were then characterized for their average molecular weights, molecular weight distribution, conformation,

and intrinsic viscosity. The effect of the level of carboxyl substitution on the polymer backbones, on their transition to viscoelastic gels in water as a function of a temperature rise, was investigated. Our results indicated that the thermo-gelling behaviour of PCBCL-PEG-PCBCL$_{pc}$ and their viscoelastic properties depend on the percentage of carboxyl group substitution on the PCBCL segment.

4.2. Experimental section

4.2.1. Materials. α-Benzyl carboxylate-ε-caprolactone (BCL) was synthesized by Alberta Research Chemicals Inc (ARCI), Edmonton, Canada based on methods reported by our group[121]. Biphenyl (≥99%), dihydroxyl-poly(ethylene glycol) (PEG) (Mw = 1450), and palladium on activated charcoal were purchased from Sigma-Aldrich (St. Louis, MO). Other chemicals such as Dichloromethane, Tetrahydrofuran, and hexane were chemical reagent grade and bought from Sigma-Aldrich.

4.2.2. Synthesis of triblock copolymers:

The synthesis of copolymers was accomplished in two steps (Figure 4-1). In the first step, ring opening polymerization of BCL as a monomer and dihydroxy polyethylene glycol (PEG) as initiator was carried out through bulk and solution polymerization as described in our previous publication [154]. Briefly, 2.4 g of BCL and 0.76 g PEG were dried at 60 ℃ in a vacuum oven for 3 h. For solution polymerization, BCL, PEG, and biphenyl (30 % w/w monomer) were mixed in an ampule and sealed under a vacuum. In bulk polymerization, only BCL and PEG, in the same quantities, were mixed and vacuum sealed. Polymerization was conducted without any catalyst at 160°C for 14 and 23 h for bulk and solution methods, respectively. The time of polymerization

reaction was optimized based on our previous study [154] to provide sufficient time for the appearance of the high molecular weight subpopulation in the produced polymers.

Prepared copolymers were then dissolved in dichloromethane and precipitated in hexane. The supernatant was discarded after 24 hours. For more purification, tetrahydrofuran (THF) and anhydrous ethyl ether were used as solvent/non-solvent systems and the above-mentioned purification procedure was repeated three times to wash off the excess monomer and other impurities, as much as possible. After purification, the product was dried under a vacuum for 24h. This step led to the production of PBCL-b-PEG-b-$PBCL_{PC}$ copolymers.

In the second step reduction or debenzylation of PBCL-PEG-$PBCL_{PC}$ copolymers was performed, which resulted in the preparation of PCBCL-b-PEG-b-$PCBCL_{PC}$. This was accomplished in the presence of hydrogen gas, palladium on activated charcoal as catalyst (10 wt.% of the polymer), and dry THF as solvent. The reaction time in this step was changed between 20 to 120 minutes to achieve different degrees of debenzylation on the PBCL section. The final product was centrifuged 2 times at 3000 rpm for 5 min to separate charcoal, then the supernatant was dried under vacuum for 24 h.

4.2.3. Characterization of copolymers

Nuclear Magnetic Resonance (NMR)

Prepared block copolymers were dissolved in $CDCl_3$ at a concentration of 5 mg/mL for ^1H NMR spectroscopy using 600 MHz Bruker NMR. ^1H NMR spectroscopy of copolymers was used to calculate the degree of polymerization (DP) and number average molecular weight (M_n) of PBCL-PEG-PBCL by comparing peak intensity of PEG (-CH_2CH_2O-, δ=3.65 ppm) to that of PCL backbone (-OCH_2-, δ= 4.05 ppm) assuming a 1450 g/mol molecular weight for PEG. The

percentage of reduction (i.e., debenzylation) in PCBCL-PEG-PCBCL was estimated using the following equation.

$$\text{Reduction (\%)} = \frac{(DP \text{ of PCBCL backbone}) - (\text{benzyl substitution on PCBCL})}{(DP \text{ of PCBCL backbone})}$$

The DP of the PCBCL backbone was calculated by comparing the area under the peak for (-CH_2O-, δ= 4.1 ppm) to that of PEG (-CH_2CH_2O-, δ=3.65 ppm). The number of benzyl substitutions on PCBCL was then estimated by comparing the area under the peak for the methylene protons of the benzyl carboxylate group (Ph-CH_2-O-C=O, δ=5.15) to that for PEG (-CH_2CH_2O-, δ=3.65 ppm).

Gel permeation chromatography (GPC)

Prepared copolymers were characterized for their average molecular weights (MW), molar-mass dispersity ($Đ_M$), intrinsic viscosity, and conformation by GPC (Agilent 1260 infinity series (Agilent, USA) with Refractive index, light scatter, and viscometer detectors) equipped with 2 columns (Styragel HR2 and styragel HR 4E from waters company, USA). The instrument was calibrated with a set of polystyrene standards covering a molecular weight range of 160-200,000 g/mol. Samples (5-10 mg/mL) were prepared in THF (HPLC grade) and filtered with a nylon syringe filter (pore size: 0.45 μm). Then 200 μL of each sample was injected to GPC which was operated at a THF flow rate of 0.7 mL/min at 35 °C. The elution time for all polymers was 30 min. During this time, the GPC chromatogram came back to the baseline but for clarity of presentation, elution time was selected from 14-24 min in all GPC graphs.

4.2.4. Dynamic rheological measurements

The viscoelasticity of the copolymer solutions in water (10 and 15 wt%) as a function of an increase in temperature was investigated by Discovery Hybrid Rheometer (TA Instruments, USA)

in parallel plate geometry and auto gap set mechanism. The heating rate was 1 °C/min (10-50 °C), with an angular frequency ω of 10 rad/s.

4.2.5. Phase diagram or state diagram

The sol-gel transition was examined by the inverse flow method at 10-20 % w/v of polymer concentration in water. Each vial contained 1 mL of copolymer solution and all samples were equilibrated at 4 °C overnight before measurements. Vials were immersed in a water bath and the temperature was raised from 10 to 50 °C at 2°C intervals. The vials containing the above samples were equilibrated for 15 min at each temperature. If the liquid inside the vial did not flow for at least 30 seconds, the sample was regarded as a gel [113] .

4.2.6. Characterization of thermo-responsive self-assembly of copolymers

The effect of a rise in temperature between 10 to 50°C on the self-assembly of prepared block copolymers was investigated using MALVERN Nano-ZS90 ZETA-SIZER (Malvern Instruments Ltd, Malvern, UK). For sample preparation, 10 mg of the block copolymer was dissolved in 1 mL of acetone, then 10 mL of distilled water was added to this solution dropwise. The mixture was stirred for 24 hours at room temperature to evaporate the acetone. The micellar diameter was determined with a zetasizer equipped laser at a wavelength of 633 nm using the intensity function. The scattered light was detected at an angle of 173°. The Z-average of self aggregated block copolymers was measured as a function of an increase in temperature.

4.2.7. Statistical analysis

The results are reported as average ± standard deviation (SD) of three independent measurements on a single batch of polymer unless mentioned otherwise. The statistical analysis was processed using GraphPad Prism software, version 8.3.1 (GraphPad Software Inc., La Jolla, CA, USA). The

significance of differences between results was assessed by one-way ANOVA analysis followed by Sidak's multiple comparison test where α=0.05 was set as the level of significance.

4.3. Results and discussion

Characterization of block copolymers

The PBCL-PEG-PBCL triblock copolymers were synthesized via ROP of BCL and PEG by two methods of bulk and solution polymerization (Figure 4-1). The reaction time for the bulk and solution methods of polymerization was selected based on the information from our previous work at 14 and 23 h, respectively. At these reaction times, the formation of the high molecular weight subpopulation in the polymer samples (due to partial cross linking of polymers) was expected [154]. The GPC analysis of PBCL-PEG-PBCL$_{PC}$ samples prepared by bulk and solution polymerization (denoted here as B_0 and S_0, respectively) provided evidence for the presence of this high molecular weight population. Specifically, a 7.9 - and 9.7-fold increase in the number of average molecular weights (M_n) as measured by GPC compared to that calculated from ^{1}H NMR spectroscopy, was observed for B_0 and S_0, respectively (Table 4-1 and 4-2) pointing to the formation of cross-linked or branched structures in the copolymer population. The purified PBCL-PEG-PBCL$_{PC}$ copolymers (B_0 and S_0) were then chemically reduced (or debenzylated) using continuous hydrogenation in the presence of palladium on activated charcoal (Figure 4-1). The degree of chemical reduction was controlled by changing the reaction time between 0-120 min as summarized in Tables 4-1 and 4-2. This led to the production of different PCBCL-PEG-PCBCL$_{PC}$ copolymers denoted as the "B" series for polymers reduced from B_0 (or PBCL-PEG-PBCL$_{PC}$ prepared by bulk ROP, Table 4-1), and the "S" series for polymers reduced from S_0 (or PBCL-PEG-PBCL$_{PC}$ prepared by solution ROP, Table 4-2).

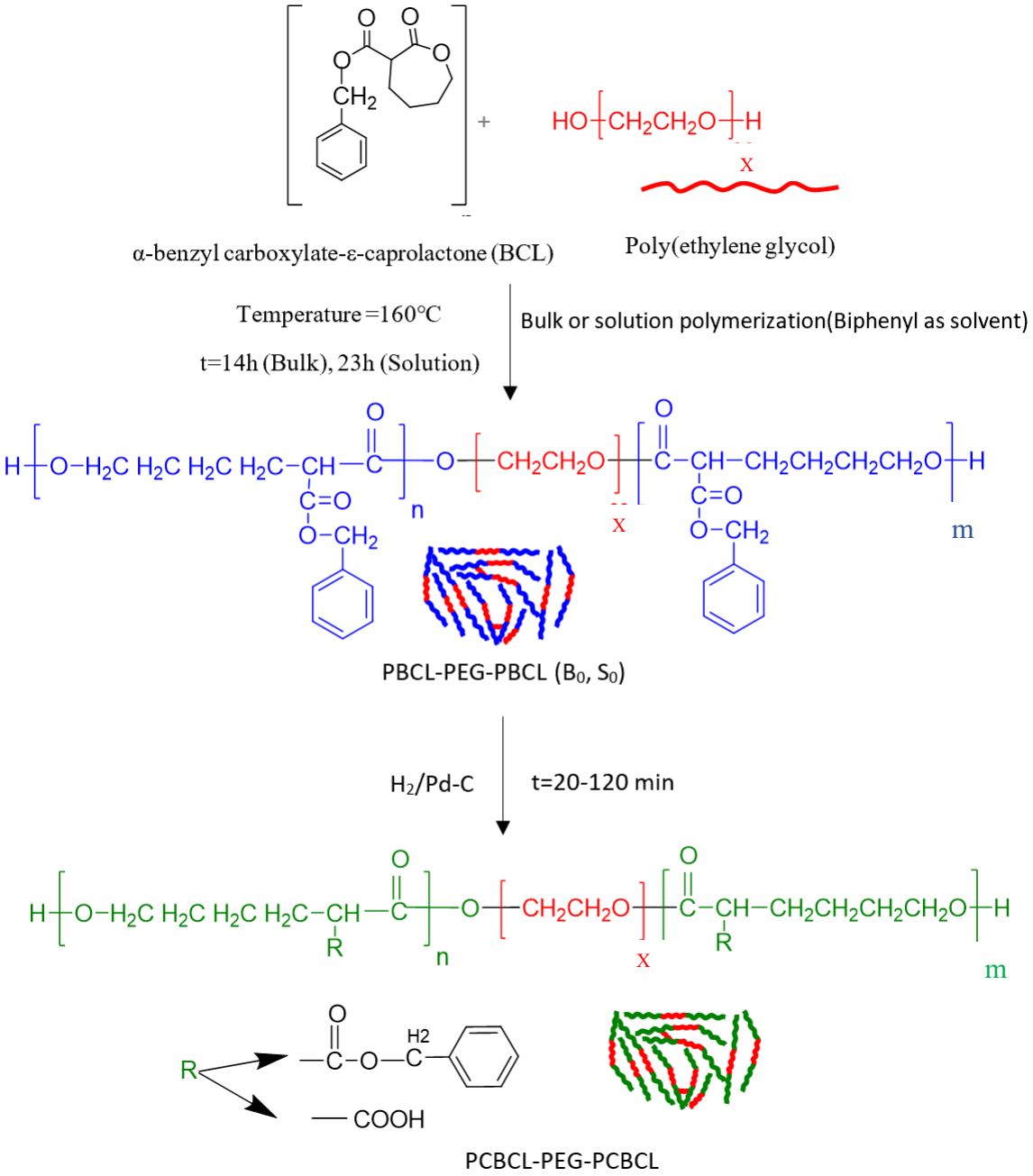

Figure 4-1. Scheme for the synthesis of PCBCL-PEG-PCBCL$_{PC}$ triblock copolymers by bulk and solution polymerization. n,m =1-18, x=33

Table 4-1. Characteristic of PBCL-PEG-PBCL$_{PC}$ copolymer synthesized by bulk polymerization (B_0) and its chemically reduced counterparts, i.e., PCBCL-PEG-PCBCL$_{PC}$ prepared at different reduction times.

Sample[a]	DP[b] Before reduction	Mol percentage of PBCL reduction	Theoretical MW (Da)	M_n (NMR)	M_n (GPC)	$\frac{Mn(GPC)}{Mn(NMR)}$	M_w (Da)	$Đ_M$	dn/dc (mL/g)
B_0	12.7	0	5910	4620	36700	7.9	69700	1.89	0.093
B_{20}	12.7	20	5580	4430	30800	7.0	64800	2.10	0.087
B_{40}	12.6	48	5110	4000	28400	7.1	63600	2.24	0.082
B_{60}	12.8	64	4843	3810	23200	6.1	60200	2.59	0.079
B_{120}	13	80	4575	3700	19900	5.4	55400	2.78	0.069

[a] B stands for Bulk polymerization. The number in the subscript shows the reduction reaction time in minutes. [b] Degree of polymerization (DP) of PBCL block measured by ^{1}H NMR in $CDCl_3$.

Table 4-2. Characteristic of PBCL-PEG-PBCL$_{PC}$ copolymer synthesized by solution polymerization (S_0) and its chemically reduced counterparts, i.e, PCBCL-PEG-PCBCL$_{PC}$ prepared at different reduction times.

Sample[a]	DP Before reduction	Mol percentage of PBCL reduction	Theoretical MW (Da)	M_n (NMR)	M_n (GPC)	$\frac{Mn(GPC)}{Mn(NMR)}$	M_w (Da)	$Đ_M$	dn/dc (mL/g)
S_0	14	0	5910	4920	47600	9.7	71300	1.50	0.103
S_{20}	14.4	20	5580	4750	41230	8.7	65760	1.59	0.102
S_{40}	14.4	35	5328	4560	37830	8.3	62600	1.66	0.100
S_{60}	14.3	52	5043	4370	30700	7.0	56900	1.85	0.094
S_{120}	14.4	72	4708	4220	21150	5.0	53300	2.52	0.055

[a] S stands for Solution polymerization. The number in the subscript shows the reduction reaction time in minutes. [b] Degree of polymerization (DP) of PBCL block measured by ^{1}H NMR in $CDCl_3$.

Upon chemical reduction of B_0, with a rise in the reaction time, the molecular weight of the polymer (measured by ^{1}H NMR) was reduced. A positive relatively linear correlation (r^2 of 0.84) was observed between chemical reduction time and degree of debenzylation for polymers in the "B" series (Figure 4-2A). With chemical increasing reduction time, M_n and M_w as measured by GPC, declined linearly (r^2=0.89 and 0.95 for M_n and M_w, respectively) (Figure 4-2B).

A similar effect was observed for "S" series, where a positive linear relationship (r^2 of 0.94) between the time of reduction and the percentage of debenzylation was noted (Figure 4-2C). The average M_n and M_w of polymer populations in the "S" series also decreased linearly with an increase in the debenzylation time (r^2=0.98 and 0.90 for M_n and M_w, respectively) (Figure 4-2D).

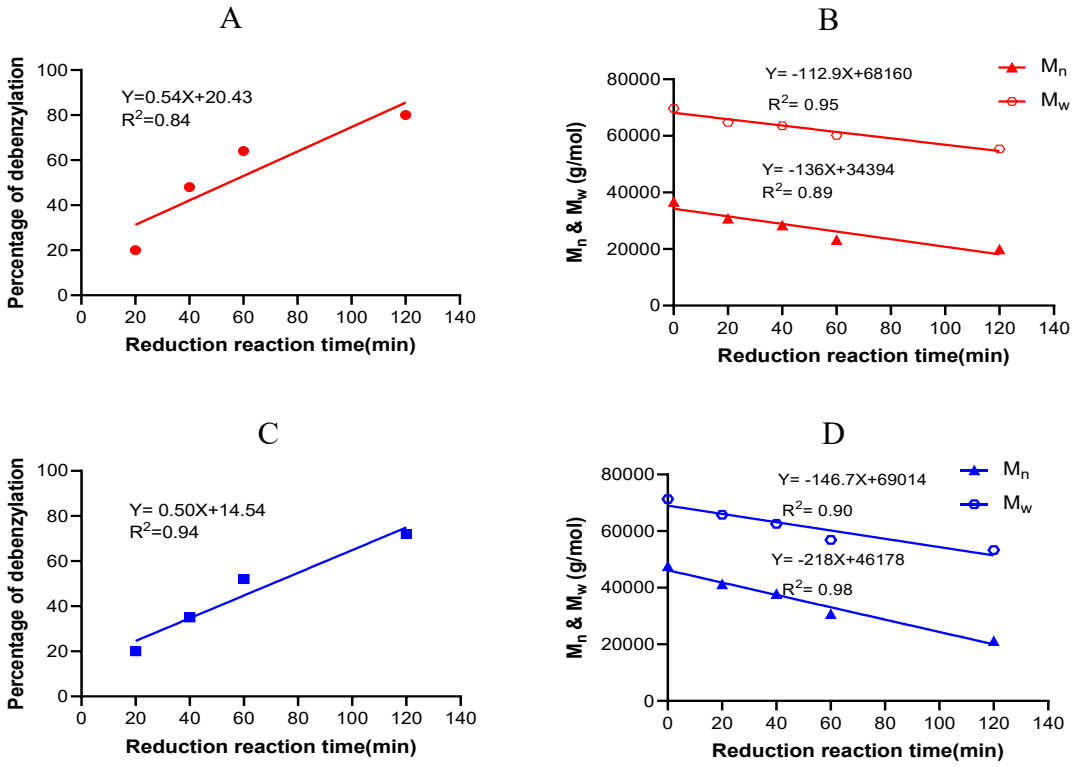

Figure 4-2. Correlation between reduction reaction time and percentage of debenzylation as measured by ^{1}H NMR spectroscopy (A & C) and M_n or M_w measured by GPC (B & D) for **A and B)** PBCL-PEG-PBCL$_{PC}$ copolymers in the "B" series (bulk polymerization); and **C and D)** PBCL-PEG-PBCL$_{PC}$ copolymers in the "S" series (solution polymerization).

The linear reduction in polymer molecular weights as a function of chemical debenzylation reaction time implies the lack of back-biting, chain- or cross-link cleavage during the reduction of PBCL-PEG-PBCL$_{PC}$ under experimental conditions.

Figure 4-3A shows the GPC profile of copolymers prepared by debenzylation of B_0 at different levels using an RI detector. Similar to the B_0 sample, the GPC elution profile of its reduced forms is bimodal and broad, indicating a wide molecular weight distribution. The elution peak at the lower retention time (peak 1) showed a 42% mole concentration of a large molecular weight population for the B_0 sample. Then based on our previous study [154] it meets the minimum requirement for producing thermogel.

The RI signal intensity depends on the concentration and the refractive index increment (dn/dc), in a concentration normalized peak, the RI signal area is an indication of the dn/dc value. It is worth noting that dn/dc is an essential parameter associated with the MW, size, shape, and concentration of polymers for several analytical techniques based on optical measurement [168]. Based on collected data from the GPC instrument (Table 4-1 and Figure 4-3A) in constant temperature, with a decrease in the MW of copolymers as a result of an increase in debenzylation, the value of dn/dc also decreased.

The molecular weight distribution (MWD) is an important factor that can affect different characteristics of the polymers and their self-assembled structures [124,169]. The $Đ_M$ was enhanced for all P**C**BCL-PEG-P**C**BCL$_{PC}$ copolymers under study as the degree of debenzylation in the polymers was raised. This happened irrespective of the PBCL-PEG-PBCL$_{PC}$ method of preparation (B_0 in Table 4-1 or S_0 in Table 4-2). This was expected and reflected the randomness of the debenzylation process. But, in general, the polydispersity of the chemically reduced polymers in the B series (Table 4-1) was higher than that of the S series (Table 4-2).The B_0 itself

has shown higher polydispersity compared to that of S_0. Again, this was expected due to lower reaction content viscosity, and higher molecular motions leading to the formation of more uniform populations in the solution polymerization products (S series) compared to the bulk polymerization ones (B series).

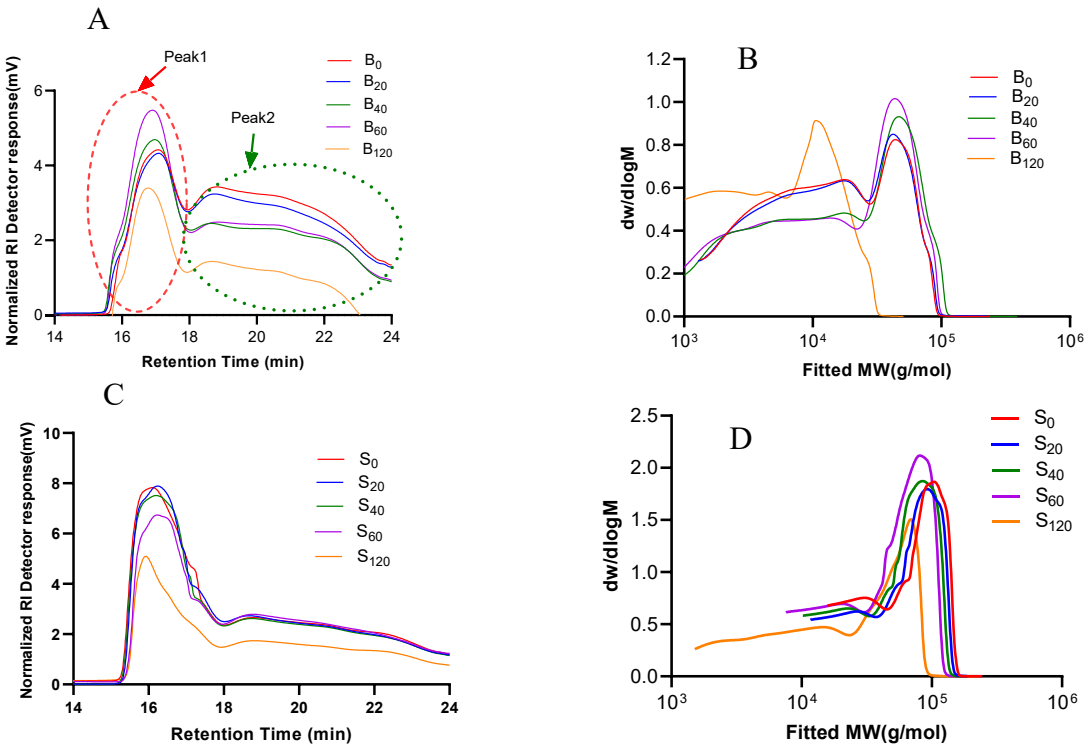

Figure 4-3. GPC elution profile detected by RI detector for **A:** "B" copolymers and **C:** "S" copolymers , **B:** Molecular weight distribution of **B:** "B" copolymers and **D:** "S"copolymers

From Figure 4-3B, it is evident that the MWD of the B_{120} has skewed to the lower molecular weight area because of the high percentage of debenzylation.

The GPC profile of "S" copolymers as detected by RI showed a bimodal shape, as well, pointing to the presence of a partially cross-linked polymer with a 51% mole concentration of high molecular weight population (Figure 4-3C). However, compared to the GPC profile for the "B" polymers, the elusion profile of "S" polymers were narrower, reflecting a lower polydispersity

index of "S" compared to "B" polymers due to the use of solution rather than bulk polymerization in the preparation of S_0 (Table 4-2).

Similar to the observation for the B_{120}, the S_{120} showed the lowest dn/dc and shifted to a lower MW area in the MWD graph (Figures 4-3C and 4-3D).

The GPC profile of the "B" copolymers based on the viscometer detector response is shown in Figure 4-4A. Again, similar to the RI response, the presence of bimodal polymer distribution is obvious. The viscosity of polymers is related to their molar mass and interaction with solvent through the Mark-Houwink-Sakurada (MHS) equation [170–172]. With an increase in the debenzylation percentage from 0 to 64 % in the "B" copolymers, the viscometer signal area increased. But the B_{120} polymer with around 80% debenzylation showed a drastically lowered detector response. The GPC elution profile of the "S" copolymers based on the viscometer detector (Figure 4-4B) and extracted data from GPC (Table 4-2) disclosed the lowest viscometer detector response and subsequently, viscosity belongs to the S_{120} sample, while average intrinsic viscosity increased by reduction time from 0 to 60 min.

The Mark-Houwink-Sakurada (MHS) equation (1) was then used to get an understanding of the polymers' molecular structure and conformation as related to these data. This equation explains the correlation of intrinsic viscosity and molecular weights from the experimental data [173] :

$$[\eta] = kM^{\alpha} \qquad (1)$$

$$\log [\eta] = \log K + \alpha \log [M]$$

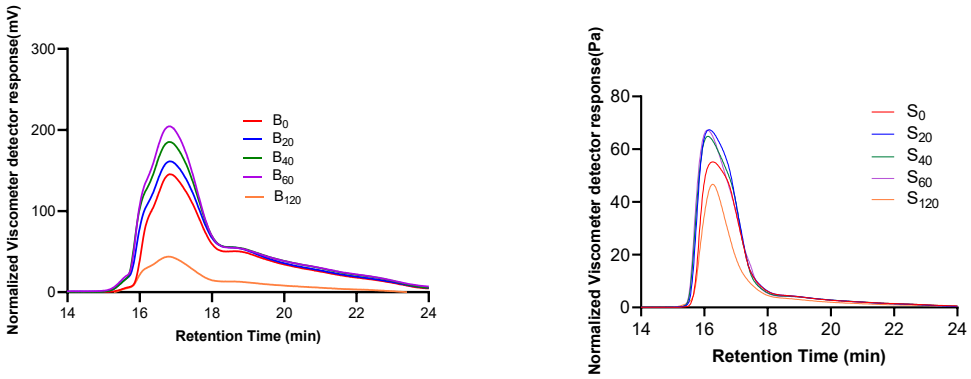

Figure 4-4. GPC elution profile measured by viscometer detector for **A:** "B" block copolymers and **B:** "S"copolymers.

Where α and K are constants depending upon the polymer type, solvent, and temperature of the viscometer detector and correspond, respectively, to the slope and intercept of the double logarithmic plot of molecular weight versus intrinsic viscosity. While α =~ 0.5-0.8 is expected for random coil polymers in a good solvent, α increases with an increase in the chain stiffness, and $\alpha < 0.5$ is related to the rigid sphere structure [173,174].

The MHS parameters for "B" polymers are shown in Table 4-3. The exponent α value of 0.73, 0.71,0.52 and 0.51 for B_0, B_{20}, B_{40} and B_{60} were obtained, respectively, which confirmed that these copolymers exist as a random coil conformation in THF at 30 °C. Whereas the exponent value for B_{120} was 0.42. Thus, the exponent value of B_{120} exhibited that the conformational structure was a spherical shape. . It is likely that at this structure carboxylic acid groups along with the C=O groups in the copolymer backbone attributed to creating spherical conformation due to the intermolecular hydrogen bonds. Similar observations were made for S_0, S_{20}, S_{40}, and S_{60} versus S_{120} in THF at 30°C (Table 4-4).

There are 2 common measurements of the molecular size based on GPC data: hydrodynamic radius (R_h) and radius of gyration (R_g). The R_h of the sample is the radius of a hypothetical sphere that

owns the same mass and density that is calculated for the sample based on molecular weight and intrinsic viscosity. The relationship between R_h, M, and [η] is shown in equation 2 (N_A is Avogadro's number).

$$[\eta]\, M = \frac{10\pi N_A}{3} . R_h^3 \qquad (2)$$

Also, R_g represents the distribution of mass center in the molecule and is calculated based on the light scatter detector response. The relationship between R_h and R_g depends on the molecular structure. For copolymers under study R_g was bigger than R_h irrespective of methods of polymerization. The average R_h and R_g for "B" and "S" series copolymers are shown in Table 4-3 and 4-4 respectively. Similar to "B" block copolymers, in debenzylated copolymers prepared from S_0, the average of R_g and R_h increased by an increase in the degree of debenzylation in the polymer.

Table 4-3. Characteristics of copolymers synthesized by bulk polymerization from GPC.

Sample[a]	Mol percentage of PBCL reduction	IV (dL/g)	α^b	K^b(dL/g)	R_h (nm)	R_g (nm)
B_0	0	0.14	0.73	4.44×10^{-5}	7.04	10.11
B_{20}	20	0.15	0.71	6.68×10^{-5}	7.05	10.16
B_{40}	48	0.16	0.52	56.94×10^{-5}	7.30	10.51
B_{60}	64	0.20	0.51	85.58×10^{-5}	7.46	10.75
B_{120}	80	0.17	0.42	331×10^{-5}	7.76	11.18

[a] B stands for Bulk polymerization. The number in the subscript shows a reduction reaction time in minutes.
[b] Mark-Houwink parameters.

Table 4-4. Characteristics of copolymers synthesized by solution polymerization from GPC.

Sample[a]	Mol percentage of PBCL reduction	IV (dL/g)	α^b	K^b(dL/g)	R_h (nm)	R_g (nm)
S_0	0	0.34	0.71	30.11×10^{-5}	7.08	9.55
S_{20}	20	0.40	0.62	84.30×10^{-5}	7.11	9.59
S_{40}	35	0.41	0.60	107.23×10^{-5}	7.17	9.68
S_{60}	52	0.42	0.56	157.37×10^{-5}	7.34	9.91
S_{120}	72	0.26	0.47	204.97×10^{-5}	7.72	10.42

[a] B stands for Bulk polymerization. The number in the subscript shows a reduction reaction time in minutes.
[b] Mark-Houwink parameters.

Thermo-responsive behaviour of the aqueous solution of block copolymers

Temperature-dependant viscoelastic gelation of the aqueous solution of "B" and "S" block copolymers under study was investigated through small amplitude oscillatory shear rheology and vial inversion test (inverse flow method). The change of storage modulus (G′), loss modulus (G″) and complex viscosity (η*) as a function of temperature for an aqueous solution of "B" copolymers at 10 and 15 wt% concentration is shown in Figure 4-5. B_{20} and B_{120} samples showed the behaviour of viscoelastic liquids, where G″ dominate G′ in all temperature (10-50°C) (Figure S4-1). The B_0, $B_{40,}$ and B_{60} samples, on the other hand, showed a distinct thermo-gelling behaviour with the sol-to-gel transition around 34, 24, and 27°C respectively, at 10 Wt%, as evidenced by the crossover of the G′ and G″ graphs and drastic increase in η* graph (Figure 4-5A).

Subsequently, we increased the concentration of B_0, $B_{40,}$ and B_{60} solution to 15 wt% (Figure 4-5B) and noticed thermo-reversible sol-gel behaviour for these samples where the transition temperatures were lowered to 23, 17, and 19°C, respectively. The lowered transition temperature can be attributed to a higher chance of polymer chain interaction and/or micellar aggregation at higher concentrations. Also, the gel window in 15wt% polymer concentration was broader compared to 10 wt% samples. By increasing the concentration of polymer solution, moduli of copolymers significantly increased indicating better mechanical stability of gel at this concentration. Among B samples under study, B_{40} showed higher moduli and viscosity compared to B_0 and B_{60} (Figure 4-5B).

The temperature dependant phase transition behaviour of the aqueous solution of $B_{0,}$ $B_{40,}$ and B_{60} at various polymer concentrations 10, 15, and 20 wt%) determined by the inverse flow method is shown in Figure 4-5C. The B_0 at 10 wt% polymer concentration formed gel at 34°C (lower transition temperature), as the temperature raised to 36°C, a turbid solution was achieved (upper

transition temperature). By raising polymer concentration from 10 to 15 and 20 wt%, the lower transition temperate declined from 34℃ to 30 and 25℃ respectively. On the other hand, upper transition temperature for B_0 increased to 38 and 40℃ by elevating polymer concentration. Similar behaviour was observed for B_{40} and B_{60} where the gel window became broader by increasing of polymer concentration.

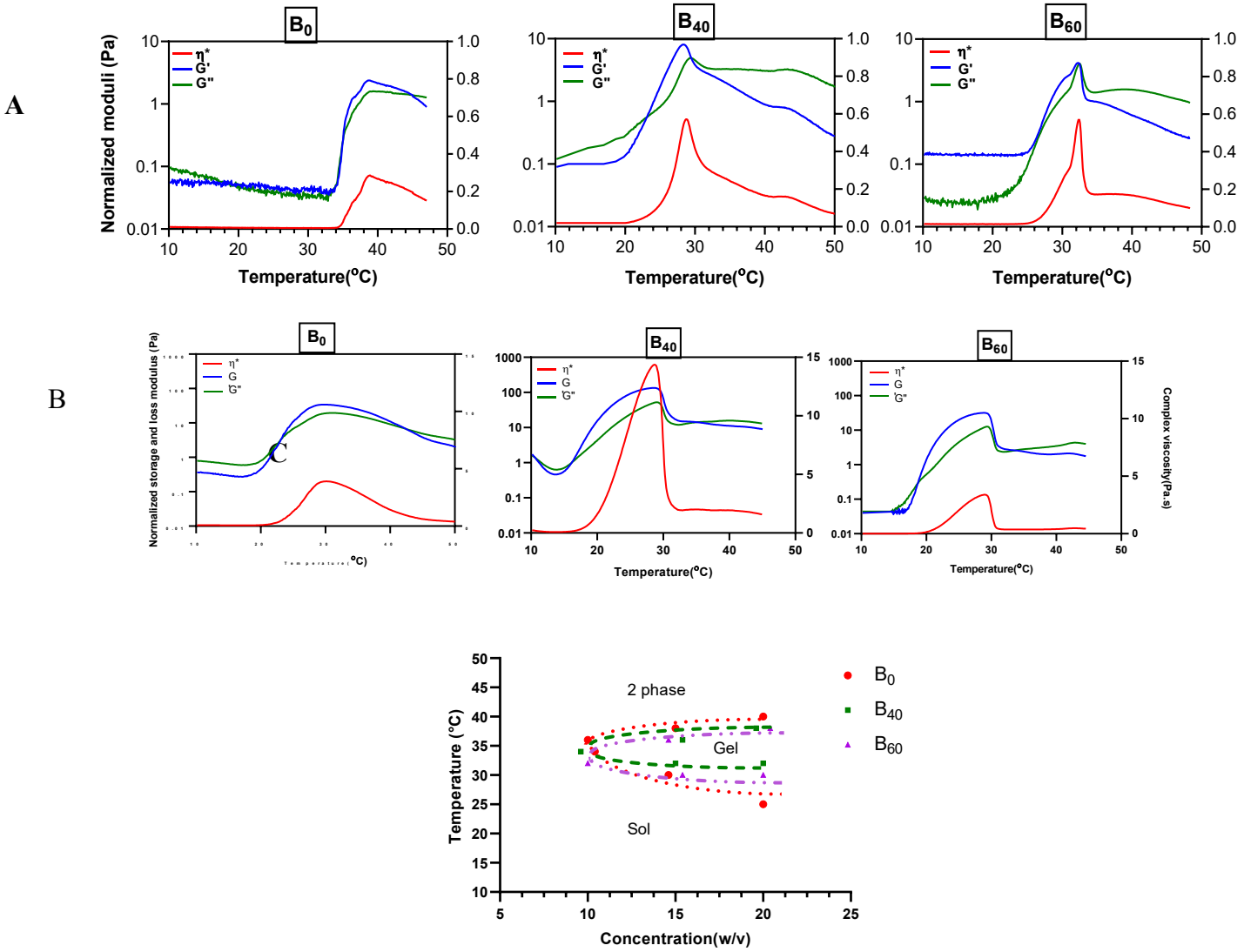

Figure 4- 5. Evolution of moduli and viscosity in a temperature ramp experiment 10-50℃ with ramp rate of 1℃/min for "B" copolymers aqueous with concentration **A:**10 wt% and **B:**15 wt% . The dash line show intersection of G′ and G″(sol-to-gel point). **C:** State diagram of Sol-gel transition for "B" copolymer aqueous solution at concentration 10, 15, 20 mg/ml.

The thermo-responsive behaviour of "S" copolymers at different concentrations is shown in Figure 4-6. The S_0 sample had very low sol-to-gel transition (around 10℃) at all concentrations under study (where G′ dominate G″). For the S_0, at 15% polymer concentration, a sol-to-gel transition around 12℃ and gel-to-sol transition around 40℃ were noted (Figure 4-6B). The S_{20} polymer did not show thermo-gelling behaviour at different concentrations under study. There was the cross-over of G' and G" modulus at 10 wt% for S_{20}, but there was no rise in η* for this sample (Figure S4-2). Rheology test revealed S_{40} has a sol-to-gel transition temperature of 24℃ and 22℃ at 10 and 15wt% respectively, while the inverse flow method showed a higher transition temperature for this sample (36℃ and 34℃ for 10 and 15 wt%, respectively). The inverse flow method showed the S_{60} sample to have lower transition temperatures of 22, 20, and 18℃ for 10, 15, and 20 wt% polymer concentrations, respectively. The upper transition temperature for S_{60} was 32, 37, and 38℃ at the above concentrations, respectively, which confirmed the rheology results. Although S_{120} showed the peak at around 16℃ for 10wt%, this sample didn't show thermo-reversible behaviour in concentration under study based on the inverse flow test (Figure S4-2).

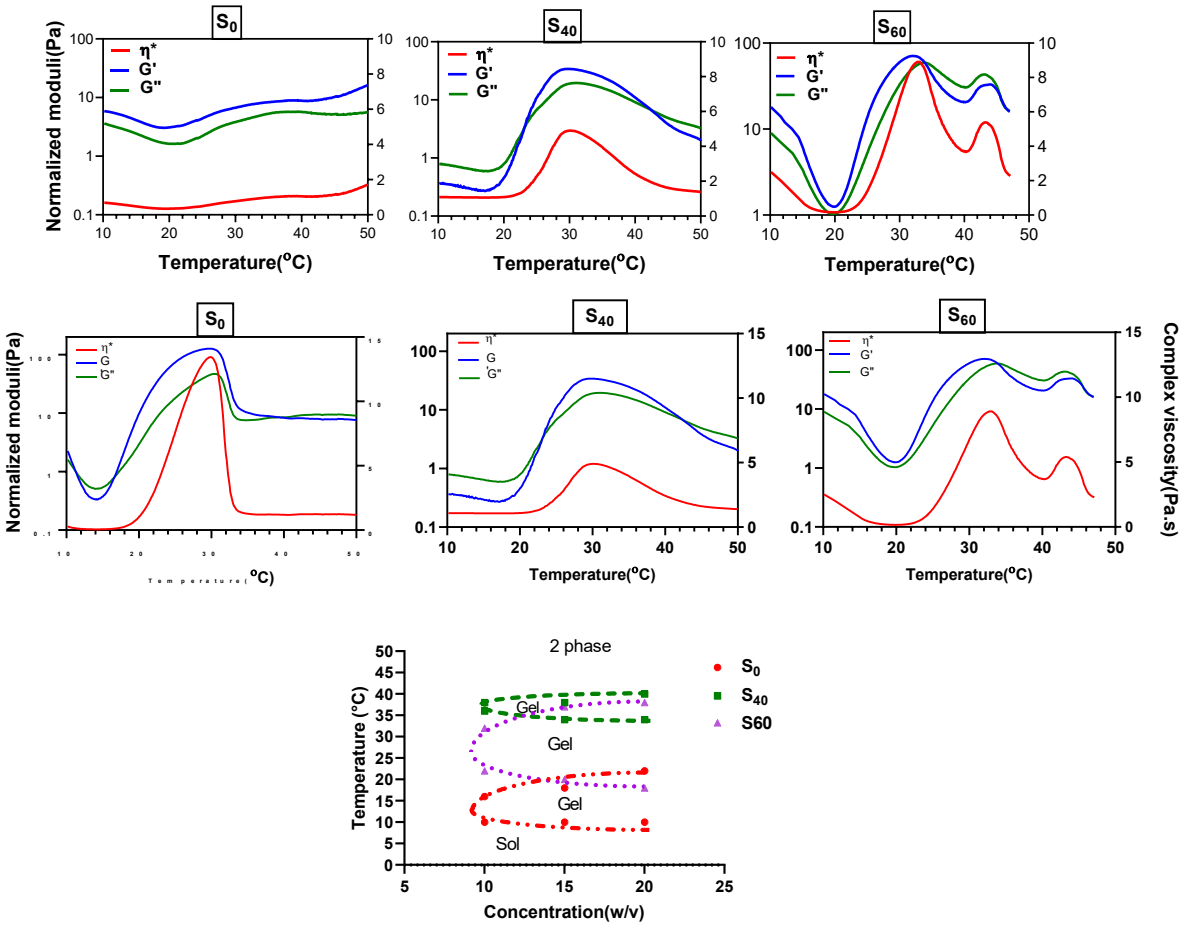

Figure 4-6. Viscoelastic behaviour of "S" copolymers aqueous solutions as a function of temperature at a heating rate 1 °C/min (10-50°C) for **A.** 10 wt% and **B.** 15 wt% polymer concentration **C:** State diagram of Sol-gel transition for "S" copolymer aqueous solution at concentration 10, 15, 20 mg/mL.

All copolymers under study (B and S series) can be self-assembled at ambient temperature in water. Figure 4-7 shows the negative correlation between the aggregate size and percentage of debenzylation or reduction time regardless of the method of polymerization. Indeed, by increasing the debenzylation time from 0 to 120 min for the "B" series, the aggregate size decreased gradually from 136 nm to 68.5 nm, this increment is more significant for the "S" series while the aggregate size of S_0 (295 nm) was declined to 68.5 nm for S_{120}.

While all copolymers under study can self-assemble into micelle in water, reverse thermo-gelling is complicated and puzzling for these copolymers. The mechanism of reversible sol-gel transition in copolymers is still unknown. Further investigation is required to define the mechanism of thermo-gelation in these polymers which may include micelle aggregation, micelle bridging and more recently percolated micelle network [40,41]. In this study, we speculated gelation of copolymers in water follow the percolated micelle network model: at low temperatures, the copolymers can self-assemble to micelles with core-corona structure, by increasing the temperature, the corona of micelles collapses due to reverse thermo-sensitivity of PEG [108]; if the corona becomes sufficiently thin, might not cover the hydrophobic core and forming semi-bare or semi-bald micelles. Owing to the hydrophobicity of the micellar core, hydrophobic interaction occurs which promotes aggregation of micelles. To explain the gelation behaviour of various copolymers under study, we focus on specifications of the hydrophobic part since the molecular weight of PEG (1450 Da) as the middle block of triblock is constant for all polymer under study.

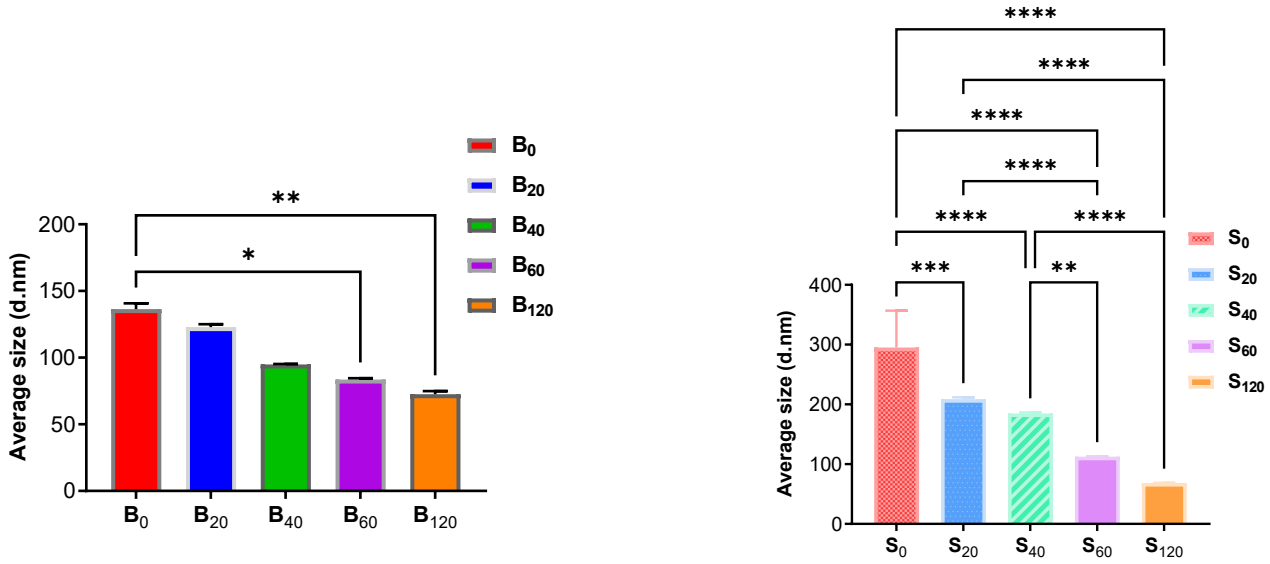

Figure 4-7. The effect of debenzylation time on the size of self-assembled structures from block copolymers synthesized by **A:** Bulk, **B:** Solution polymerization at 25ºC. ℃. Results are presented as Mean ± SD (n=3). Asterisks denote significant difference at P<0.05.

4.4 Conclusions

The results of this study showed that the percentage of debenzylation in partially cross-linked PCBCL-PEG-PCBCL copolymers to affect the thermo-gelation of aqeous solution of these samples. Copolymers with 35-60 % debenzylation, showed thermoreversible behaviour.

Chapter 5. Preparation and characterization of lipocells, liposomes encapsulating polymeric micelles, as a promising new nano-drug delivery system

5.1. Introduction

Liposomes are self-assembled phospholipids formed from natural or synthetic lipids that can be used for drug delivery. Liposomes have several advantages over other carrier systems such as biocompatibility, ability to carry hydrophilic and hydrophobic drugs, and transport ability via cell membrane [175–177]. However, liposomes have a short half-life, low stability, poor encapsulation efficiency for some drugs, and fast leakage specially for hydrophilic drugs[175,178]. Besides, the opportunity for chemical manipulation of lipids for different needs is lower than polymers. Polymeric micelles are another class of nanocarriers used for drug solubilization and targeting. Hybrid nanocarriers formed by liposomal coating of polymer based nanoparticles have been investigated for delivery small molecules[179–182], and siRNA[183,184]. These new nanodelivery system possess the complementary advantages of polymeric nanoparticles and liposomes[185].

Using copolymers incorporated liposomes can improve physicochemical stability of liposomes, provide stimuli-responsive properties for liposomes, avoid "burst release" of drugs and provide a versatile targeting platform[177,186].

In 2005, Huang *et al* developed a new drug carrier by using liposomes encapsulating the chitosan nanoparticles loaded with a model drug Fluorescein sodium (FS) for improved drug encapsulation. They showed liposome-encapsulating chitosan nanoparticles are more stable and have a slower *in vitro* release rate compared to chitosan nanoparticles or liposomes alone. The FS in liposome-encapsulating chitosan nanoparticles administered to rats exhibited prolonged circulation and higher bioavailability than FS in chitosan nanoparticles [187].

In 2013, Wang *et al*, for the first-time developed poly (acrylic acid) hydrogel in a liposome (lipogel) as a promising drug delivery vehicle for active encapsulation of the anticancer drug (17-DMAPG). They demonstrated that a pH gradient and electrostatic interactions between a cationic

drug and anionic gel in the liposomal core were critical for the active encapsulation of 17-DMAPG. Also *in vitro* cell culture studies revealed lipogel did not exert cytotoxicity on the cells [188].

Examples on the incorporation of block copolymers capable of forming polymeric micelles in liposomes are scarce in the literature. In 2015, Zhang *et al* developed a lipid-polymer carrier consisting of PCL-PEG-PCL amphiphilic copolymer as a core and folate modified shell of DSPE-PEG2000 for targeted delivery of paclitaxel. In EMT6 breast tumor model, intratumoral administration of PTX-loaded folate modified lipid-shell and polymer-core nanoparticles showed similar antitumor efficacy but lower toxicity compared to Taxol® [180].

We have reported on the synthesis and characterization of thermo-responsive triblock copolymer using polymerization of α-benzyl carboxylate-ε-caprolactone (BCL) by dihydroxy poly (ethylene glycol) (PEG) leading to the production of PBCL-*b*-PEG-*b*-PBCL [153,154], In the present study, we explore the potential for the encapsulation of partially debenzylated PBCL-PEG-PBCL block copolymer in liposomes. Triblock copolymer of poly(α-carboxyl-co-benzyl carboxylate-ε-caprolactone)-b-poly(ethylene glycol)-b-poly(α-carboxyl-co-benzyl carboxylate-ε- caprolactone) (PCBCL-PEG-PCBCL) were prepared and characterized for their molecular weight and polydispersity by ^{1}H NMR and gel permeation chromatography (GPC), respectively. Rheological methods and differential scanning calorimetry (DSC) were used to measure the gelling temperature of block copolymer solution. The triblock copolymer was labeled with Doxorubicin (DOX), as a fluorescent tag, through chemical conjugation of DOX to the free carboxyl group of PCBCL. This fluorescently tagged block copolymer was then loaded in liposome via freeze-thaw method and the resulted lipocells were purified from unloaded polymeric micelles. The encapsulation of polymers within liposomes and the morphology of the hybrid delivery system versus pure lipid or polymer based assemblies was then investigated by electron microscopy.

5.2. Experimental

5.2.1. Materials

α-benzyl carboxylate-ε-caprolactone (BCL) was synthesized by Alberta Research Chemicals Inc (ARCI), Edmonton, Canada. Hydrogenated soybean phosphatidylcholine (HSPC), N-(carbonyl methoxy polyethylene glycol 2000)-1,2-distearoyl-sn-glycero3-phosphoethanolamine sodium salt (MPEG-DSPE) and Cholesterol were purchased from Avanti Polar Lipids. Doxorubicin(DOX.HCL) was purchased from Hisun Pharmaceutical Co.(Zhejiang, China). Dihydroxy PEG (MW=1450 Da), palladium coated charcoal, *N,N*-dicylcohexyl carbodiimide (DCC), N-Hydroxysuccinimide (NHS), and solvents such as dimethylformamide (DMF), tetrahydrofuran (THF), dichloromethane (DCM), and hexane (chemical reagent grade) were purchased from Sigma-Aldrich (St. Louis, MO).

5.2.2. Methods

5.2.2.1 synthesis of PBCL-PEG-PBCL and PCBCL-PEG-PCBCL block copolymers.

The PCBCL-PEG-PCBCL block copolymer was synthesized in 2 steps (Figure 1): in the first step ring opening polymerization of BCL using PEG as initiator was accomplished as described in our previous publication[154]. In brief 0.6 g of BCL and 0.19 g of PEG were dehydrated in a vacuum oven at 70°C for 3h, then a polymerization reaction was conducted at 160 °C in a 10 mL ampule sealed under vacuum for 17 h. Prepared triblock copolymers were purified by dissolving the products in tetrahydrofuran (THF), followed by precipitation using anhydrous ethyl ether. The sediment was dried under vacuum for 24 h. In the second step, reduction or debenzylation of PBCL-PEG-PBCL was accomplished in the presence of hydrogen gas, palladium on activated charcoal as catalyst (10 wt.% of the polymer), and dry THF as a solvent for 60 min. The final

product was centrifuged 2 times at 3000 rpm for 5 min to separate charcoal, then the supernatant was dried under vacuum for 24 h.

5.2.2.2 Characterization of triblock copolymer

Gel Permeation Chromatography (GPC). Copolymer solution was analyzed for a different type of molecular weight, molecular weight distribution, and molar-mass dispersity ($Đ_M$) by gel permeation chromatography (GPC). The GPC was carried out at 35 °C and equipped with 3 detectors (Refractive index (RI), light scatter (LS), and viscometer (VS)) and 2 columns (styragel HR2 and styragel HR 4E from waters company). The instrument was calibrated with a set of polystyrene standards and THF was used as eluent at a flow rate of 0.7 mL/min. The elution time for all polymers was 30 min. During this time, the GPC chromatogram came back to the baseline while for clarity of presentation, elution time was selected from 14-24 min in all GPC graphs.

Nuclear Magnetic Resonance (NMR). ^{1}H NMR spectra were acquired by Bruker Avance III HD 600 MHz at room temperature using chloroform-d ($CDCl_3$) as solvent. The degree of polymerization (DP) and number of average molecular weight (Mn) of block copolymers were calculated by comparing the area under the peak of methylene protons of the PEG block (CH_2CH_2O-, δ=3.65 ppm) to the methylene protons of the PBCL backbone (-OCH_2-, δ= 4.1 ppm). The M_n of the PEG block was considered as 1450 g/mol for these calculations. The percentage of reduction was estimated by the following equation.

$$\text{Reduction} = \frac{(DP \text{ of PCBCL backbone}) - (\text{benzyl substitution on PCBCL})}{(DP \text{ of PCBCL backbone})}$$

Discovery Hybrid Rheometer (DHR instrument). Thermo-responsive behavior of copolymer with 10% concentration was examined by the DHR instrument which was equipped with parallel plate geometry and the heating rate was 1 °C/min (10-50°C), with angular frequency ω as 10 rad/s.

Modulated Differential Scanning Calorimetry (MDSC). In this study thermal analysis was accomplished with Q series TM 2000 modulated differential scanning calorimeter. An aqueous solution of reduced triblock copolymer at a concentration of 10%wt was prepared and kept in the refrigerator overnight. The sample was hermetically sealed. First, the sample was heated to 70°C to remove thermal history and after 5 min ramp 10°C/min to 8°C. Heating was recorded using modulated mode with an amplitude of 0.2°C every 30s, after isothermal for 5 min, ramp 0.5°C/min to 10 °C. This was followed by holding the sample at 10°C for 60 minutes, and then increasing the temperature to 70°C with the same rate under nitrogen gas. The pan filled with distilled water was used as a reference.

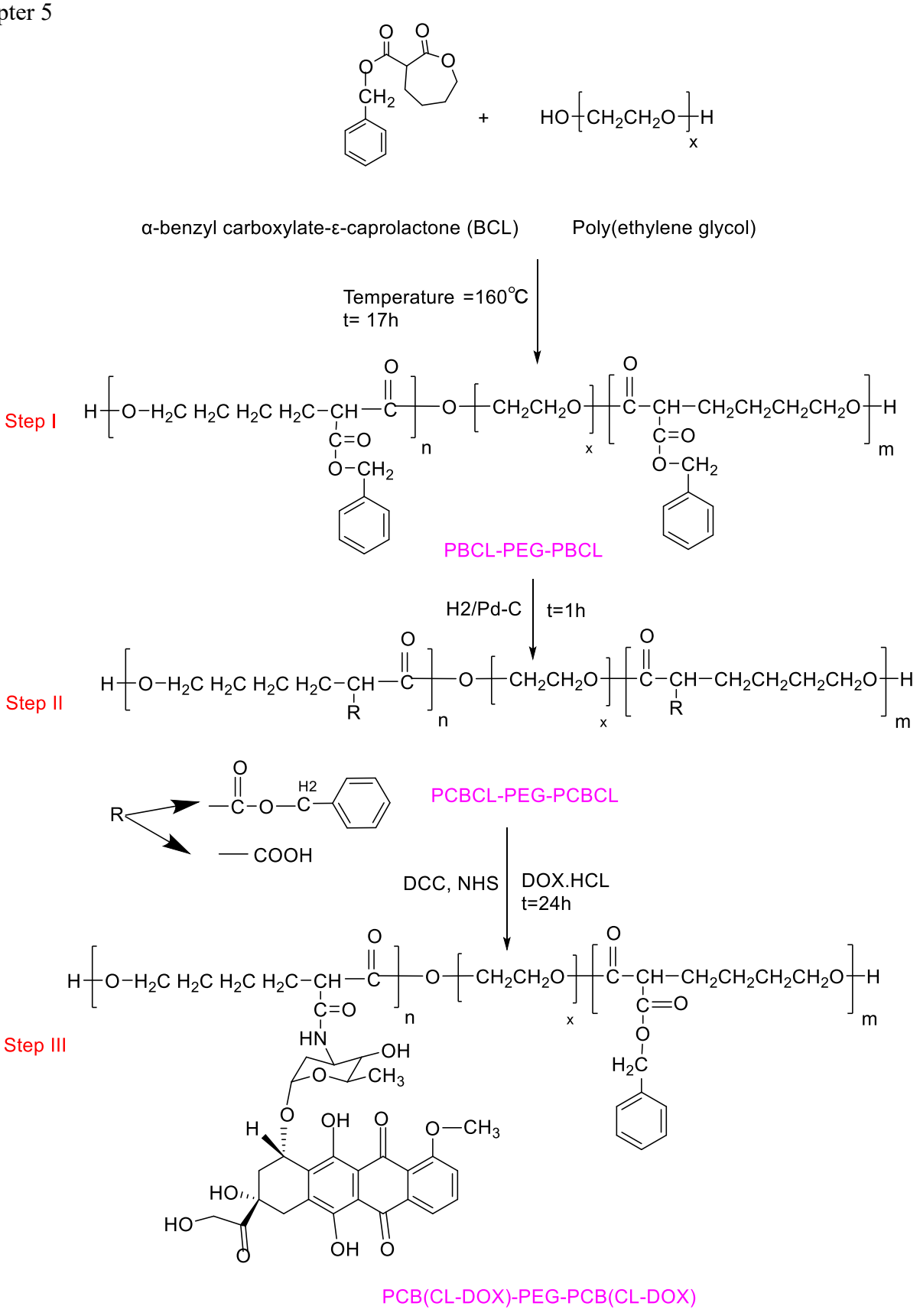

Figure 5-1.Synthetic schematic for the preparation of PCB(CL-DOX)-PEG-PCB(CL-DOX). n, m=1-18, x=33

5.2.2.3 Synthesis of PCB(CL-DOX)-PEG-PCB(CL-DOX)

PCB(CL-DOX)-PEG-PCB(CL-DOX) was prepared through the conjugation of DOX as a fluorescent probe to PCBCL-PEG-PCBCL by amide bond formation between the amino group of DOX and free carboxyl groups on the PCBCL chain using DCC and NHS (Figure **5-**1).

Briefly, DCC (82.5mg, 0.4 mmol) was added to the solution of PCBCL-PEG-PCBCL (200mg, 0.05 mmol) in 4 mL dry THF, and stirred for 20 min, then NHS (46 mg, 0.4 mmol) was added, and the reaction mixture was left under argon gas while stirring for 3 h until precipitate (dicyclohexylurea or DCU) was formed. The precipitate (DCU) was removed by centrifugation and the supernatant was dried under a vacuum. The solution of DOX.HCL (8mg, 0.014 mmol) and triethylamine (2 mg) in 10 ml dry DMF were added dropwise to the polymer solution (polymer dissolved in 3 mL dry DMF). The reaction proceeded for 24 h at room temperature under argon gas away from light. The resulting solution was centrifuged to remove the precipitate then added to 50 mL ether to remove the crude product and DMF, then freeze-dried overnight. Chemically conjugated polymer dissolved in 3 mL toluene and vortexed for 15 min then pour in hexane. After 2h supernatant and sediment were sent for thin-layer chromatography(TLC) in presence of methanol/ethyl acetate (3/1) as a mobile phase to confirm the absence of unbound free DOX. The resulted polymeric-DOX conjugate in solution was finally freeze-dried for further use.

5.2.2.4 Preparation of polymer incorporated liposomes (Lipocells)

To prepare liposome, 65.6 mg HSPC, 32.8 mg cholesterol, and 4.6 mg MPEG-DSPE (with mole ratio 2:1:0.14) were dissolved in 4 mL chloroform in a 10 mL round bottom flask. The solvent was evaporated on a rotary evaporator under vacuum for 1h. The dry lipid film was kept in a vacuum oven overnight, then the resulting dried lipid film was rehydrated with 1 mL distilled water. The flask was then rotate by rotary evaporator for 1h at 65°C for the vesicles to be formed. The size of

self assembled structures was reduced by 20 min sonication. The copolymer conjugated Dox solution (10% w/v) was added to the liposome with vigorous shaking for 30 min. Seven freeze-thaw cycles were done using liquid nitrogen and a water bath (65°C). Finally, the unencapsulated polymer was separated from the liposome through size exclusion chromatography(SEC) with sepadex LH-20 and water as eluent.

5.2.2.5 Characterization of particles

Zetasizer. A Malvern Nano-ZS90 Zeta-sizer (Malvern Instruments Ltd, Malvern, UK) was used to measure the self-assembly of copolymers and hydrodynamic diameter of the liposome and or liposcells at 25°C. Three measurements were made for each sample and the average data was reported.

TEM and cryo-TEM imaging.

The morphology of the self-assembled structure for PCBCL-PEG-PCBCL triblock copolymer solution in water, liposome, and lipocells was determined by Transmission Electron Microscopy (TEM) (FEI Morgagni TM 268, North America Nano Port, Oregon, USA). In sample preparation, the polymer with 10% w/w concentration was deposited on a copper grid, dried at room temperature for 30s, and examined using TEM by negative staining with 2% PTA (phosphotungstic acid) at 80 kV. Liposomes and lipocells were imaged by cryogenic transmission electron microscopy (cryo-TEM). A few μL of solution samples were placed on glow-discharged holey carbon grids and plunged frozen in liquid ethane using a Vitrobot vitrification device (FEI). Images were recorded with a T20 microscope (FEI) at 200 kV while sample imaging was maintained at different viewing angles.

5.3. Results and discussion

5.3.1 Synthesis and characterization of PCBCL-PEG-PCBCL copolymer

The PCBCL-PEG-PCBCL copolymers were synthesized in 2 steps: in the first step ring, opening polymerization (ROP) of BCL and PEG was accomplished by a bulk method in 17h. In the second step, the synthesized copolymer (PBCL-PEG-PBCL) was debenzylated in the presence of hydrogen gas and catalyst for 60 min. Table 5-1 shows the characteristics of synthesized copolymers based on ^{1}H NMR spectroscopy and GPC. The prepared PBCL-PEG-PBCL was expected to show thermo-responsive behavior based on our previous studies. The ratio of $M_{n(GPC)}/M_{n(NMR)}$ was 9.4. Besides, the GPC elution profile (Figure 5-2A) and molecular weight distribution (Figure 5-2B) of this sample showed a high molecular weight population in the structure. Half of the benzyl carboxylate substitution in PBCL were converted to the carboxyl group and the solution of the polymer at a concentration of 10 wt% at 30℃ created a turbid gel. The sol-gel transition of the polymer solution was investigated by rheological experiments and DSC. The PCBCL-PEG-PCBCL solution showed thermo-gelling behavior with the sol-gel transition around 27℃ as evidenced by the crossover of G′ and G″ (Figure 5-3A).

Table 5-1. Characteristic of copolymer synthesized using ring-opening polymerization of purified BCL by PEG 1450 Da. The theoretical MW of copolymers was 6000 g/mol.

Sample	DP[a]	DR[b]	M_n [c] (Da)	M_n [d] (Da)	M_n (GPC)/M_n (NMR)	M_w (g/mol)	$Đ_M$[e]	Appearance in water at 30℃
PCBCL-PEG-PCBCL	14	50%	4270	40300	9.4	85000	1.91	Gel

[a] Degree of polymerization (DP) of PBCL block measured by ^{1}H NMR. [b] Degree of reduction (percentage of PBCL debenzylation). [c] Number average molecular weight of block copolymer measured by ^{1}H NMR.[d] Number average molecular weight of block copolymers measured by GPC. [e] polydispersity index (M_w/M_n).

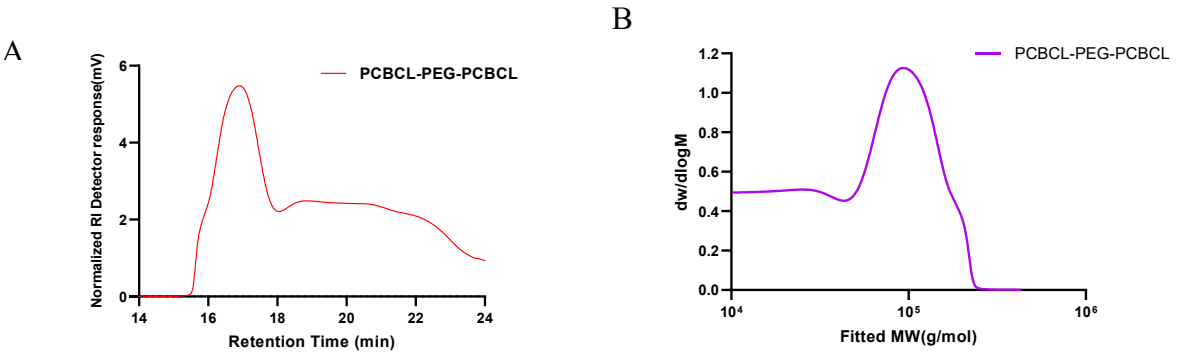

Figure 5-2. **A** GPC elution profile detected by RI detector. **B**. molecular weight distribution of copolymer

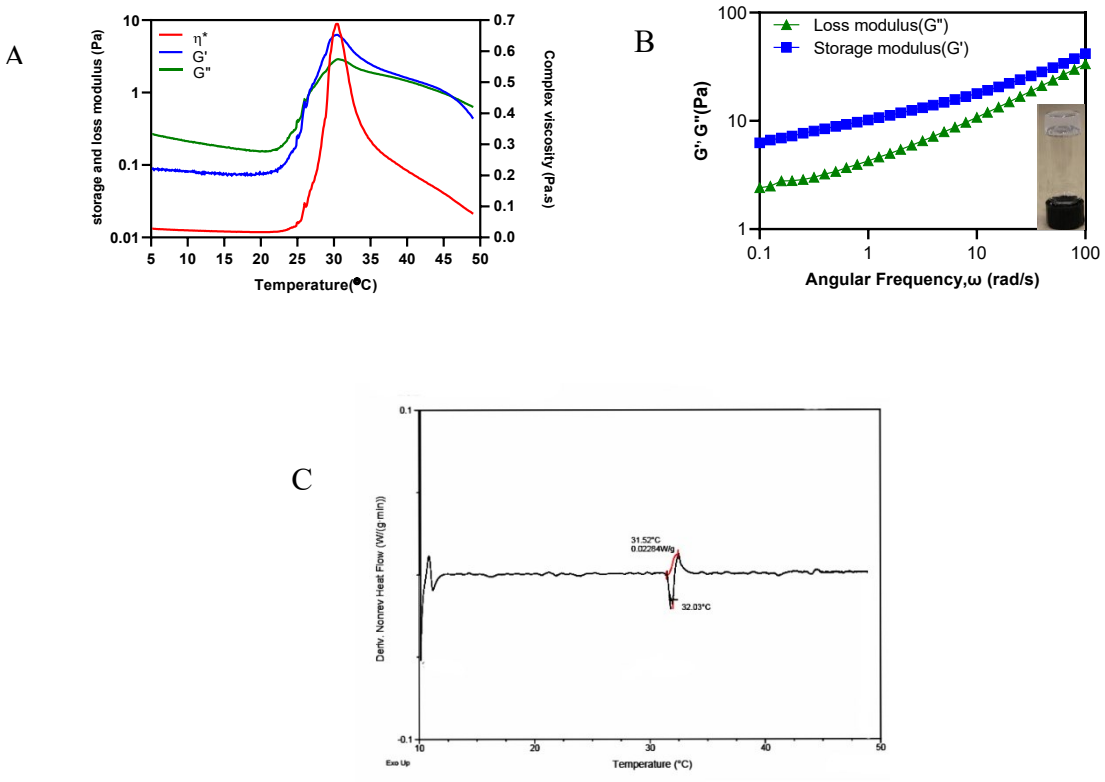

Figure 5-3. Dynamic rheology data for 10 wt% polymer solution for 2 cases: **A** storage modulus (G′), loss modulus (G″) and complex viscosity(η*) as a function of temperature and **B:** G′ and G″ plotted against frequency ω. **C:** Modulated DSC thermograms of block copolymer solution in distilled water at 10% w/w concentration.

The polymer solution showed the properties of an elastic gel which can hold its weight in a tilted vial (Figure **5-**3B) also these visual observations were quantified by dynamic rheology through measurement of storage and loss modulus as a function of frequency. The copolymer solution showed gel-like behavior and the value of G′ exceeded that of G″ independent of frequency.

5.3.2. Synthesis and characterization of PCB(CL-DOX)-PEG-PCB(CL-DOX)

Doxorubicin was chemically conjugated to the PCBCL-PEG-PCBCL via a covalent reaction of the primary amine group of Dox to the carboxylic group of the PCBCL chain using DCC and NHS as coupling agents as shown in Figure 5-1. Free and unbound Dox was separated by centrifugation and decantation. Then successful separation and removal of free DOX was examined by Thin-Layer Chromatography (TLC). As shown in figure 5-4, free Dox showed 2 spots, the lower part is related to the Dox.HCL salt and the upper part shows unionized Dox. Unlike the Pol.Dox supernatant, the sediment of Pol. Dox doesn't have free Dox. The successful conjugation between DOX and PCBCL-PEG-PCBCL was investigated by ^{1}HNMR spectra (Figure 5-5).

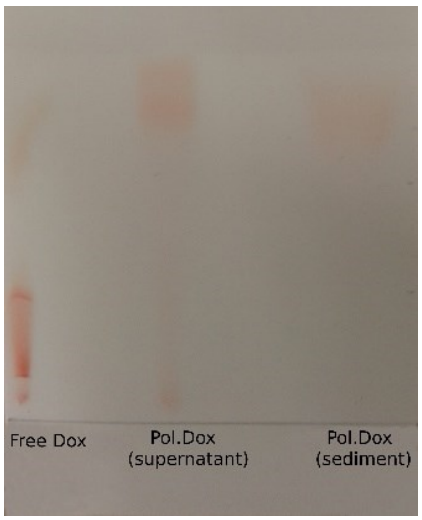

Figure 5-4. TLC of free Dox , supernatant, and sediment of PCB(CL-DOX)-PEG-PCB(CL-DOX) solution sample.

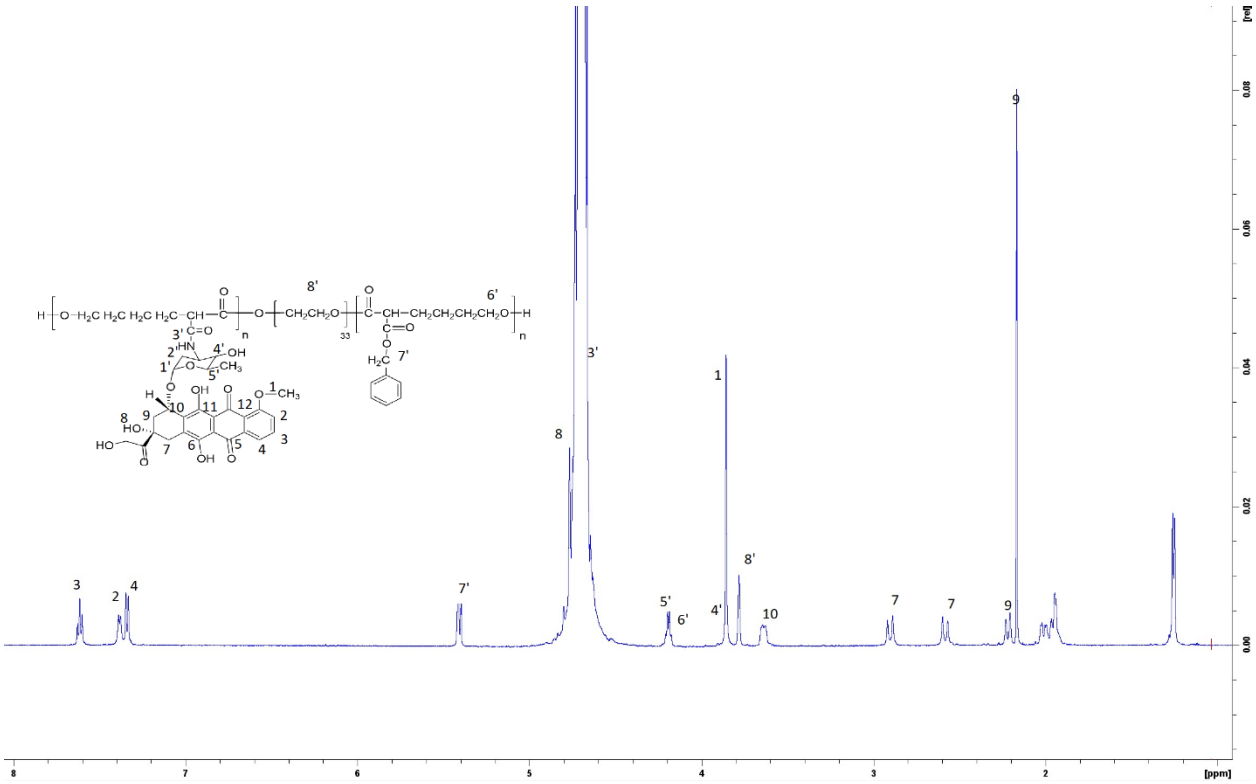

Figure 5-5.^{1}H NMR spectrum of PCB(CL-DOX)-PEG-PCB(CL-DOX) in D_2O.

3.3. Characterization of lipocells

liposome was prepared by the thin-film hydration method, then PCB(CL-DOX)-PEG-PCB(CL-DOX) was encapsulated in liposome through the freeze-thaw method. Finally, unencapsulated polymers were separated by SEC. The dynamic light scattering (DLS) technique was used to measure the hydrodynamic radius of the liposome, self-assembled structures from PCB(CL-DOX)-PEG-PCB(CL-DOX), and PCB(CL-DOX)-PEG-PCB(CL-DOX) lipocells (Figure 5-6). The PCB(CL-DOX)-PEG-PCB(CL-DOX) particle size distribution depicts uniform particle size with a Z-average of 101.5 nm and PdI of 0.271 (Figure 5-6A). The size distribution of liposomes

showed 3 peaks with average mean intensity sizes of 519.6, 88.21, and 2698 nm for peaks 1, 2, and 3 with the intensity of 66.8, 17.3, and 15.9% respectively (Figure 5-6B). For the lipocells, the size distribution represented 2 peaks with an average size of 401.3 and 74.47 nm and intensity of 76.4% and 24.6% (Figure 5-6C). Because the polymer peak and peak 2 of liposome have overlap, DLS size distribution cannot prove encapsulation of polymer inside the liposome. Then we tried to investigate encapsulation of triblock copolymer inside liposome by morphological characterization through TEM and cryo-TEM. The TEM images of PCBCL-PEG-PCBCL show the tendency of the copolymer for micellar aggregation (Figure 5-7A). Also, the TEM of liposome represents the large unilamellar vesicles (LUVs) of liposome (Figure 5-7B). In the TEM images of liposome-polymer complex (or lipocell) s, inside the liposome. There is a small spherical shape structure that is supposed to be self-assembled structures from the Dox labeled copolymer, but we can't prove the copolymer is in the core of liposome or not by TEM as the co-localization of the two structures can be an artifact of the 2-dimensional assessment by TEM.

A

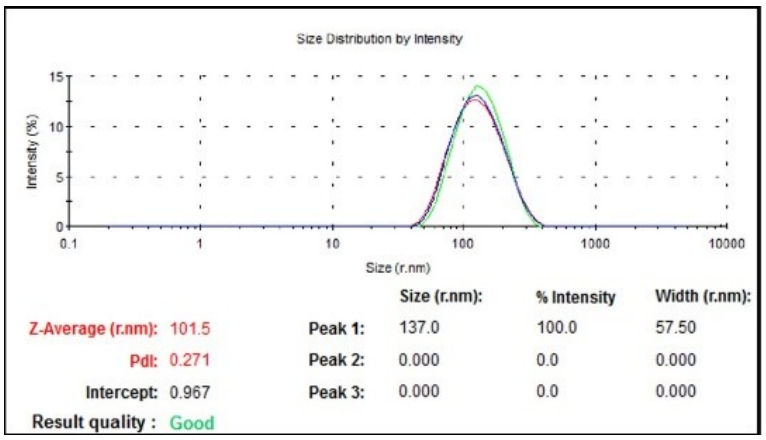

B

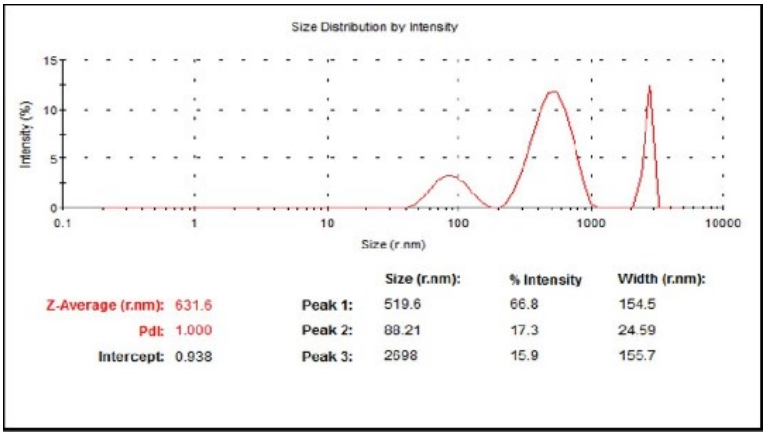

C

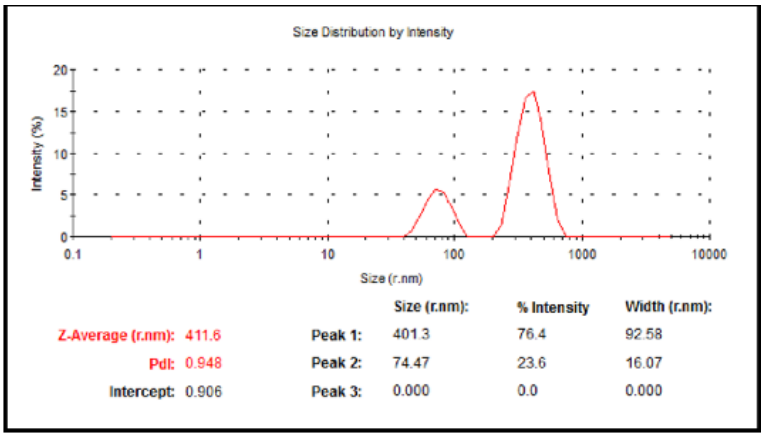

Figure 5-6. DLS data for **A:** PCBCL-PEG-PCBCL copolymer **B:** liposome and **C:** Lipocell.

cryo-TEM is a powerful technique for the structural investigation of drug delivery systems including liposomes. Due to the high contrast of the phospholipid bilayer, liposomes appear as ring-shaped structures in cryo-TEM images (Figure 5-8A). In the Lipocells depending on the angle of observation, the shape, and position of particles may be different, for example in the first row of Figure 5-8B, there is a small spherical shape inside the liposome at 25º, but it is outside of phospholipid bilayer in other angles (0 and -25º). However, in the last row (very bottom) and in the middle row, presence of some particles inside vesicular structure is apparent. As the particles is still shown inside the vesicle even after rotation of camera from -25 to +25 ° angle.

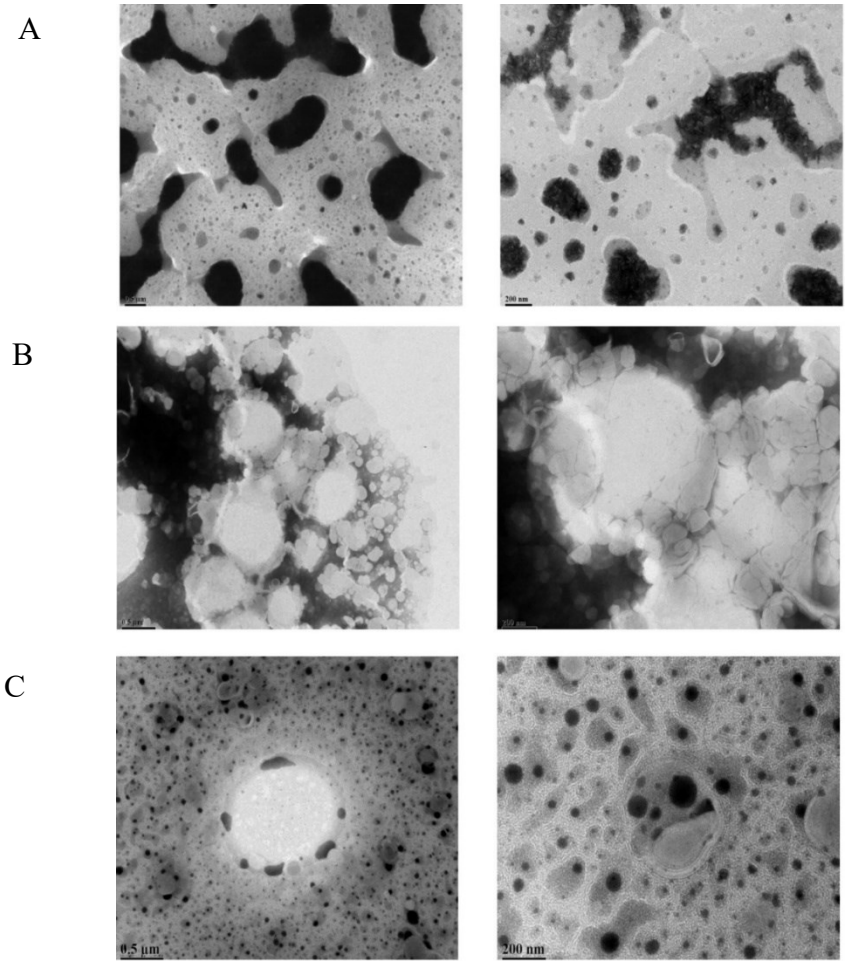

Figure 5-7. TEM images of **A.** PCB(CL-DOX)-PEG-PCB(CL-DOX) triblock copolymer. **B:** liposome and **C:** Lipocell. (Scale bar: 0.5µm and 200 nm)

A

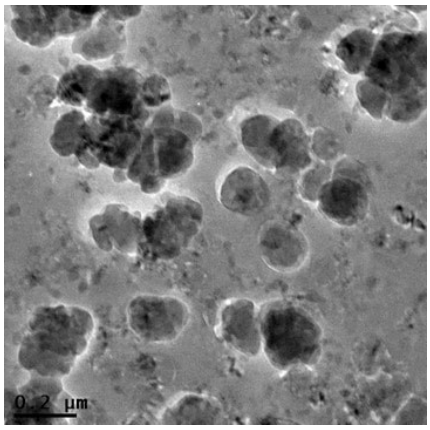

B

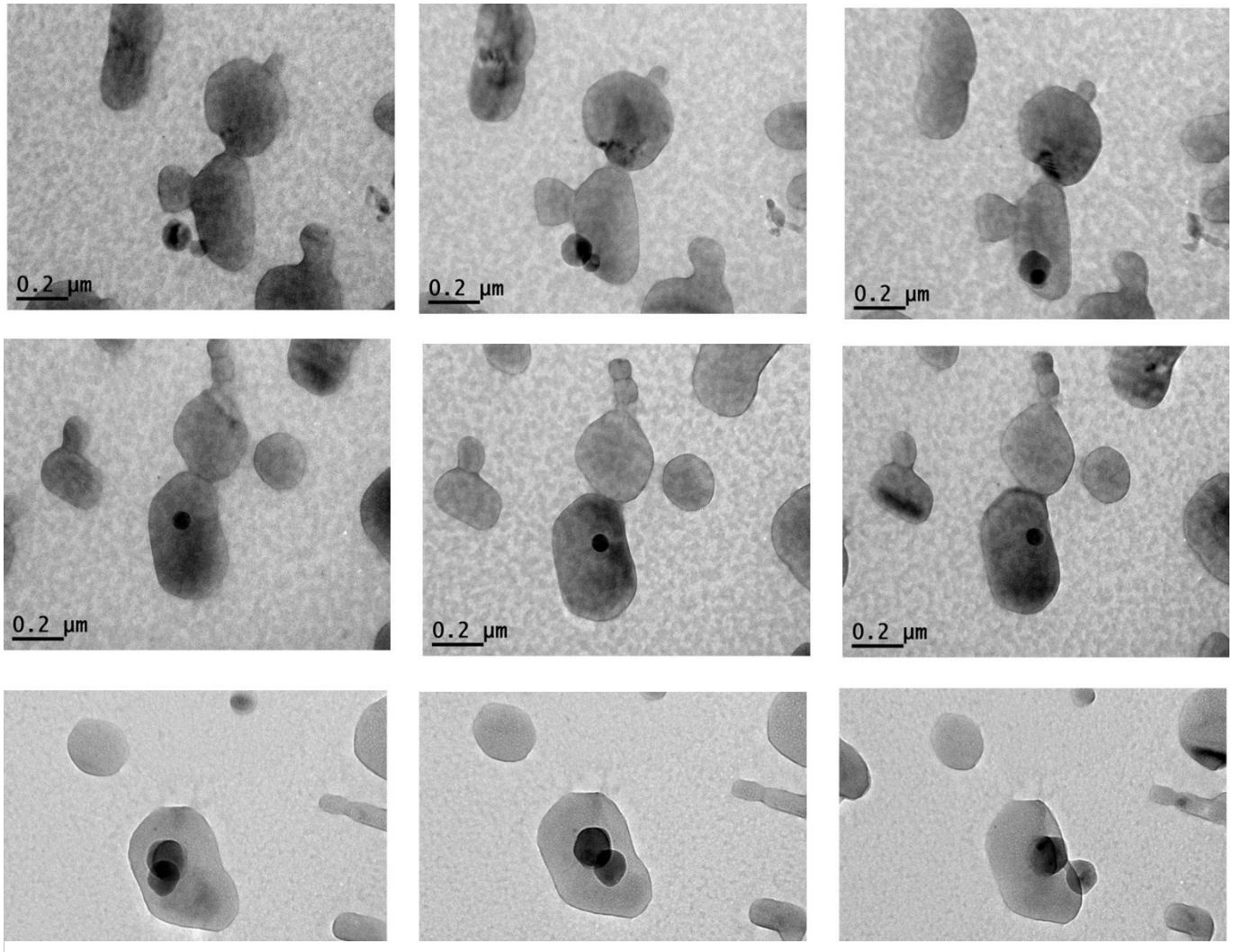

Figure 5-8. Cryo-TEM images of **A.** liposome and **B:** Lipocells in different angle (from left: -25º, 0, 25º)

4.Conclusion

Loading of triblock copolymers based on PEG and substituted polycaprolactone in liposomes was achieved through freeze-thaw method paving the way for the preparation of liposomes encapsulating polymeric micelles, or Lipocells.

Chapter 6. General Discussion, Conclusion, and Future direction

6.1. General Discussion

As a flourishing interdisciplinary field, polymer engineering facilitates the progress of many fields including medicine. Polymers are the backbone of the drug delivery system since they offer unique properties which are not comparable to any other material. Stimuli-responsive polymers mimic biological systems where an external stimulus such as temperature or pH results in a change in the properties of the polymer [189]. Stimulus responsive hydrogels made from polymers are a very interesting class of biomaterials due to stimulus responsive swelling properties, which can offer opening and closing of the pores in the hydrogel in response to stimuli. This property can be used to design stimulus responsive drug delivery systems or biosensors. Currently used thermo-responsive hydrogels have several limitations for application in biomedical fields, however. A major bottleneck is the slow and low controllability of the gelation, particularly for most amphiphilic copolymers. Since the mechanism for thermoresponsive gelation of the most block copolymers is unknown, drawing a correlation between the chemical structure of copolymers and other molecular factors such as molecular weight [112,113,124], block length [150,190], polydispersity index [112,113], and other factors [109,111] and the thermoresponsive behaviour of these materials is very challenging.

Di and tri ABCs composed of PEG and PCL have been the subject of several studies for drug delivery applications, [46] however the lack of functional groups on PCL limited the flexibility of this polymer for incorporation of diverse chemical entities. In 2006 Mahmud et al in our research group reported on the synthesis of novel PEO-PCL block copolymers containing pendant functional groups (benzyl carboxylate and /or carboxyl groups) on the PCL segment. Later Safaei et al in 2011, synthesized triblock copolymers composed of PEG and BCL through bulk ring opening polymerization, followed by debenzylation of the synthesized copolymer, i.e., poly(α-

carboxyl-ε-caprolactone)-co-poly(a-benzyl carboxylate- ε-caprolactone) -*b*-PEG- poly(α-carboxyl-ε-caprolactone)-co-poly(a-benzyl carboxylate- ε-caprolactone) (PCBCL-*b*-PEG-*b*-PCBCL), in the presence of hydrogen gas. This led to the preparation of copolymers with various degrees of free α-carboxyl to α-benzyl-ε-carboxylate groups on the hydrophobic block. She found PCBCL-PEG-PCBCL with 30-50 % COOH-substitution on the polymeric backbone to show thermo-responsive sol-gel transition above ~ 30 °C at polymer concentrations as low as 7.5 %. in the next step, she investigated the potential of prepared hydrogel for the depot delivery of small molecule peptide drug, cyclosporin A (CyA), for a potential application for dry eye syndrome.

The purpose of this thesis was to conduct a systematic study to investigate the effect of polymerization method, molecular weight distribution, chemical or physical cross-linking, and hydrophilic-lipophilic balance on thermo-responsive behaviour of triblock copolymer based on PEG and BCL, to overcome the challenge of reproducibility and control of thermo-responsiveness for hydrogels formed from PEG and functionalized PCL copolymers.

In the first chapter of the thesis (chapter 2), we focused on the optimization and control of polymerization process for the synthesis of amphiphilic triblock copolymers based on PEG and functionalized PCL (α-benzyl carboxylate-ε-caprolactone) (PBCL), (abbreviated as PBCL-PEG-PBCL). We intended to characterize the block copolymers of PBCL−PEG−PBCL synthesized by solution versus bulk polymerization methods in detail. Our goal was to define the structural characteristics of these block copolymers that can lead to the formation of viscoelastic thermo-reversible hydrogels. Gel Permeation Chromatography (GPC) was employed for a more detailed characterization of this novel copolymer. Our results showed using solvent (biphenyl) in solution polymerization to improve the controllability of polymerization. Also, for the first-time we identified the crucial role of a high molecular weight subpopulation in the prepared polymer

structures in the formation of thermoreversible hydrogels from PBCL-PEG-PBCL. Interestingly, the thermo-reversible formation of viscoelastic gels in aqueous media was only observed in polymer samples with around 40 mol % of this high molecular weight subpopulation, irrespective of the polymerization method. The evidence from the detailed characterization of polymers under study strongly pointed to the formation of the partially cross-linked or branched population in PBCL-PEG-PBCL polymer to be responsible for the appearance of this high molecular weight subpopulation. The presence of free (unreacted) PEG or monomer impurities acting as nucleophilic cross-linker, in the reaction was suggested to be responsible for the formation of this partially cross-linked (or branched) polymer subpopulation. This hypothesis was tested in chapter 3.

In chapter 3, since a potential source in partial cross-linking of the copolymer was the impurity in the monomer, we used an extra pure monomer and tries to assess the effect of polymerization time on the characteristic of PBCL-PEG-PBCL copolymer prepared by the bulk polymerization (similar to the work conducted in Chapter 2). We then investigated the thermo-gelling behaviour of prepared polymer solutions in water. Collected data indicated bulk polymerization of pure BCL by PEG as the initiator even after 40 h of reaction, did not produce a significant level of higher-than-expected Mwt polymer subpopulation. The prepared polymers, therefore, did not meet the minimum requirements (40 mol % of high molecular weight population or M_n (GPC)/M_n (NMR) ≥ 6) for having thermo-reversible hydrogel of PEG/BCL as identified in Chapter 2. In agreement with our hypothesis, the PBCL-PEG-PBCL polymers prepared using the purified monomer did not show production of the high molecular weight subpopulation and also did not form thermoresponsive gels in water. These results implied the presence of a potential cross-linker as an impurity in the monomer, i.e., BCL, to be responsible for the formation of thermogels from PBCL-PEG-PBCL.

In the next step, the role of chemical cross linking of PBCL-PEG-PBCL in the formation of viscoelastic thermogels was examined. For this purpose, then covalent cross-linking of the lineaer PBCL-PEG-PBCL prepared using a pure monomer, was accomplished using different polyol cross-linkers (dihydroxy PEG 200 and 400 Da, PCL-triol, or TMP ethoxylate). A nucleophilic acyl substitution reaction between the benzyl carboxylate pendant group of the polymer backbone and the hydroxyl groups of cross-linkers was proposed to take place in the reaction. Although the final copolymer products prepared using PCL-triol and TMP ethoxylate cross-linkers met the minimum requirements for having thermo-reversible hydrogel of PEG/BCL (identified above), only the product with PEG 400 as a cross-linker showed thermo-gelling behaviour in water. This was confirmed using both the rheological test and inverse flow method. We attributed this observation to the differences in the hydrophilicity and/or steric hindrance for the PCL-triol and TMP versus PEG. PCL-triol and TMP ethoxylate with three hydroxyl groups (three-point attachment to the backbone), may cause restriction in the freedom of conformations of the polymer backbone.

To further investigate the effect of cross-linker on the characteristics of PBCL-PEG-PBCLs and their solution in water, we used PEGs with different molecular weights (200 and 400 Da) at different molar ratios to the BCL segment. Results showed PEG 200 at different molar ratios can not act as a crosslinker as the M_n(GPC)/M_n(NMR) ratio for the polymers with PEG 200 remained around 1, following reaction with PEG200. On the other hand, when PEG 400 was used as a cross-linker, M_n(GPC)/M_n(NMR) ratio raised to 2.73, 6.60 and, 8.98 for PEG 400/BCL of 1/10. 2/10 and, 4/10 molar ratios, respectively. The use of PEG 400 Da at a PEG 400/BCL ratio of 4:10 as a crosslinker for PBCL-PEG-PBCL copolymers, was able to yield a polymer capable of forming a viscoelastic thermo-reversible hydrogel.

In chapter 4, we intended to assess how hydrophilic/lipophilic balance in the partially cross-linked triblock copolymer composed of PEG and BCL (prepared in chapter 2) can affect polymer characteristics and formation of viscoelastic thermogels from the copolymer under study. For this purpose, first PBCL-PEG-PBCL$_{PC}$ was synthesized by 2 methods of bulk and solution polymerization, then chemically reduced using continuous hydrogen gas at 0, 20, 40, 60, and 120 min. Debenzylated polymers in each category (B and S series) were characterized and a linear correlation was observed between reduction time and degree of debenzylation. Linear reduction in polymer molecular weight as a function of debenzylation time shows the lack of back-biting or cross-linking cleavage during hydrogenation of PBCL-PEG-PBCL$_{PC}$. Also, $Đ_M$ was enhanced as the degree of debenzylation raised for all copolymers under study. Based on GPC data we found reduced copolymers in "B" and "S" series exist as a random coil conformation in THF at 30 °C in all reduction times except 120 min. The B_{120} and S_{120} copolymers with 80 and 72-mole percentages of PBCL reduction, exhibited spherical shape conformation in THF which may be attributed to the intermolecular hydrogen bonds between the COOHs of a copolymer chain. Thermo-responsive behaviour of the aqueous solution of block copolymers was investigated through small amplitude oscillatory shear rheology and inverse flow method and determined copolymers under study at 0-, 40-, and 60-min reduction time showed reversible thermo-gelation. We found that thermogelation of copolymers not only depends on a high molecular weight population but also depends on hydrophilic/lipophilic balance in the copolymer segment.

After optimizing polymerization reaction and developing a more detailed understanding of the chemical and structural features in copolymers based on PEG and functionalized caprolactone on their thermo-responsive behaviour, we investigated the formation of new hybrid nano delivery systems formed through encapsulation of PCBCL-PEG-PCBCL in liposomes. This hybrid nano-

delivery system is expected to improve the flexibility of nano-carriers in the co-delivery of hydrophobic and hydrophilic entities. First, we synthesized PBCL-PEG-PBCL $_{PC}$ through bulk ROP, then purified the copolymer and subjected it to debenzylation reaction in the presence of hydrogen gas and palladium on activated charcoal for 60 min. The PCBCL-PEG-PCBCL triblock copolymer was then used to covalently conjugate by Doxorubicin through a DCC-NHS reaction. Doxorubicin was used to fluorescently label the polymer so that its interaction with the liposomes can be tracked in the Sephadex column and after. The final product after purification was characterized and encapsulated in liposome using the freeze-thaw method. Liposomes encapsulating the labeled polymer were then separated from the unloaded polymer by size exclusion chromatography using a Sephadex column. Successful encapsulation of polymer inside liposome was assessed with a transmission electron microscope (TEM) employing either a negative staining technique or a cryogenic technique (cryo-TEM). This data provides a preliminary and qualitative characterization of polymeric micelles encapsulated liposomes or Lipocells.

6.2. General Conclusion

Application of thermo-responsive polymeric hydrogels have been studied for many years. However, our understanding of the mechanism of gel formation is also very limited. As such, studies on the assessment of characteristic of copolymers leading to the formation of thermo-responsive polymeric hydrogel is scarce in the literature. In this thesis, we tried to answer this challenging question for thermogels made from copolymer based on PEG and α-carbon functionalized poly(ε-caprolactone). Our data implied a role for the presence of a high molecular weight population formed through partial cross-linking or branching of the polymer back bone in the thermo-gelling behaviour of this novel copolymer. We identified PEG 400, as a suitable cross

linker for the formation of thermogels from PBCL-PEG-PBCL. In addition to partial cross-linking or branching, the hydrophilicity of the polymer backbone was found to play a role in the formation of viscoelastic thermogels in studied structures. Prepared copolymers were shown to be loaded in liposomes, forming new nanodelivery systems termed Lipocells in this thesis, that may be used in the future as new drug delivery systems with many advantageous features.

6.3. Limitations and Future Directions

In this thesis, we provided a foundation for a theoretically reproducible and scalable synthesis protocol for the preparation of block copolymers based on PEG and α-carbon functionalized poly(ε-caprolactone) capable of the formation of thermogels. A systematic study was carried out to characterize the developed copolymers and assess chemical and structural features that can lead to the formation of a thermo-responsive hydrogel from the prepared copolymers. However, the scalability and reproducibility of the developed procedures have not been studied in an experimental setting. Future studies should focus on the experimental design approaches that can elucidate the scalability and reproducibility of PEG400 cross-linked PBCL-PEG-PBCL prepared using pure BCL in bulk and solution polymerization techniques.

Based on our data in chapter 3, an impurity in the monomer seems to be responsible for the partial cross-linking of the copolymer. This impurity needs to be identified and characterized in future studies.

We conducted a systematic study on the thermo-responsive behaviour of partially cross-linked PCBCL-PEG-PCBCL copolymer. However, based on previous studies [94,120,153] this copolymer is also pH-responsive, which was not investigated here. The effect of pH and electrolytes on the characteristics of the above copolymers and gel formation should be investigated in the future.

While we have found the high molecular weight population and hydrophilic/lipophilic balance affect the thermo-gelation of PCBCL-PEG-PCBCL, the mechanism of thermogelation for the structures developed here is still a mystery. A dynamic Monte Carlo simulation will be helpful to gain a better understanding of the internal mechanism of polymerization and gelatin of the materials developed here.

Another future development could involve the application of generated thermogels in drug delivery and assessing the effect of temperature and pH on drug loading and release for different model drugs.

Further characterization of Lipocells and application of this structure for co-delivery of hydrophilic and hydrophobic drugs (e.g., doxorubicin and paclitaxel) are also suggested.

References

1. Wei, M., Gao, Y., Li, X. & Serpe, M. J. Stimuli-responsive polymers and their applications. *Polym. Chem.* **8**, 127–143 (2017).
2. Heskins, M. & Guillet, J. E. Solution Properties of Poly(N-isopropylacrylamide). *Journal of Macromolecular Science: Part A - Chemistry* **2**, 1441–1455 (1968).
3. Schmaljohann, D. Thermo- and pH-responsive polymers in drug delivery. *Adv.Drug Deliv.Rev.* **58**, 1655–1670 (2006).
4. Zarrintaj, P. *et al.* Thermo-sensitive polymers in medicine: A review. *European Polymer Journal* **117**, 402–423 (2019).
5. Klouda, L. Thermoresponsive hydrogels in biomedical applications: A seven-year update. *European Journal of Pharmaceutics and Biopharmaceutics* **97**, 338–349 (2015).
6. Dai, S., Ravi, P. & Tam, K. C. pH-Responsive polymers: synthesis, properties and applications. *Soft Matter* **4**, 435 (2008).
7. Yusa, S. Development and application of pH-responsive polymers. *Polym J* (2022) doi:10.1038/s41428-021-00576-x.
8. Jochum, F. D. & Theato, P. Temperature- and light-responsive smart polymer materials. *Chem. Soc. Rev.* **42**, 7468–7483 (2013).
9. Thévenot, J., Oliveira, H., Sandre, O. & Lecommandoux, S. Magnetic responsive polymer composite materials. *Chem. Soc. Rev.* **42**, 7099 (2013).
10. Wang, D., Green, M. D., Chen, K., Daengngam, C. & Kotsuchibashi, Y. Stimuli-Responsive Polymers: Design, Synthesis, Characterization, and Applications. *International Journal of Polymer Science* **2016**, 1–2 (2016).

11. Yatvin, M. B., Weinstein, J. N., Dennis, W. H. & Blumenthal, R. Design of Liposomes for Enhanced Local Release of Drugs by Hyperthermia. *Science* **202**, 1290–1293 (1978).
12. Ma, G., Miao, B. & Song, C. Thermosensitive PCL-PEG-PCL hydrogels: Synthesis, characterization, and delivery of proteins. *J Appl Polym Sci* **116**, 1985–1993 (2010).
13. Patel, P., Mandal, A., Gote, V., Pal, D. & Mitra, A. K. Thermosensitive hydrogel-based drug delivery system for sustained drug release. *Journal of Polymer Research* **26**, 131 (2019).
14. Moon, H. J., Ko, D. Y., Park, M. H., Joo, M. K. & Jeong, B. Temperature-responsive compounds as in situ gelling biomedical materials. *Chem.Soc.Rev.* **41**, 4860–4883 (2012).
15. Fang, Y., Tan, J., Lim, S. & Soh, S. Rupturing cancer cells by the expansion of functionalized stimuli-responsive hydrogels. *NPG Asia Mater* **10**, e465–e465 (2018).
16. Yao, Y., Wang, Y., Li, Z. & Li, H. Reversible On–Off Luminescence Switching in Self-Healable Hydrogels. *Langmuir* **31**, 12736–12741 (2015).
17. Tavakolizadeh, M. *et al.* An environmentally friendly wound dressing based on a self-healing, extensible and compressible antibacterial hydrogel. *Green Chem.* **23**, 1312–1329 (2021).
18. Danhier, F., Feron, O. & Préat, V. To exploit the tumor microenvironment: Passive and active tumor targeting of nanocarriers for anti-cancer drug delivery. *Journal of Controlled Release* **148**, 135–146 (2010).
19. Rao, N. V., Ko, H., Lee, J. & Park, J. H. Recent Progress and Advances in Stimuli-Responsive Polymers for Cancer Therapy. *Front. Bioeng. Biotechnol.* **6**, 110 (2018).
20. Li, K. *et al.* A long-acting formulation of a polypeptide drug exenatide in treatment of diabetes using an injectable block copolymer hydrogel. *Biomaterials* **34**, 2834–2842 (2013).
21. Gong, C. *et al.* Efficient inhibition of colorectal peritoneal carcinomatosis by drug loaded micelles in thermosensitive hydrogel composites. *Nanoscale* **4**, 3095 (2012).

22. Zhao, L. *et al.* pH triggered injectable amphiphilic hydrogel containing doxorubicin and paclitaxel. *International Journal of Pharmaceutics* **410**, 83–91 (2011).
23. Surnar, B. & Jayakannan, M. Stimuli-Responsive Poly(caprolactone) Vesicles for Dual Drug Delivery under the Gastrointestinal Tract. *Biomacromolecules* **14**, 4377–4387 (2013).
24. Liu, J. *et al.* Gold Nanorods with Phase-Changing Polymer Corona for Remotely Near-Infrared-Triggered Drug Release. *Chem. Asian J.* **9**, 275–288 (2014).
25. James, H. P., John, R., Alex, A. & Anoop, K. R. Smart polymers for the controlled delivery of drugs – a concise overview. *Acta Pharmaceutica Sinica B* **4**, 120–127 (2014).
26. Mura, S., Nicolas, J. & Couvreur, P. Stimuli-responsive nanocarriers for drug delivery. *Nature Mater* **12**, 991–1003 (2013).
27. Rabiee, N., Rabiee, M., Bagherzadeh, M. & Hamblin, M. R. *Stimuli-Responsive Polymers: Nano-dimension*. (IOP Publishing, 2019). doi:10.1088/2053-2571/ab1342.
28. Gil, E. S. & Hudson, S. M. Stimuli-reponsive polymers and their bioconjugates. *Progress in Polymer Science* **29**, 1173–1222 (2004).
29. Varga, I., Gilányi, T., Mészáros, R., Filipcsei, G. & Zrínyi, M. Effect of Cross-Link Density on the Internal Structure of Poly(*N* -isopropylacrylamide) Microgels. *J. Phys. Chem. B* **105**, 9071–9076 (2001).
30. Rizzo, F. & Kehr, N. S. Recent Advances in Injectable Hydrogels for Controlled and Local Drug Delivery. *Adv. Healthcare Mater.* **10**, 2001341 (2021).
31. Kenchegowda, M. *et al.* Smart Nanocarriers as an Emerging Platform for Cancer Therapy: A Review. *Molecules* **27**, 146 (2021).
32. Stuart, M. *et al.* Emerging applications of stimuli-responsive polymer materials. *NATURE MATERIALS* **9**, 101–113 (2010).

33. Hoare, T. R. & Kohane, D. S. Hydrogels in drug delivery: Progress and challenges. *Polymer* **49**, 1993–2007 (2008).

34. Van Tomme, S. R., Storm, G. & Hennink, W. E. In situ gelling hydrogels for pharmaceutical and biomedical applications. *International Journal of Pharmaceutics* **355**, 1–18 (2008).

35. Dabbaghi, A. *et al.* Synthesis, physical and mechanical properties of amphiphilic hydrogels based on polycaprolactone and polyethylene glycol for bioapplications: A review. *Journal of Industrial and Engineering Chemistry* **101**, 307–323 (2021).

36. Hoare, T. R. & Kohane, D. S. Hydrogels in drug delivery: Progress and challenges. *Polymer* **49**, 1993–2007 (2008).

37. Yu, L., Chang, G. T., Zhang, H. & Ding, J. D. Injectable block copolymer hydrogels for sustained release of a PEGylated drug. *International Journal of Pharmaceutics* **348**, 95–106 (2008).

38. Xiong, X. Y., Tam, K. C. & Gan, L. H. Polymeric Nanostructures for Drug Delivery Applications Based on Pluronic Copolymer Systems. *j nanosci nanotechnol* **6**, 2638–2650 (2006).

39. Gong, C. *et al.* Biodegradable in situ gel-forming controlled drug delivery system based on thermosensitive PCL–PEG–PCL hydrogel. Part 2: Sol–gel–sol transition and drug delivery behavior. *Acta Biomaterialia* **5**, 3358–3370 (2009).

40. Elsayed, M. M. Hydrogel Preparation Technologies: Relevance Kinetics, Thermodynamics and Scaling up Aspects. *J Polym Environ* **27**, 871–891 (2019).

41. Zennifer, A., Senthilvelan, P., Sethuraman, S. & Sundaramurthi, D. Key advances of carboxymethyl cellulose in tissue engineering & 3D bioprinting applications. *Carbohydrate Polymers* **256**, 117561 (2021).

42. Jiang, S., Liu, S. & Feng, W. PVA hydrogel properties for biomedical application. *Journal of the Mechanical Behavior of Biomedical Materials* **4**, 1228–1233 (2011).

43. Li, R., Wu, Y., Bai, Z., Guo, J. & Chen, X. Effect of molecular weight of polyethylene glycol on crystallization behaviors, thermal properties and tensile performance of polylactic acid stereocomplexes. *RSC Adv.* **10**, 42120–42127 (2020).

44. Fujiwara, T. *et al.* Novel Thermo-Responsive Formation of a Hydrogel by Stereo-Complexation between PLLA-PEG-PLLA and PDLA-PEG-PDLA Block Copolymers. *Macromol. Biosci.* **1**, 204–208 (2001).

45. Tomme, S. R. V. *et al.* Mobility of model proteins in hydrogels composed of oppositely charged dextran microspheres studied by protein release and fluorescence recovery after photobleaching. *Journal of Controlled Release* **110**, 67–78 (2005).

46. Dabbaghi, A. *et al.* Synthesis, physical and mechanical properties of amphiphilic hydrogels based on polycaprolactone and polyethylene glycol for bioapplications: A review. *Journal of Industrial and Engineering Chemistry* **101**, 307–323 (2021).

47. Chang, H. *et al.* Amphiphilic hydrogels for biomedical applications. *J. Mater. Chem. B* **7**, 2899–2910 (2019).

48. Patrickios, C. S. & Georgiou, T. K. Covalent amphiphilic polymer networks. *Current Opinion in Colloid & Interface Science* **8**, 76–85 (2003).

49. Ulbricht, J., Jordan, R. & Luxenhofer, R. On the biodegradability of polyethylene glycol, polypeptoids and poly(2-oxazoline)s. *Biomaterials* **35**, 4848–4861 (2014).

50. Lin, C.-C. & Anseth, K. S. PEG Hydrogels for the Controlled Release of Biomolecules in Regenerative Medicine. *Pharm Res* **26**, 631–643 (2009).

51. Choi, S. W., Choi, S. Y., Jeong, B., Kim, S. W. & Lee, D. S. Thermoreversible gelation of poly(ethylene oxide) biodegradable polyester block copolymers. II. *J. Polym. Sci. A Polym. Chem.* **37**, 2207–2218 (1999).
52. Wu, K., Yu, L. & Ding, J. Synthesis of PCL–PEG–PCL Triblock Copolymer via Organocatalytic Ring-Opening Polymerization and Its Application as an Injectable Hydrogel—An Interdisciplinary Learning Trial. *J.Chem.Educ.* **97**, 4158–4165 (2020).
53. Stridsberg, K. M., Ryner, M. & Albertsson, A.-C. Controlled Ring-Opening Polymerization: Polymers with designed Macromolecular Architecture. in *Degradable Aliphatic Polyesters* vol. 157 41–65 (Springer Berlin Heidelberg, 2002).
54. Lei, N. *et al.* Therapeutic application of injectable thermosensitive hydrogel in preventing local breast cancer recurrence and improving incision wound healing in a mouse model. *Nanoscale* **4**, 5686 (2012).
55. Fu, S. *et al.* Injectable and thermo-sensitive PEG-PCL-PEG copolymer/collagen/n-HA hydrogel composite for guided bone regeneration. *Biomaterials* **33**, 4801–4809 (2012).
56. Payyappilly, S., Dhara, S. & Chattopadhyay, S. Thermoresponsive biodegradable PEG-PCL-PEG based injectable hydrogel for pulsatile insulin delivery: PEG-PCL-PEG Based Injectable Hydrogel For Pulsatile Insulin Delivery. *J. Biomed. Mater. Res.* **102**, 1500–1509 (2014).
57. Xu, S. *et al.* Sustained release of PTX-incorporated nanoparticles synergized by burst release of DOX·HCl from thermosensitive modified PEG/PCL hydrogel to improve anti-tumor efficiency. *European Journal of Pharmaceutical Sciences* **62**, 267–273 (2014).
58. Luo, Z. *et al.* Thermosensitive PEG–PCL–PEG (PECE) hydrogel as an *in situ* gelling system for ocular drug delivery of diclofenac sodium. *Drug Delivery* **23**, 63–68 (2016).

59. Gong, C. *et al.* Synthesis and characterization of PEG-PCL-PEG thermosensitive hydrogel. *Int.J.Pharm.* **365**, 89–99 (2009).

60. Ko, C.-Y. *et al. In vitro* and *in vivo* co-culture of chondrocytes and bone marrow stem cells in photocrosslinked PCL-PEG-PCL hydrogels enhances cartilage formation: Co-culture of chondrocytes and bone marrow stem cells in hydrogels. *J Tissue Eng Regen Med* **10**, E485–E496 (2016).

61. Feng, Z. *et al.* Temperature-responsive in situ nanoparticle hydrogels based on hydrophilic pendant cyclic ether modified PEG-PCL-PEG. *Biomater. Sci.* **4**, 1493–1502 (2016).

62. Dong, X. *et al.* Thermosensitive hydrogel loaded with chitosan-carbon nanotubes for near infrared light triggered drug delivery. *Colloids and Surfaces B: Biointerfaces* **154**, 253–262 (2017).

63. Liao, J., Jia, Y., Wang, B., Shi, K. & Qian, Z. Injectable Hybrid Poly(ε-caprolactone)- *b* -poly(ethylene glycol)- *b* -poly(ε-caprolactone) Porous Microspheres/Alginate Hydrogel Cross-linked by Calcium Gluconate Crystals Deposited in the Pores of Microspheres Improved Skin Wound Healing. *ACS Biomater. Sci. Eng.* **4**, 1029–1036 (2018).

64. Guo, J. *et al.* PCEC hydrogel used on sustained-release hyaluronic acid delivery with lubrication effect: Research Article. *J. Appl. Polym. Sci.* **135**, 46228 (2018).

65. Qu, Y. *et al.* Injectable and Thermosensitive Hydrogel and PDLLA Electrospun Nanofiber Membrane Composites for Guided Spinal Fusion. *ACS Appl. Mater. Interfaces* **10**, 4462–4470 (2018).

66. Ning, W., Shang, P., Wu, J., Shi, X. & Liu, S. Novel Amphiphilic, Biodegradable, Biocompatible, Thermo-Responsive ABA Triblock Copolymers Based on PCL and PEG

Analogues via a Combination of ROP and RAFT: Synthesis, Characterization, and Sustained Drug Release from Self-Assembled Micelles. *Polymers* **10**, 214 (2018).

67. Asadi, N. *et al.* Synthesis, characterization and *in vitro* evaluation of magnetic nanoparticles modified with PCL–PEG–PCL for controlled delivery of 5FU. *Artificial Cells, Nanomedicine, and Biotechnology* **46**, 938–945 (2018).
68. Nguyen, D. T., Phan, V. H. G., Lee, D. S., Thambi, T. & Huynh, D. P. Bioresorbable pH- and temperature-responsive injectable hydrogels-incorporating electrosprayed particles for the sustained release of insulin. *Polymer Degradation and Stability* **162**, 36–46 (2019).
69. Noormohammadi, F., Nourany, M., Sadeghi, G. M. M., Wang, P.-Y. & Shahsavarani, H. The role of cellulose nanowhiskers in controlling phase segregation, crystallization and thermal stimuli responsiveness in PCL-PEGx-PCL block copolymer-based PU for human tissue engineering applications. *Carbohydrate Polymers* **252**, 117219 (2021).
70. Hakemi, P., Ghadi, A., Mahjoub, S., Zabihi, E. & Tashakkorian, H. Ratio Design of Docetaxel/Quercetin Co-Loading-to-Nanocarrier: Synthesis of PCL–PEG–PCL Copolymer, Study of Drug Release Kinetic and Growth Inhibition of Human Breast Cancer (MCF-7) Cell Line. *Russ J Appl Chem* **94**, 388–401 (2021).
71. Liu, C. B. *et al.* Thermoreversible gel–sol behavior of biodegradable PCL-PEG-PCL triblock copolymer in aqueous solutions. *J.Biomed.Mater.Res.* **84B**, 165–175 (2008).
72. Baek, S. H., Kim, H. H., Doh, Y. S. & Kim, K. W. Estimation of high-temperature properties of rubberized asphalt using chromatograph. *KSCE Journal of Civil Engineering* **13**, 161–167 (January 5).
73. Ma, J. *et al.* Application of gel permeation chromatography technology in asphalt materials: A review. *Constr.Build.Mater.* **278**, 122386 (2021).

74. ‘Static light scattering technologies for GPC/SEC explained’, Malvern Instruments white paper, www.malvern.com/slsexplained.

75. Kratochvíl, P. Advances in classical light scattering from polymer solutions: *Pure and Applied Chemistry* **54**, 379–393 (1982).

76. Keeler J. *Understanding NMR spectroscopy.* (John Wiley & Sons, 2011).

77. Shapiro, Y. E. Structure and dynamics of hydrogels and organogels: An NMR spectroscopy approach. *Progress in Polymer Science* **36**, 1184–1253 (2011).

78. Hatzakis, E. Nuclear Magnetic Resonance (NMR) Spectroscopy in Food Science: A Comprehensive Review. *Comprehensive Reviews in Food Science and Food Safety* **18**, 189–220 (2019).

79. Barnes, H. A. & Hutton, J. F., Walters Kenneth. *An Introduction to Rheology*. 10 (1989).

80. Janmey, P. A. & Schliwa, M. Rheology. *Current biology : CB* **18**, R639–R641 (May 8).

81. Schippers, C., Tsarkova, L. A., Bahners, T., Gutmann, J. S. & Cleve, E. Improved Maxwell Model Approach and its Applicability toward Lifetime Prediction of Biobased Viscoelastic Fibers. *Macromol.Mater.Eng.* **n/a**, 2100443 (2021).

82. Djabourov, M., Nishinari, K. & Ross-Murphy, S. B. The sol–gel transition. in *Physical Gels from Biological and Synthetic Polymers* 64–96 (Cambridge University Press, 2013). doi:10.1017/CBO9781139024136.004.

83. Winter, H. H. Gel Point. *Encyclopedia of Polymer Science and Technology* 1–15 (2021) doi:10.1002/0471440264.pst476.pub2.

84. Nobbmann, U. *et al.* Dynamic light scattering as a relative tool for assessing the molecular integrity and stability of monoclonal antibodies. *null* **24**, 117–128 (January 1).

85. Lorber, B., Fischer, F., Bailly, M., Roy, H. & Kern, D. Protein analysis by dynamic light scattering: Methods and techniques for students. *Biochem.Mol.Biol.Educ.* **40**, 372–382 (2021).

86. Chaikov, L., Kirichenko, M. N., Krivokhizha, S. V. & Zaritskiy, A. R. Dynamics of statistically confident particle sizes and concentrations in blood plasma obtained by the dynamic light scattering method. *J.Biomed.Opt.* **20**, 1–7 (/5/1).

87. Krajina, B. A. *et al.* Dynamic Light Scattering Microrheology Reveals Multiscale Viscoelasticity of Polymer Gels and Precious Biological Materials. *ACS Cent.Sci.* **3**, 1294–1303 (12).

88. Stetefeld, J. örg, McKenna, S. A. & Patel, T. R. Dynamic light scattering: a practical guide and applications in biomedical sciences. *Biophysical Reviews* **8**, 409–427 (January 12).

89. Leyva-Porras, C. *et al.* Application of Differential Scanning Calorimetry (DSC) and Modulated Differential Scanning Calorimetry (MDSC) in Food and Drug Industries. *Polymers* **12**, 5 (2019).

90. Spink, C. H. Differential Scanning Calorimetry. in *Methods in Cell Biology* vol. 84 115–141 (Elsevier, 2008).

91. Coleman, N. J. & Craig, D. Q. M. Modulated temperature differential scanning calorimetry: A novel approach to pharmaceutical thermal analysis. *International Journal of Pharmaceutics* **135**, 13–29 (1996).

92. Deng, H., Dong, A., Song, J. & Chen, X. Injectable thermosensitive hydrogel systems based on functional PEG/PCL block polymer for local drug delivery. *J.Controlled Release* **297**, 60–70 (2019).

93. Larrañeta, E., Stewart, S., Ervine, M., Al-Kasasbeh, R. & Donnelly, R. Hydrogels for Hydrophobic Drug Delivery. Classification, Synthesis and Applications. *JFB* **9**, 13 (2018).

94. Safaei Nikouei, N. & Lavasanifar, A. Characterization of the thermo- and pH-responsive assembly of triblock copolymers based on poly(ethylene glycol) and functionalized poly(ε-caprolactone). *Acta Biomaterialia* **7**, 3708–3718 (2011).

95. Nikouei, N. S., Ghasemi, N. & Lavasanifar, A. Temperature/pH Responsive Hydrogels Based on Poly(ethylene glycol) and Functionalized Poly(e-caprolactone) Block Copolymers for Controlled Delivery of Macromolecules. *Pharm.Res.* **33**, 358–366 (2016).

96. Yu, L. & Ding, J. Injectable hydrogels as unique biomedical materials. *Chem.Soc.Rev.* **37**, 1473–1481 (2008).

97. Liow, S. S. *et al.* Thermogels: In Situ Gelling Biomaterial. *ACS Biomater.Sci.Eng.* **2**, 295–316 (2016).

98. Klouda, L. & Mikos, A. G. Thermoresponsive hydrogels in biomedical applications. *European journal of pharmaceutics and biopharmaceutics : official journal of Arbeitsgemeinschaft fur Pharmazeutische Verfahrenstechnik e.V* **68**, 34–45 (2008).

99. Liow, S. S., Karim, A. A. & Loh, X. J. Biodegradable thermogelling polymers for biomedical applications. *MRS Bull* **41**, 557–566 (2016).

100. Suntornnond, R., An, J. & Chua, C. K. Bioprinting of Thermoresponsive Hydrogels for Next Generation Tissue Engineering: A Review. *Macromol.Mater.Eng.* **302**, 1600266 (2017).

101. Cao, L. *et al.* Safe and Efficient Colonic Endoscopic Submucosal Dissection Using an Injectable Hydrogel. *ACS Biomater.Sci.Eng.* **2**, 393–402 (2016).

102. Yu, L. *et al.* Poly(lactic acid-co-glycolic acid)–poly(ethylene glycol)–poly(lactic acid-co-glycolic acid) thermogel as a novel submucosal cushion for endoscopic submucosal dissection. *Acta Biomaterialia* **10**, 1251–1258 (2014).

103. Zhang, Z. *et al.* Biodegradable and thermoreversible PCLA–PEG–PCLA hydrogel as a barrier for prevention of post-operative adhesion. *Biomaterials* **32**, 4725–4736 (2011).

104. Yu, L., Zhang, Z., Zhang, H. & Ding, J. Biodegradability and Biocompatibility of Thermoreversible Hydrogels Formed from Mixing a Sol and a Precipitate of Block Copolymers in Water. *Biomacromolecules* **11**, 2169–2178 (2010).

105. Perinelli, D. R., Cespi, M., Bonacucina, G. & Palmieri, G. F. PEGylated polylactide (PLA) and poly (lactic-co-glycolic acid) (PLGA) copolymers for the design of drug delivery systems. *Journal of Pharmaceutical Investigation* **49**, 443–458 (2019).

106. Jeong, B., Kim, S. W. & Bae, Y. H. Thermosensitive sol–gel reversible hydrogels. *Advanced Drug Delivery Reviews* **64**, 154–162 (2012).

107. Cui, S., Yu, L. & Ding, J. Thermogelling of Amphiphilic Block Copolymers in Water: ABA Type versus AB or BAB Type. *Macromolecules* **52**, 3697–3715 (2019).

108. Cui, S., Yu, L. & Ding, J. Semi-bald Micelles and Corresponding Percolated Micelle Networks of Thermogels. *Macromolecules* **51**, 6405–6420 (2018).

109. Zhang, H., Yu, L. & Ding, J. Roles of Hydrophilic Homopolymers on the Hydrophobic-Association-Induced Physical Gelling of Amphiphilic Block Copolymers in Water. *Macromolecules* **41**, 6493–6499 (2008).

110. Zhang, Y., Wang, M., Ye, J. & Lang, M. Pendant groups fine-tuning thermal gelation of poly(ε-caprolactone)-b-poly(ethylene glycol)-b-poly(ε-caprolactone) aqueous solution. *J.Polym.Sci.Part A: Polym.Chem.* **54**, 2571–2581 (2016).

111. Yu, L., Zhang, H. & Ding, J. A Subtle End-Group Effect on Macroscopic Physical Gelation of Triblock Copolymer Aqueous Solutions. *Angewandte Chemie International Edition* **45**, 2232–2235 (2006).

112. Chen, L., Ci, T., Yu, L. & Ding, J. Effects of Molecular Weight and Its Distribution of PEG Block on Micellization and Thermogellability of PLGA–PEG–PLGA Copolymer Aqueous Solutions. *Macromolecules* **48**, 3662–3671 (2015).

113. Chen, L., Ci, T., Li, T., Yu, L. & Ding, J. Effects of Molecular Weight Distribution of Amphiphilic Block Copolymers on Their Solubility, Micellization, and Temperature-Induced Sol–Gel Transition in Water. *Macromolecules* **47**, 5895–5903 (2014).

114. Nielsen, J. E. *et al.* Structural and Rheological Properties of Temperature-Responsive Amphiphilic Triblock Copolymers in Aqueous Media. *J Phys Chem B* **121**, 4885–4899 (2017).

115. Cui, S., Yu, L. & Ding, J. Strategy of "Block Blends" to Generate Polymeric Thermogels versus That of One-Component Block Copolymer. *Macromolecules* **53**, 11051–11064 (2020).

116. Yu, L., Chang, G., Zhang, H. & Ding, J. Temperature-induced spontaneous sol–gel transitions of poly(D,L-lactic acid-co-glycolic acid)-b-poly(ethylene glycol)-b-poly(D,L-lactic acid-co-glycolic acid) triblock copolymers and their end-capped derivatives in water. *J.Polym.Sci.A Polym.Chem.* **45**, 1122–1133 (2007).

117. Cui, S., Chen, L., Yu, L. & Ding, J. Synergism among Polydispersed Amphiphilic Block Copolymers Leading to Spontaneous Physical Hydrogelation upon Heating. *Macromolecules* **53**, 7726–7739 (2020).

118. Khorshid, N. K. *et al.* Novel Structural Changes during Temperature-Induced Self-Assembling and Gelation of PLGA-PEG-PLGA Triblock Copolymer in Aqueous Solutions. *Macromol.Biosci.* **16**, 1838–1852 (2016).

119. Santoveña, A. *et al.* Structure-Performance Relationships of Temperature-Responsive PLGA-PEG-PLGA Gels for Sustained Release of Bone Morphogenetic Protein-2. *Journal of Pharmaceutical Sciences* **106**, 3353–3362 (2017).

120. Safaei Nikouei, N. *et al.* Thermoreversible hydrogels based on triblock copolymers of poly(ethylene glycol) and carboxyl functionalized poly(ε-caprolactone): The effect of carboxyl group substitution on the transition temperature and biocompatibility in plasma. *Acta Biomaterialia* **12**, 81–92 (2015).

121. Mahmud, A., Xiong, X.-B. & Lavasanifar, A. Novel Self-Associating Poly(ethylene oxide)-block-poly(ε-caprolactone) Block Copolymers with Functional Side Groups on the Polyester Block for Drug Delivery. *Macromolecules* **39**, 9419–9428 (2006).

122. Li, S. & Vert, M. Synthesis, Characterization, and Stereocomplex-Induced Gelation of Block Copolymers Prepared by Ring-Opening Polymerization of l(d)-Lactide in the Presence of Poly(ethylene glycol). *Macromolecules* **36**, 8008–8014 (2003).

123. Chen, Y. *et al.* Injectable and Thermosensitive Hydrogel Containing Liraglutide as a Long-Acting Antidiabetic System. *ACS Appl.Mater.Interfaces* **8**, 30703–30713 (2016).

124. Steinman, N. Y., Bentolila, N. Y. & Domb, A. J. Effect of Molecular Weight on Gelling and Viscoelastic Properties of Poly(caprolactone)–b-Poly(ethylene glycol)–b-Poly(caprolactone) (PCL–PEG–PCL) Hydrogels. *Polymers* **12**, (2020).

125. Kaihara, S., Matsumura, S., Mikos, A. G. & Fisher, J. P. Synthesis of poly(L-lactide) and polyglycolide by ring-opening polymerization. *Nature Protocols* **2**, 2767–2771 (2007).

126. Piotr Owczarz, P. Z., Zofia Modrzejewska ,. Sławomir Kuberski and Marek Dziubiński. Rheo-Kinetic Study of Sol-Gel Phase Transition of Chitosan Colloidal Systems. *polymers* **10**, (2018).

127. Odian, G. G. *Principles of Polymerization, 2nd ed*. 297 and 545 (1981).

128. Cragg, L. H. & Manson, J. A. Normal and cross-linked polystyrene. II. Viscosity behavior of polystyrene cross-linked in emulsion polymerization. *J.Polym.Sci.* **9**, 265–278 (1952).

129. Muller, R., Gerard, E., Dugand, P., Rempp, P. & Gnanou, Y. Rheological characterization of the gel point: a new interpretation. *Macromolecules* **24**, 1321–1326 (1991).

130. Kulkarni, V. S. & Shaw, C. Chapter 2 - Surfactants, Lipids, and Surface Chemistry. *Essential Chemistry for Formulators of Semisolid and Liquid Dosages* 5–19 (2016) doi:10.1016/B978-0-12-801024-2.00002-9.

131. Kweon, H. *et al.* A novel degradable polycaprolactone networks for tissue engineering. *Biomaterials* **24**, 801–808 (2003).

132. Van Horn, B. A. & Wooley, K. L. Cross-linked and functionalized polyester materials constructed using ketoxime ether linkages. *Soft Matter* **3**, 1032–1040 (2007).

133. Garg, S. M., Xiong, X.-B., Lu, C. & Lavasanifar, A. Application of Click Chemistry in the Preparation of Poly(ethylene oxide)-block-poly(ε-caprolactone) with Hydrolyzable Cross-Links in the Micellar Core. *Macromolecules* **44**, 2058–2066 (2011).

134. Boire, T. C. *et al.* Pendant allyl crosslinking as a tunable shape memory actuator for vascular applications. *Acta Biomaterialia* **24**, 53–63 (2015).

135. Kelley, E. G., Albert, J. N. L., Sullivan, M. O. & Epps, I., T. Stimuli-responsive copolymer solution and surface assemblies for biomedical applications. *Chem.Soc.Rev.* **42**, 7057–7071 (2013).

136. Zhang, K., Xue, K. & Loh, X. J. Thermo-Responsive Hydrogels: From Recent Progress to Biomedical Applications. *Gels* **7**, 77 (2021).

137. Lei, K., Shen, W., Cao, L., Yu, L. & Ding, J. An injectable thermogel with high radiopacity. *Chem.Commun.* **51**, 6080–6083 (2015).

138. Joshy, K. S., Snigdha, S., Thomas, S. & Li, T. An Overview of the Recent Developments in Hydrogels. in *Nano Hydrogels: Physico-Chemical Properties and Recent Advances in Structural Designing* (eds. Jose, J., Thomas, S. & Thakur, V. K.) 231–246 (Springer Singapore, 2021). doi:10.1007/978-981-15-7138-1_13.

139. Mondal, S., Das, S. & Nandi, A. K. A review on recent advances in polymer and peptide hydrogels. *Soft Matter* **16**, 1404–1454 (2020).

140. Bellotti, E., Schilling, A. L., Little, S. R. & Decuzzi, P. Injectable thermoresponsive hydrogels as drug delivery system for the treatment of central nervous system disorders: A review. *Journal of Controlled Release* **329**, 16–35 (2021).

141. Chatterjee, S. & Hui, P. C. Review of Applications and Future Prospects of Stimuli-Responsive Hydrogel Based on Thermo-Responsive Biopolymers in Drug Delivery Systems. *Polymers* **13**, 2086 (2021).

142. Akimoto, J. & Ito, Y. Thermoresponsive Biodegradable Polymeric Materials for Biomedical Application. in *Sustainability & Green Polymer Chemistry Volume 1: Green Products and Processes* vol. 1372 159–172 (American Chemical Society, 2020).

143. Hogan, K. J. & Mikos, A. G. Biodegradable thermoresponsive polymers: Applications in drug delivery and tissue engineering. *Polymer* **211**, 123063 (2020).

144. Nguyen, L. T. B. *et al.* Development of thermo-responsive polycaprolactone macrocarriers conjugated with Poly(N-isopropyl acrylamide) for cell culture. *Sci.Rep.* **9**, 3477–0 (2019).

145. Doberenz, F., Zeng, K., Willems, C., Zhang, K. & Groth, T. Thermoresponsive polymers and their biomedical application in tissue engineering – a review. *J.Mater.Chem.B* **8**, 607–628 (2020).

146. Caccavo, D., Cascone, S., Lamberti, G. & Barba, A. A. Hydrogels: experimental characterization and mathematical modelling of their mechanical and diffusive behaviour. *Chem.Soc.Rev.* **47**, 2357–2373 (2018).

147. Cao, D. *et al.* An Intelligent Transdermal Formulation of ALA-Loaded Copolymer Thermogel with Spontaneous Asymmetry by Using Temperature-Induced Sol–Gel Transition and Gel–Sol (Suspension) Transition on Different Sides. *Adv. Funct. Mater.* **31**, 2100349 (2021).

148. Amirova, A. *et al.* Synthesis and Investigation of Thermo-Induced Gelation of Partially Cross-Linked Poly-2-isopropyl-2-oxazoline in Aqueous Media. *Polymers* **12**, (2020).

149. Wang, B., Zhu, W., Zhang, Y., Yang, Z. & Ding, J. Synthesis of a chemically-crosslinked thermo-sensitive hydrogel film and in situ encapsulation of model protein drugs. *Reactive and Functional Polymers* **66**, 509–518 (2006).

150. Yu, L., Chang, G., Zhang, H. & Ding, J. Temperature-induced spontaneous sol–gel transitions of poly(D,L-lactic acid-co-glycolic acid)-b-poly(ethylene glycol)-b-poly(D,L-lactic acid-co-glycolic acid) triblock copolymers and their end-capped derivatives in water. *J.Polym.Sci.A Polym.Chem.* **45**, 1122–1133 (2007).

151. Xue, K. *et al.* PCL-Based Thermogelling Polymer: Molecular Weight Effects on Its Suitability as Vitreous Tamponade. *ACS Appl.Bio Mater.* **3**, 9043–9053 (2020).

152. Amirova, A., Kirila, T., Kurlykin, M., Tenkovtsev, A. & Filippov, A. Influence of Cross-Linking Degree on Hydrodynamic Behavior and Stimulus-Sensitivity of Derivatives of Branched Polyethyleneimine. *Polymers* **12**, (2020).

153. Nikouei, N. S., Ghasemi, N. & Lavasanifar, A. Temperature/pH Responsive Hydrogels Based on Poly(ethylene glycol) and Functionalized Poly(e-caprolactone) Block Copolymers for Controlled Delivery of Macromolecules. *Pharm.Res.* **33**, 358–366 (2016).

154. Ghasemi, N., Vakili, M. R. & Lavasanifar, A. Defining Role of a High-Molecular-Weight Population in Block Copolymers Based on Poly(α-benzyl carboxylate-ε-caprolactone) and Poly(ethylene glycol) on the Formation of Thermoreversible Hydrogels. *ACS Appl.Polym.Mater.* **3**, 2608–2617 (2021).

155. Appel, J., Fölker, B. & Sprakel, J. Mechanics at the glass-to-gel transition of thermoresponsive microgel suspensions. *Soft Matter* **12**, 2515–2522 (2016).

156. Bratek-Skicki, A. Towards a new class of stimuli-responsive polymer-based materials – Recent advances and challenges. *Applied Surface Science Advances* **4**, 100068 (2021).

157. Abou-Shamat, M., Calvo-Castro, J., Stair, J. L. & Cook, M. T. Modifying the Properties of Thermogelling Poloxamer 407 Solutions through Covalent Modification and the Use of Polymer Additives. *Macromol.Chem.Phys.* **220**, 1900173 (2019).

158. Zarrintaj, P. *et al.* Thermo-sensitive polymers in medicine: A review. *European Polymer Journal* **117**, 402–423 (2019).

159. Xin, H. & Naficy, S. Drug Delivery Based on Stimuli-Responsive Injectable Hydrogels for Breast Cancer Therapy: A Review. *Gels* **8**, 45 (2022).

160. Li, J. & Mooney, D. J. Designing hydrogels for controlled drug delivery. *Nature Reviews Materials* **1**, 16071 (2016).

161. Van Vlierberghe, S., Dubruel, P. & Schacht, E. Biopolymer-Based Hydrogels As Scaffolds for Tissue Engineering Applications: A Review. *Biomacromolecules* **12**, 1387–1408 (2011).

162. Daly, A. C., Riley, L., Segura, T. & Burdick, J. A. Hydrogel microparticles for biomedical applications. *Nature Reviews Materials* **5**, 20–43 (2020).

163. Perret, R. & Skoulios, A. Synthèse et caractérisation de copolymères séquencés polyoxyéthylène/poly-ε-caprolactone. *Makromol.Chem.* **156**, 143–156 (1972).

164. Ferruti, P. *et al.* Polycaprolactone−Poly(ethylene glycol) Multiblock Copolymers as Potential Substitutes for Di(ethylhexyl) Phthalate in Flexible Poly(vinyl chloride) Formulations. *Biomacromolecules* **4**, 181–188 (2003).

165. Huynh, D. P. *et al.* Functionalized injectable hydrogels for controlled insulin delivery. *Biomaterials* **29**, 2527–2534 (2008).

166. Gong, C. Y. *et al.* Acute toxicity evaluation of biodegradable in situ gel-forming controlled drug delivery system based on thermosensitive PEG-PCL-PEG hydrogel. *J.Biomed.Mater.Res.* **91B**, 26–36 (2009).

167. Bae, S. J. *et al.* Thermogelling Poly(caprolactone-b-ethylene glycol-b-caprolactone) Aqueous Solutions. *Macromolecules* **38**, 5260–5265 (2005).

168. Han, Y. *et al.* Impact of refractive index increment on the determination of molecular weight of hyaluronic acid by muti-angle laser light-scattering technique. *Scientific Reports* **10**, 1858 (2020).

169. Gentekos, D. T., Sifri, R. J. & Fors, B. P. Controlling polymer properties through the shape of the molecular-weight distribution. *Nature Reviews Materials* **4**, 761–774 (2019).

170. Striegel, A. M. & Pitkänen, L. Detection Orthogonality in Macromolecular Separations: Role of the On-Line Viscometer in Characterizing Polymers at Conditions of "Spectroscopic Invisibility". *Chromatographia* **78**, 743–751 (2015).

171. Striegel, A. M. Viscometric Detection in Size-Exclusion Chromatography: Principles and Select Applications. *Chromatographia* **79**, 945–960 (2016).

172. Striegel, A. M. There's plenty of gloom at the bottom: the many challenges of accurate quantitation in size-based oligomeric separations. *Analytical and Bioanalytical Chemistry* **405**, 8959–8967 (2013).

173. Ahn Y, K. S., Song Y, Kim H. Physical state of cellulose in BmimCl: dependence of molar mass on viscoelasticity and sol-gel transition. Phys Chem Chem Phys. *Royal society of chemistry* 1460-1469. (2016).

174. Grinshpun, V. & Rudin, A. Measurement of Mark-Houwink constants by size exclusion chromatography with a low angle laser light scattering detector. *Makromol.Chem., Rapid Commun.* **6**, 219–223 (1985).

175. Filipczak, N., Pan, J., Yalamarty, S. S. K. & Torchilin, V. P. Recent advancements in liposome technology. *Advanced Drug Delivery Reviews* **156**, 4–22 (2020).

176. Large, D. E., Abdelmessih, R. G., Fink, E. A. & Auguste, D. T. Liposome composition in drug delivery design, synthesis, characterization, and clinical application. *Advanced Drug Delivery Reviews* **176**, 113851 (2021).

177. Lee, J.-H., Oh, H., Baxa, U., Raghavan, S. R. & Blumenthal, R. Biopolymer-Connected Liposome Networks as Injectable Biomaterials Capable of Sustained Local Drug Delivery. *Biomacromolecules* **13**, 3388–3394 (2012).

178. Aghdam, M. A. *et al.* Recent advances on thermosensitive and pH-sensitive liposomes employed in controlled release. *Journal of Controlled Release* **315**, 1–22 (2019).

179. Zhao, P. *et al.* Paclitaxel loaded folic acid targeted nanoparticles of mixed lipid-shell and polymer-core: In vitro and in vivo evaluation. *European Journal of Pharmaceutics and Biopharmaceutics* **81**, 248–256 (2012).

180. Zhu, D. *et al.* Folate-modified lipid–polymer hybrid nanoparticles for targeted paclitaxel delivery. *IJN* 2101 (2015) doi:10.2147/IJN.S77667.

181. Liao, Z. *et al.* Multifunctional Nanoparticles Composed of A Poly(dl-lactide-coglycolide) Core and A Paramagnetic Liposome Shell for Simultaneous Magnetic Resonance Imaging and Targeted Therapeutics. *Adv. Funct. Mater.* **21**, 1179–1186 (2011).

182. Wu, B. *et al.* Folate-containing reduction-sensitive lipid–polymer hybrid nanoparticles for targeted delivery of doxorubicin. *Biomater. Sci.* **3**, 655–664 (2015).

183. Tariq, I. *et al.* Lipodendriplexes: A promising nanocarrier for enhanced gene delivery with minimal cytotoxicity. *European Journal of Pharmaceutics and Biopharmaceutics* **135**, 72–82 (2019).

184. Yang, X.-Z. *et al.* Single-Step Assembly of Cationic Lipid–Polymer Hybrid Nanoparticles for Systemic Delivery of siRNA. *ACS Nano* **6**, 4955–4965 (2012).

185. Zhang, M., He, J., Zhang, W. & Liu, J. Fabrication of TPGS-Stabilized Liposome-PLGA Hybrid Nanoparticle Via a New Modified Nanoprecipitation Approach: In Vitro and In Vivo Evaluation. *Pharm Res* **35**, 199 (2018).

186. De Leo, V., Milano, F., Agostiano, A. & Catucci, L. Recent Advancements in Polymer/Liposome Assembly for Drug Delivery: From Surface Modifications to Hybrid Vesicles. *Polymers* **13**, 1027 (2021).

187. Huang, Y.-Z., Gao, J.-Q., Liang, W.-Q. & Nakagawa, S. Preparation and Characterization of Liposomes Encapsulating Chitosan Nanoparticles. *Biological & Pharmaceutical Bulletin* **28**, 387–390 (2005).

188. Wang, Y., Tu, S., Pinchuk, A. N. & Xiong, M. P. Active drug encapsulation and release kinetics from hydrogel-in-liposome nanoparticles. *Journal of Colloid and Interface Science* **406**, 247–255 (2013).

189. Schmaljohann, D. Thermo- and pH-responsive polymers in drug delivery☆. *Advanced Drug Delivery Reviews* **58**, 1655–1670 (2006).

190. Shim, M. S. *et al.* Poly(D,L-lactic acid-co-glycolic acid)-b-poly(ethylene glycol)-b-poly (D,L-lactic acid-co-glycolic acid) triblock copolymer and thermoreversible phase transition in water. *J. Biomed. Mater. Res.* **61**, 188–196 (2002).

Appendix A

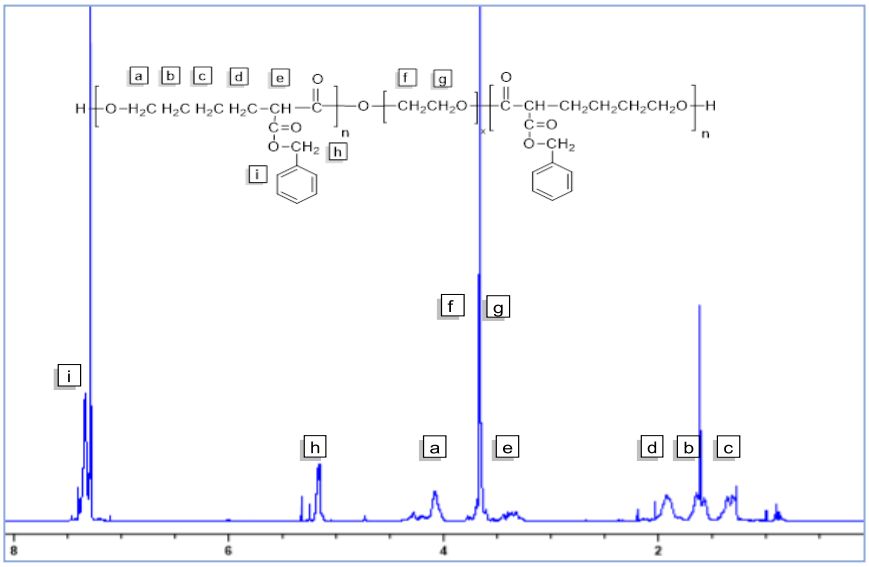

Figure S2-1. ^{1}H NMR spectrum of PBCL-PEG-PBCL block copolymers in $CDCl_3$ and peak assignments.

Appendix B

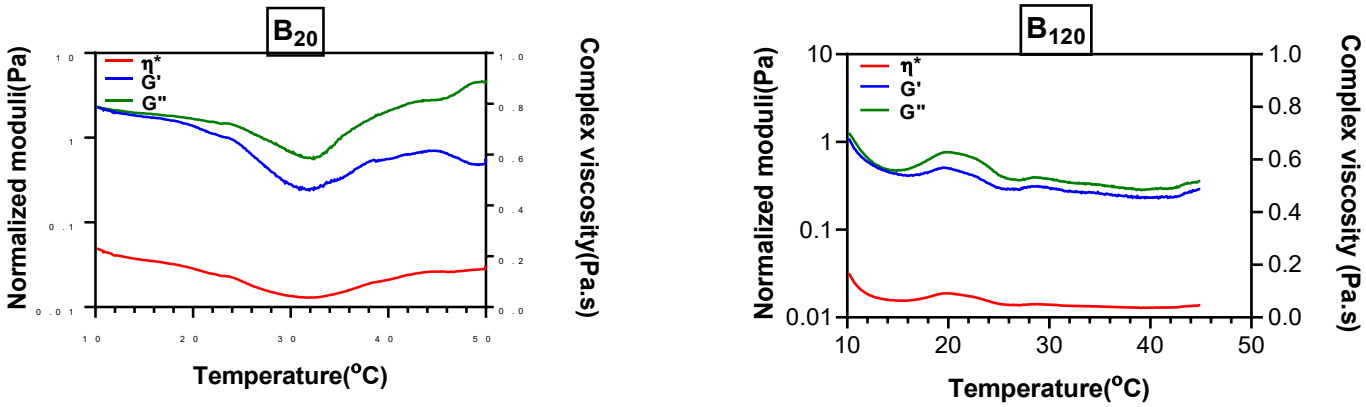

Figure S4-1. Viscoelastic behaviour of "B_{20} and B_{120}" copolymers aqueous solutions as a function of temperature at a heating rate 1 °C/min (10-50°C) and 10 wt% polymer concentration

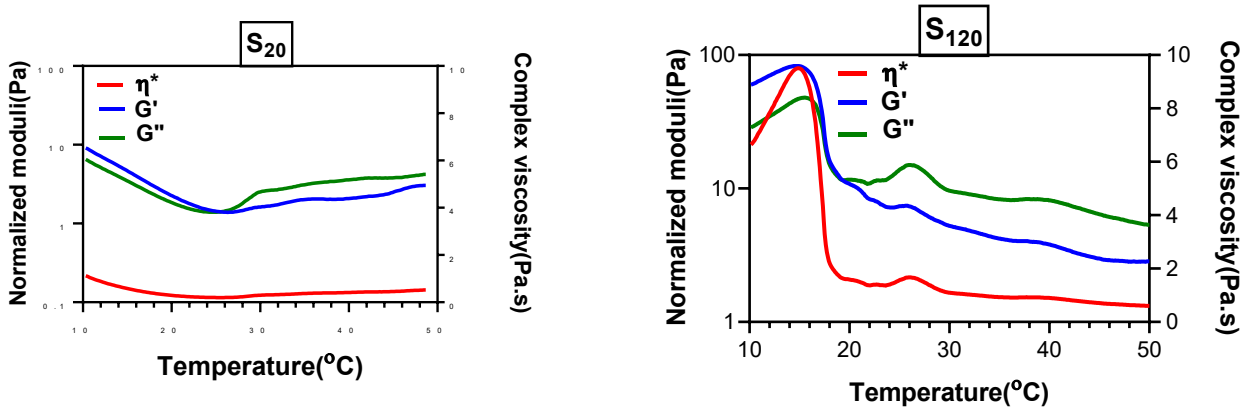

Figure S4-2. Viscoelastic behaviour of "S_{20} and S_{120}" copolymers aqueous solutions as a function of temperature at a heating rate 1 °C/min (10-50°C) and 10 wt% polymer concentration.